Isoconversional analysis for the prediction of mass-loss rates during pyrolysis of biomass

Lina Norberg Samuelsson

Doctoral Thesis, 2016
KTH Royal Institute of Technology
Energy Processes
Department of Chemical Engineering and Technology
SE-100 44 Stockholm, Sweden

TRITA CHE Report 2016:23
ISSN 1654-1081
ISBN 978-91-7595-997-9

Akademisk avhandling som med tillstånd av KTH i Stockholm framlägges till offentlig granskning för avläggande av teknisk doktorsexamen 10 juni kl. 10.00 i sal F3, KTH, Lindstedtsvägen 26, Stockholm.

Abstract

Biomass is the only renewable carbon source that can compete with fossil energy sources in terms of production of materials, chemicals and fuels. Biomass can be transformed into charcoal, liquid and gas through pyrolysis, i.e. pure thermal decomposition. By changing the pyrolysis conditions either solid, liquid or gaseous fractions can become the main product and pyrolysis is thus a very versatile process. Pyrolysis is also the first step in combustion and gasification, two important thermal processes in our society. The importance of biomass pyrolysis has led to extensive research in this area but due to the complexity of the process there is still no general understanding of how to describe biomass pyrolysis, which is essential in order to optimize thermal processes. The research presented in this thesis thus aims at finding a simple yet accurate way to model the decomposition rate of biomass during pyrolysis.

Thermogravimetric analysis, a well known method that is simple to use, was chosen to collect the experimental data used for kinetic evaluation. The reaction kinetics were derived using two different model-free, isoconversional methods, i.e. the non-linear form of the Friedman method and the incremental, integral method of Vyazovkin. By using these two methods and experimental data, complete reaction rate expressions could be derived for commercial cellulose, Norway spruce and seven different samples originating from kraft cooking, the most common process to produce pulp for the paper industry. The derivation of model-free rate expressions have never been performed before for these materials and since the rate expressions are model-free, no assumptions or knowledge about the pyrolysis reactions were required. This is a great advantage compared to the commonly used model-fitting methods that rely on information about these aspects. All the rate expressions were successful in predicting mass-loss rates at extrapolated pyrolysis conditions. This is a clear indication of the soundness of the methodology presented in this thesis.

Keywords: Pyrolysis, biomass, kinetics, cellulose, spruce, black-liquor, model-free, isoconversional, prediction

Sammanfattning

Biomassa är den enda förnybara kolkällan som kan konkurrera med fossila energikällor när det gäller produktion av material, kemikalier och bränslen. Biomassa kan omvandlas till biokol, bioolja och gas med hjälp av pyrolys, dvs termisk nedbrytning. Genom att variera de processförhållanden som råder under pyrolysen kan man få antingen fast, flytande eller gasfasiga ämnen som huvudprodukt, något som gör pyrolys väldigt flexibelt. Utöver detta är pyrolys även betydelsefull vid förbränning och förgasning, två viktiga processer i dagens samhälle. Vikten av biomassapyrolys har resulterat i omfattande forskning inom området men pga biomassas komplexa natur råder det ännu ingen enighet gällande hur biomassapyrolys bör modelleras. Detta försvårar utveckling och optimering av termiska processes matade med biomassa. Forskningen som presenteras i denna avhandling fokuserar således på att finna en enkel men noggrann metod för att beskriva hastigheten med vilken biomassa bryts ned under pyrolys.

Termogravimetrisk analys, en vanligt förekommande metod som är enkel att använda, valdes för att samla in experimentell data som kan användas för att undersöka hastigheten för termisk nedbrytning, dvs kinetiken. Två olika metoder som på engelska går under benämningen “model-free” och “isoconversional” har använts, nämligen den icke-linjära formen av Friedmans metod och den stegvisa, integrala metoden som utvecklats av Vyazovkin. Genom att använda dessa två metoder och experimentell data kunde kompletta reaktionshastighetsuttryck tas fram för kommersiell cellulosa, gran och sju olika material framställda genom sulfatprocessen, den idag vanligast förekommande pappersmassaprocessen. Pyrolyskinetiken för dessa material har aldrig tidigare analyserats med dessa två metoder och fördelarna med metoderna gjorde det möjligt att bestämma hastighetsuttryck utan någon kunskap om de pågående reaktionerna. Detta är en viktig fördel jämfört med andra metoder som är beroende av sådan information. Alla framtagna reaktionshatighetsuttryck kunde användas för att framgångsrikt förutsäga minskningen av massa vid extrapolerade pyrolysförhållanden. Detta är en tydlig indikation på att metoden använd i denna avhandling fungerar väl.

Nyckelord: Pyrolys, biomassa, kinetik, cellulosa, gran, svartlut, model-free, isoconversional, förutsägelse

Publications

This thesis is based on the following publications:

1. Lina N. Samuelsson, Rosana Moriana, Matthaus U. Babler, Monica Ek and Klas Engvall. Model-free rate expression for thermal decomposition processes: The case of microcrystalline cellulose pyrolysis. *Fuel*, 143:438-447, 2015.

2. Lina N. Samuelsson, Matthaus U. Babler and Rosana Moriana. A single model-free rate expression describing both non-isothermal and isothermal pyrolysis of Norway Spruce. *Fuel*, 161:59-67, 2015.

3. Lina N. Samuelsson, Matthaus U. Babler, Elisabet Brännvall and Rosana Moriana. Pyrolysis of kraft pulp and black liquor precipitates derived from spruce: Thermal and kinetic analysis. *Fuel Processing Technology*, 149:275-284, 2016.

4. Lina N. Samuelsson, Kentaro Umeki and Matthaus U. Babler. Mass-loss rates for wood chips at isothermal pyrolysis conditions: a comparison with low heating rate powder data. Manuscript in preparation.

Some of the Figures in this thesis have been reprinted from Paper 1-3, with permission from Elsevier.

Peer-reviewed conference contributions not appended to this thesis

1. CEEC-TAC2, Vilnius (2013): "Isoconversional Study of Cellulose Pyrolysis Kinetics" (poster presentation)

2. tcbiomass2013, Chicago (2013): "A New Methodology to Model Torrefaction Kinetics" (oral presentation)

3. ESTAC11, Espo (2014): "Modeling isothermal pyrolysis of cellulose with rate expression derived from dynamic TG experiments" (poster presentation)

Author contributions

- Paper 1:
  - I performed most of the experiments as well as all the data analysis of those experiments. I wrote all the code for the data analysis as well as most of the paper. I was in charge of the design and planning of the study.
- Paper 2:
  - I performed all the experiments except for the proximate analysis, the wet analysis characterization and the preparation of the sample. I wrote most of the paper and did all the data analysis. I contributed to the design and planning of the study.
- Paper 3:
  - I performed all the experiments except the proximate analysis for seven of the eight samples, the wet analysis characterization and the preparation of the eight samples. I contributed to the design and planning of the study and wrote most of the paper. Elisabet Brännvall and Daniel Tavast provided the description of the kraft cooking experiments as well as the description of the wet characterization analysis. Elisabet and Daniel prepared all the kraft cooking samples and the wet analysis of these samples.
- Paper 4:
  - I planned and performed the experiments, performed all the data analysis and wrote most of the paper.

Contents

List of Symbols

β_i	Heating rate of experiment i
α	Conversion
β	Heating rate, dT/dt
δc_α	Error in c_α
$\delta c'_\alpha$	Error in c'_α
δE_α	Error in E_α
δJ^2	Variance of the δJ_i's
δJ_i	Error in J_i
$\Delta\alpha$	Increment of conversion for which the kinetic parameters c_α and E_α are assumed constant
$\hat{E}_\alpha$	Optimized apparent activation energy
$\langle J_i(\hat{E}_\alpha)\rangle$	Average of the time integrals evaluated at $\hat{E}_\alpha$
$\langle J_i\rangle$	Average of the time integrals evaluated at $\hat{E}_\alpha$
$\langle X_i\rangle$	Average of the X_i's
A	Arrhenius frequency factor (pre-exponential factor)
A_α	Apparent pre-exponential factor at conversion α
c_α	Conditioned effective prefactor at conversion α
c'_α	Effective prefactor at conversion α
$d\alpha/dt$	Conversion rate (reaction rate)
E	Arrhenius activation energy
E_α	Apparent activation energy at conversion α
$f(\alpha)$	Reaction model (conversion function)
$g(\alpha)$	Integral form of conversion function $f(\alpha)$
i	Index of experiment, $i \neq j$
j	Index of experiment, $j \neq i$
J_i	Time integral evaluated at $\hat{E}_\alpha$
$J_i(\hat{E}_\alpha)$	Time integral evaluated at $\hat{E}_\alpha$
$J_i(E_\alpha)$	Time integral (from $t_{i,\alpha-\Delta\alpha}$ to $t_{i,\alpha}$) of the exponent in the Arrhenius temperature function evaluated at E_α
$k(T)$	Arrhenius rate constant (temperature function)
$k(T_0)$	Arrhenius rate constant at T_0
$m(t)$	Sample mass as a function of time
m_1	Dry sample mass
m_2	Sample mass at T_2 (at complete conversion)

n	Number of experiments for which the kinetic evaluation is performed
R	Gas constant
$r_{i,\alpha}$	Approximate conversion rate (numerical differential of $d\alpha/dt$ at conversion α for experiment i)
T	Temperature
t	Time
T_0	Reference temperature
T_1	Temperature for which the sample is dry ($\alpha = 0$)
T_2	Temperature for which the char yield becomes a function of heating rate
T_α	Characteristic temperature at which α is reached
$T_{i,\alpha}(t)$	Temperature at which a conversion α is reached in the i-th experiment
T_{iso}	Isothermal temperature
T_{peak}	Peak temperature, the temperature for which the conversion rate reaches a maximum
X	Vector containing the X_i
X_i	Derivative of $J_i(E_\alpha)$ with respect to E_α, evaluated at the optimized apparent activation energy

Chapter 1

Introduction

1.1 Motivation

Bedtime story year 2050

Once upon a time there was a society that used fossil fuels to create almost everything they needed. From coal, oil and natural gas they could produce heat and electricity, plastics, medicines and even fabrics. On top of that, pretty much their whole transportation fleet was relying on fossil fuels. The discovery of fossil fuels had made the society wealthy and industrialized but soon the first problems became evident. Forests and lakes were suffering from acid rain, and smog appeared over the cities. Conflicts arose around the world between countries fighting for the valuable resources. The weather on the planet started to change, and when whole societies disappeared into the oceans people started to worry about the future for real. Something had to be done to limit the damage, and fast. Researchers all over the world started to look for renewable alternatives to minimize the use of the ever so convenient fossil fuels. With wind, water and sun, the societies could get renewable electricity and hydrogen. This was definitely valuable but how about all the rest? How about all the hydrocarbo... Eureka, the answer is biomass! This is the only renewable alternative to all the products manufactured from fossil energy sources. By fermenting biomass, biogas for electricity, heat and fuel can be produced and by thermochemical conversion biomass can be converted into biocoal, synthesis gas and bio-oil. With this idea, the societies abandoned the fossil resources and focused on using the renewable carbon-sources everywhere around them. It was a tough balance between food and fuel production but with algae they could make use of non-arable land and salt water instead of fresh water. This time they used their resources in a sustainable manner and lived happily ever after.

Although greatly simplified, this short story explains the motivation for this thesis, i.e. the importance to study thermochemical conversion of biomass. We are all aware of the greenhouse effect resulting mainly from carbon dioxide, water vapor and methane as a result of our daily life here on earth. By using biomass instead of fossil energy sources the build-up of carbon dioxide in the atmosphere can be decreased. The decrease of the carbon dioxide build-up rate is possible since the time scale to go from carbon dioxide to biomass is very short compared to the time it takes to create fossil fuels. The carbon dioxide released during combustion of biomass can quickly be removed from the atmosphere due to growth of new biomass.

Simply switching from using coal, oil and natural gas to using biomass is for economic, legislative and technical reasons difficult. Biomass is any renewable hydrocarbon such as straw, wood, algae, compost, fish bones, manure, sewage sludge, paper, slaughter waste, nut shells etc.[1, 2]. Biomass is thus a very diverse group of materials, all having different physical and chemical properties. In 2007 the share of energy from biomass (wood, agricultural sources and municipal solid waste) in the world was 10 %. Based on the available biomass and technology, this share is estimated to have the potential to increase to 25-30 %, taking into account sustainable biomass production[3]. The research in this thesis focuses on lignocellulosic biomass, i.e. biomass from plants. Using wood as an example and comparing it to coal will illustrate some of the problems related to the use of biomass in conventional thermochemical technology developed for fossil fuels. A majority (more than 95 %) of all commercial burners and gasifiers are powder fed[4]. Since wood is a hard, fibrous material it is very energy intensive to grind it into fine particles, a fact that severely limits the application of biomass in today's technology. Coal on the other hand is brittle and easy to mill. Secondly, wood contains up to 45 wt% water which has to be removed before combustion or reduced to 10-15 wt% before gasification[5]. Coal, being a hydrophobic material, has much lower moisture levels (10-15 wt%)[6]. The hydrophilic nature of wood also prevents easy storage outdoors. Wood adsorbs moisture and it is prone to biological degradation from bacteria and fungi. Coal has none of these problems[6]. Thirdly, due to the bulky nature of stems and branches, and the high water content, wood is expensive to transport. The energy density of wood is 2-3 GJ/m^3 while the corresponding value for coal is 18-23 GJ/m^3, based on the lower heating value[6].

Thermochemical conversion can transform biomass into a solid biocoal, a gas or a liquid[1]. Usually all three phases are produced simultaneously but in varying proportions. All thermochemical processes are initiated with a pyrolysis step[7, 8]. During pyrolysis the biomass is thermally decomposed in the absence of an oxidation agent like oxygen. Depending on the process conditions the main product can be solid, liquid or gas and pyrolysis can thus be very versatile in terms of product distributions. During combustion on the other hand, the biomass is oxidized in an atmosphere having an excess of oxygen. All carbon and hydrogen atoms in the

biomass are oxidized to carbon dioxide and water and after complete conversion only ash is left as a solid residue. In addition to these two processes there is gasification, in which biomass is decomposed under sub-stoichiometric oxidant conditions. Steam, oxygen or air are usually used as oxidation media and the desired product is hydrogen and carbon monoxide, so called synthesis gas. This synthesis gas can be upgraded to a variety of organic molecules such as pharmaceutical drugs, diesel fuel and plastics[9].

Returning to the issues related to the use of biomass as a feedstock for commercial coal applications, one solution to the feeding, storage and transportation issues is torrefaction. The temperatures associated with this low temperature pyrolysis process are usually between 473 and 623 K[10]. Except for the fact that heating is performed in an inert atmosphere no established definition of torrefaction seems to exist. Reports from ECN (Energy research Centre of the Netherlands)[11, 12] state that, in addition to the already mentioned criteria on temperature and atmosphere, torrefaction is characterized by low heating rates (< 50 K/min), atmospheric pressure and relatively long residence times (around 1 h). Torrefaction transforms biomass into a solid with improved grinding and feeding properties[12–14], makes it hydrophobic[15, 16], resistant to biological degradation[6] and increases the specific energy density up to six times compared to that for raw biomass[6, 11, 14, 17]. Additionally, since the process temperature for torrefaction is low, waste heat from other processes might be used and the energy efficiencies in such industries would thus be improved[18]. After an increase in the research activities on torrefaction, in 2015 the first commercial plants were finally operating[19].

Some gasification and combustion technologies can use coarse biomass particles such as pellets and chips, which avoid the expenses of milling biomass. Examples of such technologies are fixed or moving bed gasifiers and fluidized bed gasifiers[5]. The aim of gasification is to produce a synthesis gas but unfortunately, biomass gasification also gives tar. Tar, usually defined as volatile hydrocarbons that condense at room temperature[7, 20], is detrimental to the gasification system since it leads to clogging of pipes and other downstream problems[1, 21]. Additionally it reduces the yield of synthesis gas since some of the biomass is used to produce tars[1]. A way to minimize the tar issues is to use staged gasification[22–24]. By performing pyrolysis in a preceding reactor the tars evolved during pyrolysis can be separated from the process stream before performing gasification in the following stage. Gasification of biochar gives less tar[23–25] and additionally, the pyrolysis vapors can be burned to add heat to the process in an efficient way.

1.1.1 Model-fitting and model-free isoconversional methods

The importance of pyrolysis, both as a process on its own, e.g. torrefaction, and as a part of gasification and combustion, has led to extensive research in this area[8]: Especially the kinetics of the pyrolysis process has been given a lot of

attention[26]. In order to optimize pyrolysis processes a process model describing the transport phenomena and the reaction rate is required. The reaction kinetics of biomass is usually studied by thermogravimetric analysis (TGA)[27, 28], an experimental technique giving mass-loss data as a function of time and temperature. The kinetic models derived from such data can be used to describe the overall conversion (mass-loss) and, if the vapors are condensed, the product distribution between volatiles (tar) and gas. The methods used when deriving kinetic parameters from experimental thermal analysis data can be categorized into model-fitting and model-free methods.

In model-fitting methods a reaction scheme, *e.g.* $Wood \rightarrow Gas + Char$, is selected and for each step in this scheme a reaction model, also called conversion function, describing the influence of conversion on the reaction rate, is assumed. The unknown parameters in the resulting system of equations are found from experimental data using regression. The parameters giving the best fit are chosen, giving these methods the name *model-fitting*. The name refers to the need to choose a reaction model for each step in the reaction scheme but it could also be refered to as "reaction scheme fitting". If experimental data from several temperature programs are used then the model-fitting methods can give parameters applicable for prediction at extrapolated conditions[29–32]. This is not different from model-free methods. Indeed, it has been shown that kinetic parameters derived from single temperature program data is not reliable and should be avoided[31]. Due to simultaneous derivation of several parameters the model-fitting methods give rise to correlated parameters that are not unique solutions to the minimization problem[30]. Additionally, the model-fitting methods are dependent on detailed information about the process chemistry in order to choose a suitable reaction scheme and conversion functions[30, 31]. If an erroneous conversion function is chosen the derived kinetic parameters will be erroneous. Some of the mathematically more complicated model-fitting methods are the distributed activation energy models (DAEM), modeling a reaction step as an infinite number of parallel reactions, each with its own apparent activation energy[33, 34]. The frequency factor is usually the same for all of the reactions[26]. This method has been found successful for complex materials[27, 31, 35, 36] but it has also been criticized for introducing an unnecessary number of reactions[26]. It is also not trivial to know what value to choose for the frequency factor and a reaction scheme is still needed.

The problem with uniqueness of the derived kinetic parameters and the difficulties in choosing a reaction scheme and conversion functions were partly solved by the introduction of model-free methods[27]. In these methods, the apparent activation energy can be determined independent of conversion function and the frequency factor, giving a unique apparent activation energy. The term *model-free* refers to this fact, i.e. that no conversion function is needed. In the so-called isoconversional model-free methods, this is possible by making the assumption, referred to as the isoconversional principle, that at a certain conversion the reaction rate is

only a function of temperature. This enables separation of the conversion function and the temperature function in the reaction rate expression (see Eq. (2.1) on page 17) which results in apparent activation energies valid at a certain conversion. In other words, the apparent activation energy is derived as a function of conversion, explaining the name *isoconversional*. The isoconversional principle comes with a limitation since the biomass pyrolysis process is assumed to follow a reaction scheme consisting of several reactions in series. The applicability of the isoconversional principle must be validated and this is most easily done by using a Friedman plot, i.e. for a range of conversion values, α, the natural logarithm of the conversion rate, $d\alpha/dt$, is plotted as a function of the inverse of temperature. This is done for a minimum of three different temperature programs and if the relationship is linear for a certain conversion then the isoconversional principle holds at that conversion[37]. The isoconversional principle has been shown to be valid for a range of different processes such as *e.g.*, thermal degradation of polymers, curing, dehydration and crystallization[38] as well as for oxidation of crude-oil[37, 39] and pyrolysis of calcium carbonate[40].

Another advantage (in addition to the derivation of a unique value of the activation energy, independent of conversion functions) of isoconversional analysis, compared to model-fitting methods, is that, due to the availability of the activation energy as a function of conversion, these methods can be used to predict conversion as a function of time based solely on the derived apparent activation energy. The so called kinetic triplet (i.e. the conversion function, apparent activation energy and frequency factor) does not need to be determined explicitly. Unfortunately, it is quite rare that the derived apparent activation energy is used in this way, at least in the field of biomass pyrolysis. The success of a prediction is a good indication of the soundness of the derived kinetic parameters. Except for the mentioned advantages with isoconversional analysis there are also some disadvantages. Since the apparent activation energy is derived as a function of conversion, the experimental data needs to have high resolution and the definition of conversion needs to be applicable to to the whole dataset[30]. The importance to define the conversion in a consistent way can be understood easily if we understand the isoconversional principle: at one and the same conversion, the same reaction is rate limiting and the kinetic parameters are only a function of temperature. Performing pyrolysis experiments on wood at different temperatures give varying final yields of solid residue as a function of temperature and the definition of conversion as “100 % conversion at the end of the process” can thus not be used. Another drawback with isoconversional methods is that the derived reaction rate expression can only be used to describe processes with the same underlying reaction mechanism. This limits the applicability of these methods since, as discussed in Section 2.2.1.1 on page 11, pyrolysis product ratios are strongly dependent on the reaction conditions. Such relationships between process conditions and product yields can be included in reaction schemes in model-fitting methods but not for isoconversional

methods[30].

1.1.2 Problem statement

Pyrolysis of biomass has mainly been modeled using global reaction schemes[41, 42]. In these methods, wood is usually described as one[43] or three components[44] decomposing individually into the lumped products char (biocoal, biochar), gas and tar (bio-oil). As explained, if data from several different temperature programs is used, model-fitting methods can give kinetic parameters that are successful in predicting pyrolysis conversions[29–32], but the success of model-fitting relies upon a proper choice of a reaction scheme and conversion functions for each step in the mechanism. Reaction schemes applying distributed activation energy models (DAEM) to describe the reaction rates for each step is also commonly used for biomass[33, 34]. Despite the importance of finding kinetic models for biomass pyrolysis, so far there is no consensus on how to model the kinetics of lignocellulosic biomass pyrolysis[27, 34, 41, 42, 45]. Already in 1970 Roberts [46] discussed the significant spread in the kinetic parameters derived for woody biomass pyrolysis, and the spread is still considerable in recent studies[42]. The same is true for pyrolysis of cellulose: the derived kinetic parameters reported in literature are widely scattered[47]. Even though cellulose is chemically much less complex than biomass, the literature suggests many different reaction schemes and conversion functions to describe cellulose pyrolysis[41, 47, 48]. Although there is still no complete understanding of the kinetics of cellulose pyrolysis, recent mechanistic modeling results have confirmed many of the experimental findings in literature, increasing the understanding of cellulose pyrolysis on a mechanistic level[49]. A reason for the spread in the values for the kinetic parameters, at least for biomass, could be due to actual differences in the reaction kinetics for the studied samples, resulting from differences in sample composition or experimental conditions. The spread could also result from the use of different reaction schemes and reaction models, a hypothesis that is strengthened by the scattered results achieved for the more homogeneous cellulose.

The scattered kinetic data is not only present in the field of biomass kinetics and as a response to this fact the Kinetics Committee of the International Confederation for Thermal Analysis and Calorimetry (ICTAC) recently (2011) published recommendations on how to estimate thermal decomposition kinetics of solids[31]. One of their recommendations is to use isoconversional methods to derive the apparent activation energy as a function of conversion. As mentioned, isoconversional methods are not dependent on information about the ongoing processes, hence an understanding of the processes that take place can be obtained without any hypothesis of the reaction mechanism and reaction model(s). This is an important feature that facilitates kinetic analysis of complex materials like biomass, since the same protocol can be used for different samples.

The importance of biomass pyrolysis for our future society, the advantages of isoconversional analysis[31] and the fact that there is still no consensus in how to model biomass pyrolysis kinetics, clearly motivates the work presented in this thesis.

1.2 Aim and scope

The overall aim of the present thesis was to find a simple way to model and predict the pyrolysis rate of biomass. The research has been performed with an engineering perspective, which means that the ability to model the studied process is the aim. The method should be simple to use to allow for industry or other interested stakeholders to include it as part of their process control routine. Additionally the data for the model should be easy to collect. With these requirements in mind we used isoconversional methods to derive biomass pyrolysis kinetics from TGA-data. More precisely, we investigated the possibility to derive isoconversional reaction rate expressions for pyrolysis of microcrystalline cellulose, spruce powder, pulp and black liquor precipitates from kraft cooking of spruce. Furthermore, the predictive capabilities of the rate expressions were investigated. As said, the experimental data used for deriving the rate expression came from TGA, a commercial, widely distributed analysis method that is easy to use.

The microcrystalline cellulose was chosen since it is a commercially available material that has been extensively studied in the literature using mainly model-fitting methods. There is thus a lot of available literature data to which our results can be compared. Since the end of 1990's there has been an increase in isoconversional studies on cellulose pyrolysis kinetics[50–56], but in these studies only the apparent activation energy is obtained in a strictly model-free manner. The kinetic triplet (i.e. the frequency factor, activation energy and conversion function) has been completed through a combination of model-fitting and isocoversional methods. In paper 1, we applied two different isoconversional methods to this substrate in order to i) compare the reliability of the two methods, ii) investigate if cellulose pyrolysis follows the isoconversional principle, iii) extend the isoconversional methodologies to enable derivation of a complete reaction rate expression (without model-fitting) and iv) properly test the derived rate expression at extrapolated conditions. To the best of our knowledge, prior to our cellulose study, there were no other biomass pyrolysis studies that had derived a complete rate expression isoconversionally and tested the predictability at extrapolated conditions. Strictly model-free rate expressions have been used before (and in some cases for prediction) to describe combustion of pyrolysis char from pine[57], NiS recrystallization[58], pyrolysis of calcium carbonate[40] and the self-accelerating decomposition temperatures of explosives[59].

In paper 2, the developed methodology was applied to Norway spruce, the major

wood species grown in Sweden[60]. The aim with this study was to obtain a rate expression for biomass pyrolysis that can be used to model industrial processes. At the same time we could test the developed methodology on a material that is more complex than cellulose. The reliability of the derived rate expressions were properly checked at extrapolated conditions.

Wood is a relatively expensive source of energy since it is also needed *e.g.* as a construction material and as feedstock for the paper industry. Except for the feeding, storage and transportation issues, wood is a good fuel with low ash content. Wood is also a good candidate for research since it is relatively homogeneous compared to waste materials like straw and branches. As a feedstock for the biofuel industry though, it is more logical to use waste sources of biomass, like demolition wood, agricultural waste or industrial waste streams. In paper 3, we thus studied the applicability of isoconversional analysis to model the pyrolysis of black-liquor precipitates as well as wood pulps. Today the black-liquor streams in kraft pulp plants are combusted to regenerate cooking chemicals and supply the mill with electricity and heat[61]. Since modern, heat integrated kraft pulp mills are net producers of heat[62–64], some of the organic matter in the black liquor might instead be extracted and converted to high-value renewable products. For example, hemicellulose can be used to produce sugars[65] or plastic films and coatings[66] while lignin could be pyrolyzed to produce functional char materials[67] or be depolymerized to produce aromatic building blocks for the chemical industry[68]. Also, lignin could be recovered in form of a powder suitable for thermal applications[69]. The aim in paper 3 was to investigate the potential to create char from both pulps and black liquor precipitates and derive the rate expressions necessary to model such conversion processes.

As we learned, milling of wood is expensive and for many thermal applications, *e.g.* torrefaction, wood chips are used[6]. In the fourth paper we investigated to what extent the rate expression derived from spruce powder at low heating rate conditions could be used to predict the conversion rate for wood chips at high heating rate conditions, mimicking the sudden feeding of chips into a preheated reactor.

Outside the scope of this thesis lie the determination and modeling of reaction heats, gas and vapor species formed as well as the modeling of heat and mass transfer phenomena, shrinkage and fragmentation of the fuel. No product analysis was performed.

Chapter 2

Biomass pyrolysis

This chapter presents background information provided with the intention of helping the reader to understand the results in this thesis.

2.1 Woody lignocellulosic biomass

The word biomass includes all organic materials that due to their production rate can be regarded as renewable[1, 2]. The biomass samples studied in this thesis are so called lignocellulosic biomass, i.e. biomass from the plant kingdom[2]. The word *lignocellulose* is easy to understand knowing that plant based biomass is mainly composed of cellulose, hemicellulose and lignin[1]. Cellulose and hemicellulose are polysaccharides, i.e. polymers consisting of sugar monomers. Together with starch and pectic substances they constitute the carbohydrate part of biomass[70]. Cellulose is a crystalline non-branched polymer of glucose while hemicellulose is a branched polymer that in softwoods consists mainly of galactoglucomannan (galactose, glucose and mannose) and arabinoglucuronoxylan (arabinose, glucose and xylose)[65]. The third main component in wood is lignin. Lignin is not a carbohydrate but a complex aromatic network built up of mainly coniferyl alcohol, together with sinapyl alcohol and p-coumaryl alcohol[67, 70]. Cellulose, hemicellulose and lignin together constitute about 90 % of the dry solid mass of wood, the remaining 10 wt% consisting of ash (usually below 1 wt%) and extractives[70, 71].

Norway spruce (Picea abies) wood is one of the materials studied in this thesis. Spruce is a so called softwood, a gymnosperm, in contrast to hardwoods that belong to the group angiosperms[70]. Some differences between softwoods and hardwoods are differences in the cells that the wood consists of and differences in

the macromolecules and their relative amounts[70]. For example, softwoods contain approximately 40 wt% cellulose, 30 wt% hemicellulose and 30 wt% lignin while for hardwoods the corresponding general composition is 45, 25 and 30 wt% (ash, moisture and extractive free basis)[65, 70]. A comprehensive review of the organic and inorganic phase composition of biomass is given in[72].

2.2 Pyrolysis processes

In this thesis, the word pyrolysis is used to describe the thermal decomposition in the absence of an oxidation agent, i.e. in an inert atmosphere. The term pyrolysis is sometimes also used to describe thermal degradation at the specific conditions suitable to produce bio-oil[71, 73].

The different chemical nature of the three main components of wood, i.e. hemicellulose, cellulose and lignin, result in different thermal properties for the components and for the composite biomass. In general, at low heating rates the decomposition temperatures for hemicellulose, cellulose and lignin are 493-598 K, 598-648 K and 523-773 K, respectively[41, 43]. Wider ranges have also been reported[74, 75] and the ranges may vary depending on the origin of the biomass and the chemical structure of the components. The thermal decomposition range will be a function of the heterogeneity of the molecules in the sample and as such, cellulose usually has the most narrow decomposition range, followed by hemicellulose and lignin[8].

2.2.1 Chemistry of biomass pyrolysis

During pyrolysis of wood, three product groups are achieved, i.e. gas, volatiles and char. The product distribution from biomass pyrolysis is strongly influenced by process parameters like heating rate, temperature and pressure but also factors like sample size and ash content[41, 76]. Examples of gases are carbon dioxide, carbon monoxide and methane[41, 43]. In some literature, these species are denoted as volatiles[43, 77] but that is not the nomenclature used in this thesis. The term volatiles is in this thesis used to denote the tars and other species that are condensible at room temperature. Tars can be classified as primary, secondary and tertiary[7, 41, 78], depending on the temperature range in which they are formed. Examples of primary tars, also called oxygenates, are acids, ketones, phenols and furans[21, 78]. Primary tars are formed at temperatures up to 673-773 K while secondary and tertiary tars are formed at about 773-1123 K and 1123-1223 K, respectively[41, 78]. Secondary tars are *e.g.* phenols, while tertiary tars are *e.g.,* PAH, polyaromatic hydrocarbons[21, 78]. In some literature only organic molecules with high boiling points are considered as tars since these pose the biggest problems during gas cleaning downstream of gasification[79]. Another

classification is to divide the volatile species into non-polar, high molecular weight organic species, called bio-oil or tar, and species soluble in water[80]. The term bio-oil is sometimes used to denote all condensibles, even water soluble species like acids[20, 81]. The water that evolves due to drying and as a reaction product is not classified as a tar. A good overview of volatile species evolved during pyrolysis of biomass is given by Anca-Couce [77].

Char is the solid fraction resulting from pyrolysis at temperatures above ca. 573 K[25]. Char consists of mostly carbon but it may also include ash[20, 80]. The term fixed carbon sometimes used in this field refers to the amount of carbon, or the combustible fraction in char. Due to the different chemistry of the three main components in wood, the volatile fractions are mostly resulting from pyrolysis of the carbohydrates (cellulose and hemicellulose) while char, being mainly carbon, results from mainly lignin[43, 82]. However, such characterization is only quantitative and, as shown in paper 3 in this thesis, the amount of char formed during pyrolysis is not a linear function of lignin content.

Pyrolysis of biomass is not well understood[73]. This is readily seen from the complex influence of process parameters, sample composition and sample form on the product ratio. In general, the pyrolysis pathways for cellulose and hemicellulose (xylan) are similar[8, 43]. One of the first steps is the cleavage of glucosidic bonds, i.e. the covalent ether-linkage between a carbohydrate and another molecule (could be a carbohydrate). This process is called transglycosylation and starts around 573 K[43]. This creates light tars such as levoglucosan and other anhydro-sugars. If levoglucosan is prevented from further reactions this is the main product from cellulose pyrolysis[73]. Furfural is one of the major components from hemicellulose[8]. Meanwhile, dehydration and elimination reactions are present, together with ring opening and fragmentation reactions[8]. The products formed during cellulose pyrolysis usually results from several of these mechanisms. A good overview of the pyrolysis chemistry of cellulose is given by Emsley and Stevens [83], Lin *et al.* [84] and Mamleev *et al.* [85]. The decomposition of lignin differs from that of the carbohydrates: between 423 K and 573 K dehydration gives water and formaldehydes from oxygenated propyl chains, at 473 K ether linkages can break giving phenolic compounds with alkyl chains while at temperatures above 573 K alkyl chains decompose to give phenolic compounds[8].

At temperatures above about 773 K secondary reactions of the formed volatiles are initiated. These reactions are called secondary pyrolysis since the products from the initial decomposition act as reactants[20]. Secondary reactions give rise to so called secondary products.

2.2.1.1 Pyrolysis product ratios: fast, intermediate and slow pyrolysis

The ratios between char, volatiles and gas are influenced by process parameters and sample properties. Examples of the most important process parameters are heating

rate, pressure, gas residence time and temperature. Regarding sample properties, important factors are sample size, sample composition, ash amount and moisture amount. There is a lot of research regarding the product distribution (see [41] and references therein) and there is consensus that high heating rates and low vapor hold-up time in contact with the solid material give more liquids, while a high vapor hold-up time in combination with low heating rates and high pressures favor char formation[1, 20, 25, 86]. In general, low temperatures favor solid products, medium temperatures favor vapors while at high temperatures mostly gases are formed[20]. The strong influence of heating rate on the product distribution has lead to the somewhat arbitrary classification of pyrolysis into slow (conventional, carbonization), intermediate (or fast) and fast (or flash) pyrolysis[1, 71, 80].

2.3 Biomass pyrolysis kinetics

2.3.1 Thermogravimetric analysis (TGA)

The most commonly used experimental technique to study biomass pyrolysis kinetics is thermogravimetric analysis[27, 28]. Thermogravimetric analysis, referred to as TGA in this work but also known as TG in some literature[28, 87], is a thermal analysis (TA) technique used to study mass-change phenomena induced by temperature changes. The temperature changes in the samples are achieved by external heating or cooling, but it can also be the result of processes within the sample. Since the method measures mass-change, TGA can only be used to study thermal processes leading to a change in sample mass. Other thermally induced processes such as melting and crystallization can not be studied using TGA but are instead analyzed using DSC, differential scanning calorimetry. As the name reveals, DSC measures the difference in heat flux to the sample compared to that to a reference. This allows for determining reaction and phase transformation enthalpies.

Due to the limited information that can be gathered using TGA, i.e. mass as a function of time and temperature, the technique is often combined with DSC in a so called simultaneous thermal analyzer, STA. To further increase the information that can be collected about a thermal event the evolved gases and/or vapors can be analyzed using evolved-gas analysis (EGA)[27]. The term EGA is also used to denote thermally stimulated exchanged gas analysis[87] but that is not the meaning of EGA used here. EGA can give either qualitative or quantitative information and examples of EGA are mass-spectrometry (MS), Fourier-transform infrared (FTIR) spectroscopy and gas chromatography (GC). In addition to TGA and DSC there are also other thermal analysis methods. Examples of such are differential thermal analysis (DTA), thermomechanical analysis (TMA), thermomanometric analysis, thermoelectrical analysis (TEA), thermomagnetic analysis, thermooptical analysis

(TOA) and thermoacoustic analysis (TAA). To my knowledge, none of these methods are used for studying kinetics of thermal decomposition of biomass, and these methods are thus not further discussed. An overview of thermal analysis methods can be found in[87].

Before presenting some technical aspects of TGA, let's illustrate what can be measured with TG-EGA. Calcium oxalate monohydrate is used as an example. Due to its relatively simple mass-loss curve this chemical compound is commonly used as a control substance in TGA[88–91]. Calcium oxalate monohydrate, $CaC_2O_4 \cdot H_2O$ is a salt that during pyrolysis decompose in three successive reactions:

Dehydration: $CaC_2O_4 \cdot H_2O(s) \rightarrow CaC_2O_4(s) + H_2O(g)$

Decarbonylation: $CaC_2O_4(s) \rightarrow CaCO_3(s) + CO(g)$

Decarbonation: $CaCO_3(s) \rightarrow CaO(s) + CO_2(g)$

These three processes all give rise to mass-loss steps since for each step water vapor, carbon monoxide and carbon dioxide, respectively are evolved from the sample. Since the material is stable and does not adsorb water due to its already hydrated form, it is convenient to use as a control substance to check the accuracy of the balance and the attached gas analysis equipment. By carefully loading a well defined sample mass in the TGA the theoretical mass loss for each step is easily calculated. The mass-loss recorded during TGA can then be compared to the theoretical value to get an estimation of the accuracy of the balance system. By connecting a mass-spectrometer to the TGA the amount and type of evolved gas for each step can be recorded. The time difference between the actual evolution of the gas and the detection in the EGA can easily be established for the setup, which will be useful when studying other, unknown processes. Even though the decomposition of calcium oxalate monohydrate is easily illustrated by the three above reactions, the actual thermogravimetric mass-loss curves can vary significantly as a function of process conditions and experimental setup[92]. Since this is true for this relatively simple system, we must be aware that the same can be true for other systems studied with TGA. The influence of process parameters, sample characteristics and gas flow configurations will be discussed in connection to biomass in Section 2.3.2.

There are some concepts that are of importance when discussing TGA. A *temperature program* describes the alterations in sample temperature. It is the term used to denote the program made by the TGA operator but it can also be used to describe the temperature of the sample, caused by both the programmed temperature schedule and/or reaction heat. If the temperature program consists of only heating rate segments (heating ramps), i.e. is non-isothermal, then the program can be described as being *dynamic*[87]. Correspondingly, the term dynamic TGA experiments is used to denote experiments with a linear heating rate from start to end

of the run. Contrary to this, isothermal experiments apply a constant temperature throughout the whole process. This mode of operation is very hard to achieve in practice since, even though a sample is dropped down into an already hot furnace, the sample has a finite heat capacity which prevents instantaneous heat-up[28]. In literature, the term isothermal is often used incorrectly to describe so called quasi-isothermal experiments. Quasi-isothermal experiments are experiments that for the main part consist of an isothermal segment but which are initiated by a heating ramp to reach the desired isotherm.

A key concept in studies of thermal decomposition kinetics is *thermal lag*. Thermal lag means that the actual temperature of the sample is not following the desired temperature program used in the TGA[27]. This will result in the mass-loss being logged at a temperature not corresponding to the actual sample temperature, which will give erroneous kinetic parameters. The deviation between the programmed temperature and the actual sample temperature can be a result of the finite heat capacity of the sample or a finite heat transfer rate, as well as self-heating or self-cooling of the sample due to reaction heat or evaporation of evolved gases. Finally, the *buoyancy effect* and the *correction* or *blank run* is sometimes mentioned. The buoyancy effect give rise to mass changes due to changes in gas density as a function of temperature. All non-isothermal runs or other processes where the gas atmosphere around the sample changes in density need to be corrected with a correction or blank run. Such a run is performed using the same temperature program but without any sample. The resulting blank curve is then subtracted from the experimental curve to give the mass-loss for the sample.

2.3.2 Collecting kinetic information of biomass pyrolysis using TGA

The data available from TGA is the mass-change as a function of sample temperature and time. In order to get data representing the kinetics of the sample decomposition process, the process rate (mass-change per time) needs to be governed by the rate of the ongoing chemical reactions. Other processes that may be governing the rate are heat and mass transfer processes, as well as thermodynamic phenomena such as equilibrium. The short compilation below tries to address important aspects to take into account when conducting TGA experiments on biomass in order to obtain reliable kinetic data. For more general, but detailed guidelines of how to collect thermal analysis data for kinetic evaluation the reader is referred to the paper by the Kinetics committee of ICTAC (International Committee of Thermal Analysis and Calorimetry) published in 2014[28].

2.3.2.1 Sample size and sample mass

The sample particle size and sample mass should be chosen to avoid thermal lag and to obtain a representative sample composition. The sample size also influences the presence of secondary reactions.

The heterogeneous nature of most biomass needs to be taken into account during the planning of the experiments. To obtain representative kinetic parameters each sample should be prepared so that the whole biomass composition is represented. In the case of wood, this can be achieved by milling and mixing and by removing heterogeneous parts like branches and bark. Milling will also decrease the particle size, which can decrease intra-particle temperature gradients that otherwise can occur. Extensive milling may result in a dense powder which may affect the pyrolysis process due to trapping of evolved gas species (secondary pyrolysis). To test if this effect is present several experiments with different sample layer thickness or different sample crucibles and gas flow configurations and flow rates can be used. If milling is not desired then the number of repetitions should be high to ensure capturing representing kinetic properties.

The actual sample mass that can be used is usually dependent on the instrument accuracy and maximum loads for the balance. The sample mass can also be limited by the size of available crucibles. In general, for kinetic investigations a lower mass is preferred since this minimizes the thermal lag and the presence of secondary reactions (due to decreased hold-up time of vapors in the solid matrix). Low mass will increase the signal to noise ratio and the difficulty to obtain homogeneous samples. Ideally, tests with different sample mass and heating rates are performed to make sure that the chosen sample mass is not resulting in thermal lag for the chosen heating rates. Additionally, one has to make sure that the balance is calibrated and that the buoyancy effect is accounted for[28]. One final thing to remember is that a smaller sample particle size will increase the surface to bulk ratio. If the reactions at the surface are different to those in the bulk, this may be of importance[27, 93].

2.3.2.2 Temperatures and heating rates

The aim with the kinetic studies performed in this thesis is to develop a reaction rate expression that can be used to describe pyrolysis processes, preferably at industrially relevant conditions. The heating rate in some industrial applications can be several hundreds of Kelvin per second[94]. In most commercial TGA the maximum heating rates achievable are much lower than this, partly as a result of large thermal inertia in the furnaces used. The question to ask then is if the kinetics determined in a TGA at lower heating rate conditions can be used to model the high heating rate processes in industry. One thing that is important to remember is that even though the heating rate is high on the surface of the particle the in-

ternal heating rate is not necessarily high[94, 95], which suggests that, at least at lower process temperatures, TGA may give relevant information. From a scientific perspective, low heating rates are advantageous since they will decouple overlapping mass-loss rate peaks which enables separate analysis of the sub-processes. A lower heating rate will also decrease the thermal lag. If high heating rates are desired then the sample mass needs to be low. Thermal lag between the furnace and the sample thermocouple can be accounted for with temperature calibration as described in *e.g.* [28]. The thermal lag inside the sample can not be accounted for by calibration but instead needs to be avoided through the choice of sample mass and crucible type, or, for macroscopic particles, measured by intra-particle thermocouples. Comparing the temperature for which the maximum mass-loss is achieved for different sample masses and heating rates provides a simple measure to assess the thermal lag in the system. During kinetic analysis, systems with thermal lag, resulting in a lower actual sample temperature than the measured temperature, will give rise to apparent kinetic parameters that are lower than if thermal lag was not present[85]. The opposite is true in cases where the sample temperature exceeds that of the temperature program, *e.g.* during sample self-heating due to exothermal reactions.

Essential for isoconversional methods but also very important for model-fitting methods is that the experiments are performed with a minimum (preferably more) of three different heating rates or temperature programs[31].

2.3.2.3 Gas atmosphere and flow rate

For simplicity, in kinetic studies of biomass pyrolysis the gas flow and atmosphere is usually chosen to minimize the influence from secondary pyrolysis processes[28]. This should be tested by varying the gas flow rate and making sure that it does not influence the mass-loss curve. No lid on the sample crucible is used in these cases and a high gas flow rate is important. The gas flow configuration will also be an important factor to vary. The gas should be inert, i.e. no oxidizing agent like water or oxygen should be present. This is very important especially during long runs and runs at high temperature, where even trace amounts of oxygen can lead to detectable mass-loss[28]. The choice of inert gas will be a function of price, availability, thermal conductivity and density. A higher thermal conductivity of the gas will improve the heat transfer between the furnace and the sample, which may decrease thermal lag.

2.3.2.4 How to assure high accuracy of the collected data

The accuracy of the collected data, i.e. how well the data reflects the rate of the ongoing chemical processes will depend on the sample size, sample mass, temperature program, gas flow rate and gas type. In addition to this it will depend

on the quality of the temperature calibration, balance calibration, buoyancy effect correction, cleanliness of the system and the crucibles, as well as on how good the reproducibility in sample preparation and handling is. Additionally, all the hard work done during calibration, cleaning and planning can go to waste if the TGA is not placed in a vibrational free environment at constant atmospheric conditions. All these factors are discussed in details in [28] and thus not further discussed here. Two final things that may influence the data quality is the sampling rate and the automatic smooting that exists in some commercial TGA softwares.

2.3.3 Thermal decomposition kinetics

The Kinetics Committee of ICTAC recently published recommendations on how to estimate thermal decomposition kinetics of solid[31]. In addition to the importance of having high quality data they recommend i) using data from a minimum of three different temperature programs, ii) using an isoconversional method to derive the apparent activation energy as a function of conversion, iii) complete the reaction rate expression and finally, iv) validate the derived rate expression with experimental data not included in the derivation of the kinetic parameters. All these recommendations have been followed in this thesis.

In thermal analysis, processes initiated by a change in temperature are studied. The reaction rate for such processes, having no pressure dependence, is often described as:

$$\frac{d\alpha}{dt} = k(T)f(\alpha) \tag{2.1}$$

where $k(T)$ is a rate constant (temperature function), α is the conversion, t is the time and $f(\alpha)$ is the conversion function (reaction model). Equation (2.1) describes the rate of a single step process. Depending on the process studied α can be evaluated as *e.g.* a fraction of the total mass-loss or a fraction of the total heat absorbed or released in the process. Regardless of what fraction α denotes it always increases from 0 to 1 as the process progresses[38]. Since decomposition rates during thermal analysis of complex materials reflect the overall transformation of reactant to product the rate constant derived for a process found to obey a single step equation is likely not describing a process consisting of a single step. Instead the process probably involves several steps where one step is much slower than the others and thus determines the overall kinetics[31]. The Arrhenius equation, i.e. $k(T) = A\exp(-E/RT)$, is, almost without exceptions, applied to describe the temperature dependence of the thermal decomposition process[38], where R is the gas constant and T is the temperature. The experimentally determined activation energy, E, and frequency factor, A, should be denoted as effective, apparent, empirical or global since they may deviate from the intrinsic kinetic parameters[31, 38];

even though the studied process is limited by the reaction rate, the measured quantities reflect the sum of all ongoing reactions, and probably not the rate of a single elementary reaction step. There is actually a vivid discussion in the thermal analysis community whether the Arrhenius expression should be used as a temperature function in solid state reactions or not[27, 47]. As of yet there is no agreement. The motivation to use other temperature functions is that i) the data from TGA can not give information on separate energy boundaries of elementary reactions, ii) it would decrease the interpretation of the apparent kinetic parameters E and A as kinetic parameters with physical meaning described by the transition state theory[96] and iii) the temperature integral (see Section 2.3.3.1) would be avoided, since with other temperature functions there can be an analytical solution[97]. Since the temperature integral is easily solved using modern computers the third of these motivations is redundant. Regarding the reaction model, $f(\alpha)$ in Eq. (2.1), also called the conversion function, several different expressions have been used to describe solid-state kinetics. There are power law models, diffusion models, contracting sphere models, Avrami-Erofeev models and the Mampel model. Some examples of what $f(\alpha)$ may look like are found in[31]. Once the kinetic triplet (E, A and $f(\alpha)$) is determined the rate expression, *e.g.* Eq. (2.1) can be used to model the process (there are model-free methods where only the apparent activation energy is needed, see Section 2.3.3.1).

Before presenting an overview of the modeling work done on biomass pyrolysis kinetics, isoconversional methods used in the literature are shortly described, focusing on their different accuracy. A description of the two isoconversional methods used in this thesis is found in Section 3.2.

2.3.3.1 Isoconversional methods

The isoconversional methods can be divided into differential and integral methods. The Friedman method[98] is a differential method developed in 1964. It is called differential since the rate expression is evaluated in its differential form. The basic equation of Friedman's differential method is readily obtained by taking the logarithm of Eq. (2.1):

$$\ln\left(\frac{d\alpha}{dt}\right) = \ln(Af(\alpha)) - \frac{E}{RT}. \tag{2.2}$$

This method is very simple to apply and it is the isoconversional method based on the fewest number of assumptions[31, 99]. An often mentioned drawback with the Friedman method is the need to differentiate the data, i.e. to estimate the derivative $d\alpha/dt$, which in the case of TGA data may result in significant levels of noise[31, 100]. To avoid this problem, the integral methods can be used[90, 99]. The first integral methods were the method by Ozawa[101], developed in 1965, as

well as the method of Flynn and Wall[102, 103], from 1966. The integral methods are based on the integral form of the rate equation, given in Eq. (2.1):

$$g(\alpha) = \int_0^{\alpha} \frac{A}{f(\alpha)} d\alpha = A \int_0^{t} \exp\left(\frac{-E}{RT}\right) dt. \tag{2.3}$$

Here, $g(\alpha)$ is the integral form of the conversion function. From Eq. (2.3) we can immediately see one of the limitations of the earlier integral methods, i.e. the constant apparent activation energy and frequency factor over the time 0 to t. This will cause an averaging of the determined apparent activation energies, which can lead to significant errors[90, 100]. This averaging is present in the most commonly used integral isoconversional methods, i.e. the Ozawa-Flynn-Wall (OFW) method and the Kissinger-Akahira-Sunose method (KAS)[30]. Another reason for the low accuracy of these methods compared to the more recent integral methods (see below) is the application of an approximation for the temperature integral in Eq. (2.3). The integral in the time domain can easily be transformed to the temperature domain for linear heating rate programs where the heating rate $\beta = dT/dt$. The low accuracy in the OFW method[99, 100] has resulted in ICTAC clearly advising against using this method[31]. The temperature integral can not be solved analytically for a non-isothermal temperature program and much effort has been put into finding an as accurate approximations for the integral as possible. A review of this work has been written by Órfão [104]. If an accurate approximation for the temperature integral is used the error connected to this approximation is less than 1 % [99]. With the availability of modern computers the numerical solution of the temperature integral is trivial and there is no need to apply approximations for the integral. The error introduced by the averaging of the apparent activation energy still remains for these methods though. Notice that if the process consists of a single reaction, described by a single activation energy, then the averaging will not induce any errors.

The more modern integral isoconversional methods avoid the problem with the temperature integral approximation by solving the integral numerically. The averaging of the apparent activation energy is also avoided by using increments of temperature for which the integral is solved. An example of an advanced isoconversional method is the integral incremental method of Vyazovkin[90]. This method has been criticized for being unnecessarily complex and thus also making it difficult to analyze the error propagation in the derived apparent kinetic parameters[99]. The method has also been criticized for being computationally slow[105, 106]. Several papers exist (*e.g.* [30, 40, 57, 58, 100, 105, 107, 108]) that compare the accuracy of the most commonly used isoconversional methods in terms of the derived apparent activation energy. Overall, the advanced isoconversional methods are of similar accuracy or more accurate than the older isoconversional methods (KAS, OFW). The methods used in this thesis is the non-linear

form of the Friedman method[98] as well as an extended version of the integral incremental method of Vyazovkin[90]. The mathematical details of the applied methods are presented in Section 3.2 and a compilation of the differences between the applied methods and similar methods is found in Section 3.2.3.1.

Finally, an interesting observation by Vyazovkin[38] in 2015 is that the most inaccurate among the integral isoconversional methods, i.e. the OFW method, is the most commonly used. This method is as simple to use as the much more accurate method by Kissinger-Akahira-Sunose[109] and the method of Starink[99]. The most versatile methods, i.e. methods that can handle data from arbitrary temperature programs (*e.g.*, the Friedman method and the integral incremental method by Vyazovkin) are not as frequently used as one could expect.

2.3.4 Literature overview of biomass pyrolysis kinetics based on TGA data

This section gives an overview of the published work applying model-fitting and isoconversional methods to derive the pyrolysis kinetics of biomass. Pyrolysis models describing heat and mass transfer are not reviewed. Due to the vast amount of different reaction schemes developed for biomass this overview is by no means complete. The review is focusing on studies investigating woody biomass. Studies dealing with samples consisting of the main components of biomass, i.e. pure cellulose, hemicellulose and lignin are only shortly mentioned. Review papers and other studies giving good overviews of the pyrolysis models used for cellulose are found in [47–49, 52, 76, 77, 83–85, 89, 110, 111]. The main findings of these articles are presented at the end of this section, together with some findings for hemicellulose and lignin.

Furthermore, this section is limited to biomass pyrolysis literature that use so called lumped reaction models[34, 41]. This means that they do not describe the actual reaction mechanisms but instead lump the evolved products together in categories denoted solid, volatiles (tar) and gas. This has also been called visible kinetics[45] and semi-global models[27]. This kind of models are the most commonly used but there are studies where the kinetics of specific gas species are also modeled (*e.g.* [112–115]). Recently, studies using quantum calculations to estimate the energetically most favorable decomposition pathways have also entered the field[49, 77]. A final limitation to this literature compilation is that mainly studies based on simultaneous analysis of experimental data from several different temperature programs are reviewed. This limitation is based on the now widely recognized fact that it is not possible to derive reliable kinetic parameters from data based on a single temperature program[31].

2.3.4.1 Model-fitting woody biomass literature

A first mathematical model describing pyrolysis kinetics was set up by Bamford *et al.* in 1946[116–118]. Since then, a range of kinetic models have been developed to describe the pyrolysis reactions in biomass and lignocellulosic materials. Model-fitting methods are the most commonly used, something made clear from the many reviews of the area[27, 34, 41, 42, 45]. These methods apply reaction schemes involving pseudo components with various degree of complexibility. The reviews also make it clear that there is no consensus on how biomass pyrolysis kinetics should be modeled and that most models are based on single temperature program data, although lately the number of such papers seems to be decreasing. The models suggested for biomass pyrolysis can be divided into "one component mechanisms", "one step models", also called "total devolatilization model", "multi-component models", "competing and parallel reaction models", and models with secondary tar cracking[41, 45]. Criticism against the one step models is that these models can only predict char yield, and not gas and tar yield, as a function of time[115]. The use of three parallel single step reactions, illustrating the decomposition of cellulose, hemicellulose and lignin, also has this drawback.

Models that have been proposed in the literature to describe the pyrolysis mass-loss of biomass are:

- three parallel *n*th order reactions (water-washed beech wood, 0.5-108 K/min) [119]
- three parallel reactions where lignin is a third order reaction, the others are first order (waste softwood, 5-20 K/min) [120]
- two parallel first order reactions (water-washed beech wood 3-108 K/min, untreated beech wood, 5-80 K/min wood) [121]
- either six first order parallel reactions or four *n*th order parallel reactions (willow and poplar wood, 10-20 K/min and stepwise isothermal) [122]
- three parallel first order reactions (beech wood, 5-20 K/min) [115]
- three parallel reactions (two DAEM and one autocatalytic) (spruce and birch, 5-40 K/min, isothermal, modulated, "controlled reaction rate" and two stepwise isothermal programs) [32]
- four parallel first order reactions (beech and pine, 20-40 K/min and stepwise isothermal programs) [123]
- three parallel autocatalytic reactions (non-wood pulps, 5-20 K/min) [124]
- DAEM (pine sawdust, 0.0833-1 K/s) [125].

From this compilation it is clear that biomass often is modeled as three parallel reactions, motivated by the independent decomposition of the three main components in wood. The different reaction schemes and conversion functions proposed could result from differences in biomass studied, different sample mass, particle size[121], heating rates and influence of mass and heat transfer[41, 121]. Four of the above studies, i.e. [32, 115, 123] and [125] verify the developed rate expressions at extrapolated conditions. Two of the studies apply distributed activation energy models to describe the decomposition[32, 125]. A review paper on DAEM studies on biomass pyrolysis reveal that this method is quite successful in the field [33]. Due to the engineering perspective of this thesis, and the fact that different reaction schemes and models are used, the actual fitting parameters (E, A, $f(\alpha)$) derived in the above mentioned studies are not reported here. The success of the model to predict conversion rates at extrapolated conditions is much more interesting.

2.3.4.2 Isoconversional woody biomass literature

Literature dealing with isoconversional analysis of pyrolysis of woody biomass is presented. A phenomena seen quite often in studies using isoconversional methods is the determination of apparent activation energies only, i.e. no complete rate expressions are derived. Isoconversional predictions can be performed using only the apparent activation energy. Unfortunately to the best of my knowledge there are no pyrolysis articles presenting such predictions for woody biomass (not even among studies completing the rate expression) and such studies thus provide very limited information to the field. In the seemingly first isoconversional study on pyrolysis of woody biomass (2008) Yao *et al.* [126] used the Friedman method on TGA data to derive the apparent activation energies for pine wood fibers. One year later, Park *et al.* [127] derive a complete rate expression for oak wood consisting of two parallel reactions and one secondary tar reaction. The apparent activation energies were derived from TGA data using the Friedman method. Wood powder (undefined wood species) was also studied by Gašparovič *et al.* [128] in 2010. They found good agreement between the TGA data and their model developed from TGA data by using apparent kinetic parameters derived with the method of Friedman, together with an nth order reaction for each conversion value. Two years later Slopiecka *et al.* [129] used the OFW and KAS methods, together with a single step first order reaction to describe the pyrolysis of poplar wood in TGA. Finally, in 2014 two papers appeared. Chen *et al.* [130] derived the apparent activation energies for poplar wood using the Friedman method while Wu *et al.* [131] used the Cai-Chen iterative linear isoconversional method[57] to derive the apparent activation energy of oak and pine wood.

2.3.4.3 Model-fitting cellulose literature

The complexity of thermal decomposition of biomass has lead to the study of cellulose as a first step in the quest to understand the pyrolysis process. Several investigations have been performed and many different global models have been suggested to describe the pyrolysis kinetics. Milosavljevic and Suuberg [110] found that cellulose decomposes through two different mechanisms, as a function of temperature. In their literature review, Antal and Varhegyi [76] found that cellulose can be accurately described to decompose through a first order single step reaction. The same year, Conesa *et al.* [111] performed simultaneous regression of three heating rate curves and concluded that a scheme consisting of two parallel steps with one of the steps decomposing into gas and char gave the best results. More than ten years later, Völker and Rieckmann [119] used multivariate regression to conclude that microcrystalline cellulose can be modeled using two parallel reactions, one of them being a series of two reactions. In 2009, Lin *et al.* [84] suggested that cellulose pyrolysis is independent of heating rate and that a first order single step reaction coupled to a model that accounts for thermal lag is accurate enough to describe cellulose pyrolysis in a TGA. Opposite to many of the previous suggestions, in 2009 Mamleev *et al.* [85] suggested a reaction scheme consisting of two parallel reactions representing β-elimination and transglycosylation, respectively. Two years later Cai *et al.* [132] instead found that an *n*th-order logistic DAEM is suitable to describe the pyrolysis process. In the review by Lédé [48] (2012) it was concluded that there was still no consensus of how to model pyrolysis of cellulose. Şerbănescu [47] also noticed the scattered data in her review in 2014 but concluded that the first order single step reaction scheme can be used with success, partly because of the similarity of the resulting apparent activation energy with those derived with isoconversional methods. Finally, in the recent review by Burnham *et al.* [49] reasons for why a single step first order reaction clearly cannot govern the kinetics of cellulose pyrolysis are given. Additionally, recent experiments, as well as quantum chemical calculations suggest that the global pyrolysis kinetics for cellulose follows a sequential, nucleation-growth or random-scission model, all being sigmoidal[49].

2.3.4.4 Isoconversional cellulose literature

Regarding isoconversional studies on cellulose pyrolysis kinetics there are now quite a few. The first use of isoconversional analysis in the biomass field seems to be by Antal in 1982[89] where they derived the apparent activation energy for cellulose pyrolysis with the Friedman method. Three years later Antal *et al.* [133] found that the Friedman method gave apparent activation energies that supported the reaction scheme of cellulose pyrolysis suggested by Bradbury *et al.* [134]. Since their experimental results did not confirm the Bradbury reaction scheme

they finally concluded that due to thermal lag, the Friedman method is useless for datasets with widely different heating rates, i.e. data influenced by thermal lag[89]. Except for this early study and one study in 1997[50] all isoconversional cellulose studies are published after 2003. Except possibly one, i.e. the study of Cabrales and Abidi [53], none of the studies derive complete rate expressions in a strictly model-free manner and test the derived rate expressions at extrapolated conditions. In the study of Cabrales and Abidi [53] the integral, non-incremental method of Vyazovkin was used. They used a commercial software and, although the details are missing, it seems like they predicted isothermal conversion rates from dynamic heating rates. Reynolds and Burnham [50] used the Friedman method and a modified Coats-Redfern method to conclude that a three parameter nucleation model governed the reaction rate of cellulose during pyrolysis. Capart *et al.* [54] also found that a nucleation model together with Friedman activation energies gave the best description of both quasi-isothermal and linear heating rate data. An Avrami-Erofeev function was found suitable by Kim and Eom [135] who applied the Friedman method as well as model-fitting to find the apparent kinetic parameters. The Capela-Ribeiro non-linear isoconversional method was used to determine the apparent activation energy of three different celluloses by Barud *et al.* [136]. A one step reaction scheme described by an Avrami–Erofeev conversion function was also found suitable by Barud *et al.* [136]. Shaik *et al.* [137] used the mean activation energy derived from the Friedman method together with a single step first order reaction to describe cellulose pyrolysis kinetics. Sánchez-Jiménez *et al.* [55] concluded that a chain scission model together with the mean apparent activation energy from the Friedman method gave satisfactory results for cellulose decomposition. Cellulose pyrolysis apparent activation energies have also been derived with the inaccurate OFW method[138–140]. Moriana *et al.* [140] used Friedman derived apparent activation energies together with a single step *n*th order reaction at low conversion (below 0.3) followed by a single step first order reaction at high conversion (0.3-0.7).

2.3.4.5 Hemicellulose and lignin literature

To conclude this section, there are also some studies dealing with hemicellulose and lignin pyrolysis kinetics. Völker and Rieckmann [119] used multivariate regression and found that xylan pyrolysis kinetics was best modeled using three reactions in series and organosolv lignin needed two parallel series reactions. Beis *et al.* [141], Ferdous *et al.* [142] and Mani *et al.* [143] used either first order or first order gaussian DAEM to describe the pyrolysis kinetics of different lignins. As commonly seen, none of the above studies test the derived apparent kinetic parameters at extrapolated conditions. Several other studies using both model-fitting and isoconversional methods to study the pyrolysis kinetics of lignin and hemicellulose exist [56, 144–148]. As was the case for woody biomass and cellulose, these

studies reveal that more research is needed to get a coherent understanding of the pyrolysis properties of these materials.

Chapter 3

Experimental and numerical methods

This section first describes the experimental work performed in this thesis, including sample characteristics, sample preparation, run parameters and instrument specifications. After this, the numerical methods, i.e. the isoconversional methodology, used in this thesis is presented.

3.1 Experimental details

3.1.1 Samples

- Paper 1: Sigmacell cellulose type 20 (Sigma Aldrich) was used as received. Sigma Aldrich technical service reports a particle size of 20 μm, 36-40 kDa average molecular weight and an approximate degree of polymerization of 200.
- Paper 2: Norway spruce (Picea Abies) powder (40 mesh, 0.4 mm) was prepared from chips free of knots and bark using a ball mill. The chips were delivered by StoraEnso (Stockholm, Sweden). Proximate analysis, carbohydrate and lignin analysis is found in Tab. 3.1 on page 29 and a description of the analysis procedure is found in Section 3.1.3 on page 32. This sample is referred to as W, for wood.
- Paper 3: Two kraft pulps and five kraft black-liquor precipitates were prepared from a pilot-scale kraft cooking setup. The relationships between the seven samples and wood can be seen in Fig. 3.1. The two pulps (P1 and P2),

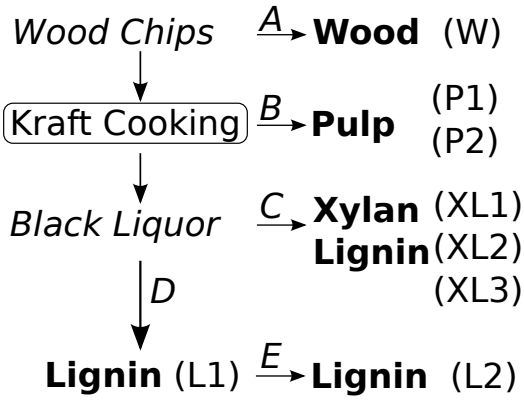

Figure 3.1: The relationship between wood and the seven kraft cook samples. The denotations for the samples are enclosed in parentheses. The letters A to E denote the preparation methods used.

prepared according to the description in Section 3.1.2, were produced at different kraft cooking times which resulted in differences in lignin amounts, see Tab. 3.1. Among the five precipitates, three of them were precipitated at pH 3, resulting in considerable amounts of xylan and lignin and therefore denoted as XL1, XL2 and XL3. The XL-samples differ in cooking time (see Tab. 3.1). The fourth precipitate, denoted L1 for lignin, was precipitated at pH 9, giving a sample consisting of lignin and carbohydrates. By subjecting L1 to acid hydrolysis a pure lignin sample was achieved, denoted L2. A description of the preparation of the black-liquor precipitates is found below in Section 3.1.2. The proximate, carbohydrate and lignin analysis is found in Tab. 3.1 and a description of the analysis procedures is found on page 32.

- Paper 4: Norway spruce (Picea Abies) chips were prepared by hand from knots and bark free chips. Chips of three different thicknesses were prepared and are hereafter referred to as thin, medium and thick. The chip dimensions are found in Tab. 3.2. A photography of the three chip sizes is seen in Fig. 3.2. Notice that the chips were prepared so that the fiber direction runs in parallel to the chip side. A schematic of the chip dimensions is found in Fig. 3.3. The wood chips and the wood powder used in paper 2 and 3 are from the same source and the proximate, carbohydrate and lignin content for these are thus the same (see Tab. 3.1).

Table 3.1: Cooking time, organic content, based on carbohydrate analysis and Klason lignin amount (including ash), and proximate analysis results for each sample.

Sample	Cooking time [min]	Organic content (wt% dry basis)						Proximate analysis (wt% dry)		
		Arabinose	Galactose	Glucose	Xylose	Mannose	Klason lign.	VM	FC	Ash
W	0	0.5	2.0	49.1	2.3	12.6	33.5	82.9 ± 1.7	14.9 ± 0.4	2.2 ± 2.1
P1	300	0.5	0.7	80.0	3.1	8.6	7.1	88.8 ± 0.9	10.6 ± 0.1	0.6 ± 0.5
P2	100	0.7	0.7	71.0	2.7	8.1	16.8	81.7 ± 0.1	16.7 ± 0.0	1.5 ± 0.1
XL1	50	7.3	5.0	3.2	38.7	1.7	44.1	63.8 ± 0.2	32.1 ± 0.1	4.1 ± 0.2
XL2	150	5.2	4.8	1.7	24.2	0.7	63.4	62.7 ± 0.2	34.7 ± 0.1	2.6 ± 0.0
XL3	250	3.7	6.1	1.9	23.5	0.6	64.2	64.0 ± 0.2	33.4 ± 0.2	2.6 ± 0.1
L1	300	1.2	20.0	11.1	4.1	1.9	61.7	62.4 ± 0.0	33.6 ± 0.1	4.0 ± 0.2
L2	300	no carbohydrates present					100.0	58.5 ± 1.6	40.6 ± 0.1	1.2 ± 1.2

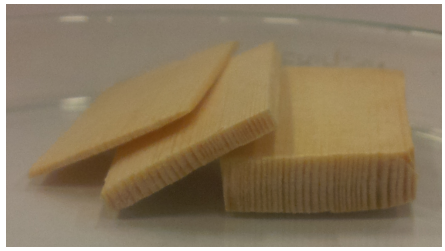

Figure 3.2: Photograph of the (from left to right) thin chip, medium chip and thick chip used in paper 4.

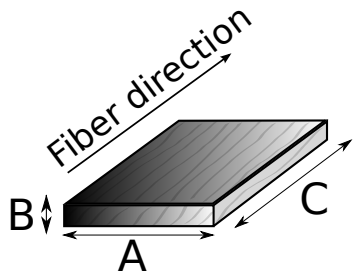

Figure 3.3: Schematic of the dimensions of the chips. The chip thickness (B) is perpendicular to the fiber direction.

Table 3.2: Sample dimensions and sample masses.

Sample	Dimensions [mm]			Mass [mg]
	Width (A)	Thickness (B)	Length (C)	
Thin chip	13-15	≤ 1	15-20	163±10
Medium chip	14-15	1-2	20-24	301±9
Thick chip	13-15	4 < B < 7	20-24	691±65

3.1.2 Preparation of kraft samples

Fig. 3.1 summarizes the eight samples studied in paper 3. The samples are all different and their denotations are seen in parenthesis in the figure. Each preparation step, denoted by the letters B to E are explained below. Step A consists of grinding in a ball mill.

3.1.2.1 Kraft cooking (step B)

Wood chips were placed in a rotating steel autoclave and vacuum was established for 30 minuted, using a vacuum pump. While keeping the vacuum, white liquor (1.5 M Na^+, 1.2 M OH^- and 0.26 M HS^-) at room temperature was added in 4:1 ratio (liquor : wood). The autoclave was heated by rotating it in a polyethylene glycol hot bath slightly inclined, to increase the contact between the wood chips and the cooking liquor. The cooking was performed at 157°C during 100 or 300 minutes, including 10 minutes allowance to reach the cooking temperature. After the cooking, the autoclave was immediately cooled in a water bath and the weak black liquor and pulp were collected and separated. The collected pulp was treated by displacement washing, using deionized water, in a washing cylinder immersed in a washing bath. The washed pulp was oven dried at 40°C. This cooking procedure is step B in Fig. 3.1.

3.1.2.2 Precipitation procedure pH 3 (step C)

The XL-samples were prepared by precipitation of the weak black liquor produced during kraft cooking (step B). The precipitation was done according to the procedure presented by Axelsson et al. [25], with one exception; the final washing step was performed with acetone instead of ethyl ether. Acetic acid was slowly added to the black liquor until the volume added equaled the volume of the black liquor sample, changing the pH of the solution to pH 3. The black liquor-acetic acid mixture was poured into a volume of ethanol 3 times the volume of the mixture. The solution was then placed in a refrigerator at a temperature of 277 K for 16-24 hours while xylan and lignin formed a precipitate. The supernatant was separated by decantation and the precipitate was washed twice with an ethanol-water mixture (volumetric ratio 1:2), three times in pure ethanol and finally three times with acetone. The precipitate was centrifuged after each washing step with a ROTOFIX 32A centrifuge for 20 minutes at a speed of 4 000 rpm. After the washing process, the precipitate was dried in a desiccator under vacuum to remove acetone. The dry solid weight was measured with an infra-red balance, Mettler Toledo LP-16.

3.1.2.3 Precipitation procedure pH 9 (step D and E)

Sample L1 was precipitated from weak kraft black liquor at pH 9 and 343 K. The pH of the solution was reduced from 12 to the precipitation pH by adding 20 wt% H_2SO_4 solution while stirring. The beaker with the precipitated lignin was cooled in an ice bath and then put in a refrigerator overnight at 278 K, allowing for the precipitated lignin to settle at the bottom of the beaker. The acidified black liquor supernatant was decanted through a high pH filter and the remaining lignin was dispersed in distilled water. The lignin was washed with acid water of pH 2 while

stirring, to decrease the concentration of sodium ions and organic contaminants. The solution was then filtered through a low pH filter. The lignin filtrate had a gel like texture; it was put on glass dish and then dried in a ventilated oven at 338 K for 12 hours. The resulting dry powder is the L1 sample. The L2 sample was obtained by subjecting part of the L1 sample to acid hydrolysis with sulphuric acid (398 K, 60 min), according to SCAN-CM 71:09 (Scandinavian pulp, paper and board testing committee).

3.1.3 Carbohydrate and lignin analysis

The carbohydrate content and type was determined after acid hydrolysis; it was analyzed according to SCAN-CM 71:09, using a high-performance anion exchange chromatograph equipped with pulsed amperometric detection (HPAEC-PAD) and a CarboPac PA1 column (Dionex, Sunnyvale, Ca, USA). The amount of Klason lignin in the samples was determined gravimetrically, after hydrolysis with sulphuric acid (398 K, 60 min), according to SCAN-CM 71:09. The amounts are collected in Tab. 3.1.

3.1.4 Proximate analysis

Proximate analysis was performed for W, P1, P2, XL1, XL2, XL3, L1 and L2 to determine the moisture (M), volatile matter (VM), fixed carbon (FC) and ash (A) content. The results can be found in Tab. 3.1.

The proximate analysis was performed with the Netzsch STA 449 F3 apparatus described in Tab. 3.5. Thermocouple signals were calibrated with the metal standards for the same purge flow used in the temperature program developed for proximate analysis, and a heating rate of 10 K/min.

Alumina crucibles, $85\mu l$, were used and care was taken to ensure that the sample was evenly distributed in the crucible. This to minimize heat and mass transfer gradients between the surrounding and the sample. The sample size (mean of two repetitions) can be found in Tab. 3.4. The volumetric gas flow rate was 80 ml/min.

The temperature program used was based on the works of García *et al.* [149] and Dean *et al.* [150]. Nitrogen gas (98.75% purity) and technical air was used as inert and oxidative atmosphere, respectively. The temperature program used is described in Table 3.3. Limitations in the TGA applied in this work, resulted in that the temperature program could not be followed exactly and the actual sample temperatures measured during analysis is seen in Tab. 3.3.

Table 3.3: Temperature program used for the proximate analysis performed in this study. *Passive cooling. ** Overshoot to 1239 K at start of isothermal step

Segment	T [K]	β [K/min]	Dwelling t [s]	Process
Initial	298	-	-	Drying, N_2
Heating from	298	20	-	
Isothermal	402	-	600	
Heating from	402	50	-	Pyrolysis, N_2
Isothermal	1223**	-	1200	
Cooling	-	*	-	
Heating from	638	50	-	Combustion, Air
Isothermal	1223**	-	1200	
Cooling	-	*	-	

Table 3.4: Dry sample mass. The values are mean of two runs per sample. The samples deviated at most 0.4 mg from each other.

Sample	Dry sample mass [mg]
W	9.88
P1	9.8
P2	10.1
XL1	10.0
XL2	10.1
XL3	10.0
L1	10.0
L2	9.9

3.1.5 Pyrolysis experiments

Three different TGA setups have been used in this thesis. Their specifications and the experiments performed in each one of them are presented in this section. The TGA setups did not include any instrumentation for gas analysis which limits us to predict solely the solid mass fraction as a function of temperature and time.

3.1.5.1 Instrument specifications

Some of the specifications from the manufacturers for the equipment used in this work are collected in Tab. 3.5. By comparing the two commercial setups it is easy to understand that the Mettler Toledo TGA/DSC 1 system was used for almost all of the experiments. The installed auto-sampler, together with the fast cooling of the furnace after finished runs make this instrument suitable for kinetic studies needing many repetitions at several heating rates. The reason that the DSC was not used is that DSC is often used with a lid on the crucible. The lid is put both on the reference cup and on the sample cup in order to minimize effects due to different emissivity of the two cups (due to the color of the sample). Using a lid (with a pin hole) will trap the evolved gases and volatiles and prolong the residence time for these species close to the solid. As mentioned in Section 2.2.1.1, this promotes secondary pyrolysis reactions which complicates the overall kinetic study since the reaction rate will to a larger part be pressure dependent. A second reason for not using DSC in this thesis is that processes coupled to mass loss are inherently difficult to study with DSC, resulting in that DSC is not commonly used for mass-loss processes[38]. For the same reasons DSC was not used in the Netzsch system studies.

3.1.5.2 TGA/DSC 1 Star System

The Mettler Toledo system was used to collect data for all four papers. The crucible type, gas quality and volumetric flow rate was the same in all studies, see Tab. 3.5. To correct for the buoyancy effect all runs performed at the same day were proceeded with one blank run, för each heating rate, as described in Section 2.3.1. Care was taken to ensure that the sample powder at the bottom of the pan was evenly distributed and spread in a reproducible way.

- Paper 1: Cellulose samples with three different sample masses were pyrolyzed in order to investigate the influence of sample mass on the thermal lag and the kinetics. The sample masses were 1.6 ($\pm$5 %), 4.0 ($\pm$3%) and 9.9 ($\pm$2 %). Pyrolysis was performed from room temperature to 1023 K. All sample masses were pyrolyzed at 3, 5, 7, 10 and 15 K/min while the two highest sample masses also were pyrolyzed at 2 K/min. For each heating rate

Table 3.5: Instrument specifications and details of relevance for the experiments performed in this thesis. TC = thermocouple.

Instrument→	TGA/DSC 1 Star system	STA 449 F3 Jupiter	macro-TGA
Manufacturer:	METTLER TOLEDO	NETZSCH	Home built
Instrument category:	STA	STA	TGA
Temperature range:	Ambient-1100C	Ambient-1250C	Ambient-900C
Heating rates:	0.002-150 K/min	0.001-50 K/min	3 K/min approximately
Cooling system:	Forced air (cool down in 25 min)	Passive	Passive
Auto-sampler installed:	Yes	No	No
Mass resolution:	0.1μg	0.1μg	1000 μg
Temperature accuracy:	$\pm$2 K	$\pm$1 K	$\pm$10 K
Sample TC position:	Under crucible, in contact	Under crucible, in contact	Under crucible
Balance:	Horizontal, UMX5	Top-loaded	Hanging basket
Balance calibration:	Scheduled service	Self-calibration	Tare
Temperature calibration:	Scheduled service (In, Zn, Al, Au))	Metal standards (Sn, Bi, Zn, Al, Au)	-
Crucibles:	Cylindrical (depth 3.5 mm), no lid, alumina, 70μl	Cylindrical, no lid, alumina, 85μl	Ni-Cr wire basket (home made)
Atmosphere and flow rate:	N_2 (99.999%), 70 ml/min	Ar (99.999 %), N_2 (98.75%), Technical Air, 80 ml/min	N_2 (99.999%), 5000 ml/min

and sample mass, 2-4 repetitions were performed. In addition to the three masses, a fourth mass of 2.7 mg was used. With this mass, four repetitions at 15 K/min were performed to further investigate the presence of thermal lag. The dynamic experiments with heating rate 2 or 3 to 15 K/min were used to perform kinetic analysis. To validate the derived kinetic parameters, two quasi-isothermal runs at 553 and 573 K, using 4 mg of sample. A heating rate of 10 K/min was used to reach the isotherm. A high sampling rate resulting in 29×10^3 to 54×10^3 data points per curve.

- Paper 2: Spruce powder with a sample mass of 4.01 ($\pm$2.8%) mg was pyrolyzed from 303 K to 1173 K using heating rate 1, 2, 5, 7, 10, 15, 20, 40, 80 and 100 K/min. Three to four repetitions were performed for each heating rate. To investigate the influence of sample mass on thermal lag and the amount of char formed, two other masses were used: 1.66 ($\pm$7.2%) mg and 9.95 ($\pm$1.0%) mg. These sample masses were pyrolyzed at 10, 15, 20, 40, 80 and 100 K/min from room temperature to 1173 K. Additionally, four quasi-isothermal experiments at 539, 571, 621 and 650 K were performed. The ramp used to reach the isotherm was 10 K/min and the isotherm was kept for 300 min. A high sampling rate was used resulting in 52.5×10^3 to 5.25×10^3 data points per curve for 2 K/min and 100 K/min, respectively.

- Paper 3: Seven kraft cooking samples were studied and the thermal and kinetic properties were compared to those for spruce (at 1-10 K/min, previously published in paper 2). The samples were heated from 303 K to 1173 K using four different heating rates: 2, 5, 7, and 10 K/min. The sample mass was 4.01 ($\pm$2%) mg (during loading, all samples and repetitions included). A fifth heating rate of 15 K/min was used for kinetic evaluation purposes for samples P1, XL1, L1 and L2. Additionally, sample L2 was pyrolyzed quasi-isothermally at 572, 592, 622, 652 and 672 K. The isothermal temperatures were reached with a ramp of 10 K/min. The dwelling time at the isothermal temperature was 300 min. Two to four runs were performed for each heating rate and sample, resulting in a minimum of 11 curves per sample. For the quasi-isothermal data, three repetitions were run at 672 K, while single runs were performed for the other isotherms. All pyrolysis runs were performed with a high sampling rate, resulting in a minimum of 25 $\times10^3$ points per curve.

- Paper 4: Some supplementary runs, with 4 mg wood chip cubes, used during kinetic evaluation were run in the Mettler Toledo TGA/DSC 1 Star System. The experiments are described in the supplementary material for paper 4.

3.1.5.3 STA 449 F3 Jupiter

The Netzsch system was used to perform the proximate analysis for paper 2, 3 and 4 and the comparison of char yields in paper 3.

- Paper 2, 3 and 4: The proximate analysis is described in detail in Section 3.1.4.

- Paper 3: Three spruce powder runs with a sample mass of 4.6±0.15 mg were performed in argon (purity 99.999 %, 80 ml/min) from room temperature to 1173 K using heating rate 1, 2 and 10 K/min. One run per heating rate.

3.1.5.4 Macro-TGA

A macro-TGA setup, home-built by researchers at the Department of Engineering Sciences and Mathematics at Luleå University of Technology, was used to study pyrolysis of wood chips in paper 4. The macro-TGA consists of a vertical tube furnace with an inner diameter of 100 mm. From the top of the furnace a sample basket, connected to a balance (model FZ-120i, A&D weighing) with a wire, can be inserted. An illustration of the system is seen in Fig. 3.4. The purge gas flow rate is 5 normal L/min and the pyrolysis gas flow rate is 7 normal L/min. Nitrogen (99.997 %) was used. For each experiment a pre-dried (12-24 h at 377 K) chip was put in an upright position in a wire basket (801 mg, Ni-Cr wire) and lowered down into the purge zone to remove oxygen. After a minimum of two minutes the sample basket was manually lowered down from the purge zone into the furnace. The time that elapsed from the start of the sample insertion into the heated zone to the start of the sampling mass logging was 5-10 s. The mass was sampled every 2 s with an accuracy of 1 mg. The sample temperature, measured with a thermocouple (accuracy ±2 K) placed 1.5 cm below the sample basked and 2 cm off center, was sampled once per second and varied on average with a standard deviation below 4 K from the isothermal temperature. After each pyrolysis experiment the sample basket was withdrawn from the furnace and placed in the purge zone to cool down before removing the char from the basket. The mass of the pre-dried sample chip and the resulting char was measured in an external balance (LPW-723, VWR). For all chip thicknesses the sample mass measured in the external balance varied less than 10 mg from the value measured in the macro-TGA. 3-5 repetitions were performed at each isothermal temperature, i.e. at 574, 597, 615, 637 and 676 K. The minimum dwelling time for the medium and thick chips was 44 min and the longest time was 240 min.

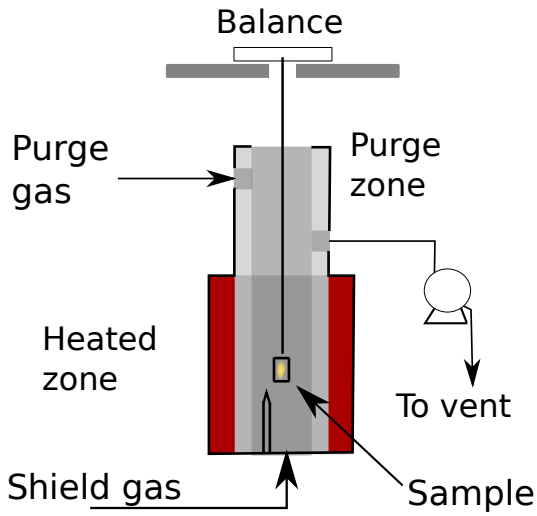

Figure 3.4: The isothermal macro-TGA setup.

3.2 Isoconversional analysis

3.2.1 Kinetic analysis methods used in this thesis

Two isoconversional model-free methods were used in this thesis, namely, the non-linear form of the differential method originally proposed by Friedman [98] and the incremental integral method introduced by Vyazovkin [90]. The differential method was chosen because of its ease of implementation and since it is built on the least number of assumptions[31]. It can also easily be used for an arbitrary temperature program, which is very important for engineering purposes. The incremental integral method was chosen since it does not lead to an averaging of the apparent activation energy, which is the case for the simpler OFW and KAS methods (see Section 2.3.3.1 on page 18). Additionally, it can be used for an arbitrary temperature program and, compared to some of the iterative isoconversional methods using linearization (see Section 3.2.3.1 on page 44), it introduces less modification of the raw data. Two methods were used since both of them have their own drawbacks and advantages.

Isoconversional methods are based on the isoconversional principle stating that, at a certain extent of conversion, the rate of decomposition is uniquely determined by the current sample temperature. In this thesis, conversion is defined as:

$$\alpha(t) = \frac{m_1 - m(t)}{m_1 - m_2}, \tag{3.1}$$

where m_1 is the mass of the dry sample, $m(t)$ is the sample mass at time t, and m_2 is the sample mass at the end of the pyrolysis reaction. The end for the pyrolysis reaction, i.e. the temperature for which the sample mass m_2 is reached, was found from experimental data and reliability testing as discussed in Section 4.2.1.

The simplest model following the isoconversional principle is:

$$\frac{d\alpha}{dt} = k(T(t))f(\alpha), \tag{3.2}$$

where $k(T(t))$ is the temperature function, $T(t)$ is the sample temperature at time t, and $f(\alpha)$ is the conversion function. The temperature function is typically assumed to follow Arrhenius law:

$$k(T) = A\exp\left(-\frac{E}{RT}\right), \tag{3.3}$$

where A is the apparent pre-exponential factor (frequency factor), E is the apparent activation energy and R is the gas constant.

Isoconversional methods are called model-free since the apparent activation energy as function of conversion can be determined without making any assumptions on the conversion function (reaction model) $f(\alpha)$. In this thesis, we extended the isoconversional methods in order to also determine an effective prefactor, defined as:

$$c'_\alpha = A_\alpha f(\alpha) \tag{3.4}$$

As seen, the effective prefactor is the product of the apparent pre-exponential factor (at a conversion α), and the conversion function. As shown below, E_α and the prefactor c'_α are extracted as discrete values for a given conversion. The set of the E_α and the c'_α for α going from 0 to 1 forms a complete reaction rate expression.

The differential method of Friedman is based on approximating the rate of conversion, i.e. the derivate on the left hand side of Eq. (3.2), from the experimental data. For a given conversion α, this approximated rate is denoted by $r_{i,\alpha}$, where i denotes the index of the experiment, as illustrated in Fig. 3.5. Applying this together with Eq. (3.4), (3.3) and (3.2) gives the non-linear rate expression for the Friedman method:

$$r_{i,\alpha} = c'_\alpha \exp\left(-\frac{E_\alpha}{RT_{i,\alpha}(t)}\right), \tag{3.5}$$

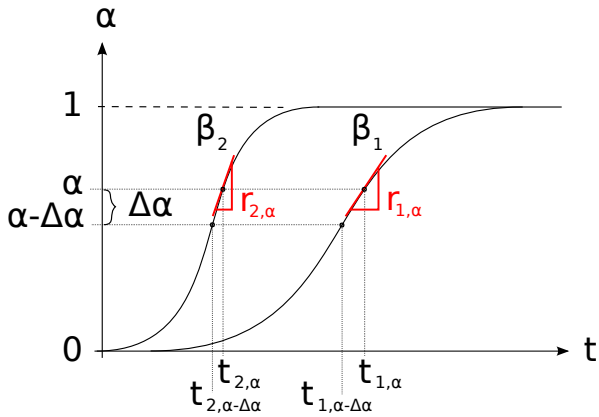

Figure 3.5: Schematic of the evolution of conversion at two heating rates β_1 and β_2, and the quantities used in the isoconversional methods (see text for details).

where $T_{i,\alpha}(t)$ is the temperature at which a conversion α is reached in the i-th experiment. For a given conversion, each experiment provides a value for $r_{i,\alpha}$ and $T_{i,\alpha}(t)$. Fitting Eq. (3.5) to these values presents a non-linear optimization problem with the two unknowns c'_α and E_α. In the original paper by Friedman [98], this problem is transformed into a linear problem by taking the logarithm of Eq. (3.5) which then allows for determining c'_α and E_α from a plot of $\ln r_{i,\alpha}$ vs. $1/T_{i,\alpha}(t)$. Although widely applied, this linearization of Eq. (3.5) will affect the experimental error in $r_{i,\alpha}$ and has a tendency to overestimate the uncertainty in experiments with a low heating rate (for which $r_{i,\alpha}$ is small). This suggests to remain with the non-linear problem as given in Eq. (3.5) and use a least-square solver for finding c'_α and E_α. The numerical details of this procedure are given in paper 1.

The integral method is based directly on the isoconversional principle, i.e. over a small enough increment of conversion the kinetics are governed by a single reaction (only a function of temperature) and accordingly, over this small increment, c'_α and E_α can be treated as constants. Eq. (3.2) can then be applied for each increment of conversion[151]. Denoting such an increment by $\Delta\alpha$, integration of Eq. (3.2) gives:

$$\Delta\alpha = c'_\alpha J_i(E_\alpha), \tag{3.6}$$

where

$$J_i(E_\alpha) = \int_{t_{i,\alpha-\Delta\alpha}}^{t_{i,\alpha}} \exp\left(-\frac{E_\alpha}{RT_i(t)}\right) dt, \tag{3.7}$$

and $T_i(t)$ is the temperature evolution in the i-th experiment; the integration limits indicate the times at which the conversions $(\alpha - \Delta\alpha)$ and α, respectively, are reached in experiment i (see Fig. 3.5). For a given conversion, Eq. (3.6) holds for any experiment, which implies that for a given conversion the $J_i(E_\alpha)$'s should be equal. The optimization problem to find E_α is thus to minimize the variation of the $J_i(E_\alpha)$'s. In the method proposed by Vyazovkin [90], this is done by minimizing the following function:

$$\Phi(E_\alpha) = \sum_{i=1}^{n}\sum_{j\neq i}^{n} \frac{J_i(E_\alpha)}{J_j(E_\alpha)}, \tag{3.8}$$

where n is the number of experiments. Having found E_α from minimizing Eq. (3.8), we can recompute the $J_i(E_\alpha)$'s, which allows for extracting the prefactor c'_α:

$$c'_\alpha = \Delta\alpha / \langle J_i(\hat{E}_\alpha)\rangle, \tag{3.9}$$

where $\langle J_i(\hat{E}_\alpha)\rangle$ is the average of $J_i(\hat{E}_\alpha)$ evaluated at the optimized activation energy $\hat{E}_\alpha$. Details on the implementation of both methods can be found in paper 1-3.

3.2.2 Error estimation and conditioning

Having determined the kinetic parameters E_α and c'_α through optimization of a certain set of experimental data, including experimental uncertainly, it is important to estimate the uncertainty in the determined parameters. The uncertainty estimation for the apparent activation energy derived with the integral method was addressed in a paper by Vyazovkin [152]. Although the method applied in this work is different from that in [152], both methods use the same starting criteria. This starting criteria, i.e. the isoconversional principle, states that for a given conversion interval, independent on heating rate, the time integral $J_i(E_\alpha)$ should be equal for all experimental curves. The variation in the J_i's, evaluated with the optimized activation energy, $\hat{E}_\alpha$, can therefore be seen as the error (or residual) of the minimization problem. We define this error as (in the following $J_i \equiv J_i(\hat{E}_\alpha)$):

$$\delta J_i = J_i - \langle J_i\rangle. \tag{3.10}$$

The error δJ_i is related to the error in the activation energy, δE_α, through[153]:

$$\delta J_i = X_i \delta E_\alpha, \tag{3.11}$$

where $X_i = (\partial J_i/\partial E_\alpha)_{\hat{E}_\alpha}$ is the derivate of Eq. (3.7) with respect to E_α, evaluated at the optimized activation energy. From Eq. (3.11), the error in the activation energy follows as[154]:

$$\delta E_\alpha = \sqrt{\delta J^2 (X^T X)^{-1}} \tag{3.12}$$

where δJ^2 is the variance of the δJ_i's, and X is the vector containing the X_i. From the error in the activation energy given in Eq. (3.12) we can proceed and deduce the error in the effective prefactor. The error in $\hat{E}_\alpha$ propagates to the estimation of the prefactor c'_α, whose error is:

$$\delta c'_\alpha = \frac{\Delta\alpha}{\langle J_i \rangle^2} \delta J. \tag{3.13}$$

This expression deserves a closer look. Indeed, Eq. (3.13) gives an error $\delta c'_\alpha$ that is of similar magnitude as the estimated parameter c'_α (cf. Eq. (3.9)). This is readily seen from an order of magnitude estimate of the quantities entering Eq. (3.13): Writing Eq. (3.11) as $\delta J \sim |X|\,\delta E_\alpha$ with $|X| \sim J/RT_\alpha$, where T_α is the characteristic temperature at which conversion α is reached, we can use Eqs. (3.9) and (3.13) to obtain:

$$\frac{\delta c'_\alpha}{c'_\alpha} \sim \frac{\delta E_\alpha}{RT_\alpha}, \tag{3.14}$$

which for typical values of δE_α and T_α is $O(1)$.

This large error in the estimation of the prefactor c'_α presents a severe limitation of our methodology, and Eq. (3.9) actually may lead to meaningless results. To overcome this difficulty, we introduce a preconditioning of the kinetic model by substituting the original Arrhenius expression (Eq. (3.3)) with a conditioned form,

$$k(T) = k(T_0) \exp\left[-\frac{E_\alpha}{R}\left(\frac{1}{T} - \frac{1}{T_0}\right)\right], \tag{3.15}$$

where $k(T_0)$ is the rate constant at a reference temperature T_0 chosen within the range of interest, e.g where the conversion rate is at a maximum. In the use of kinetic data, $k(T_0)$ takes on a similar role as the pre-exponential factor A while the treatment of its uncertainty is substantially simplified. To illustrate this, let us repeat the derivation from above by using Eq. (3.15) instead of Eq. (3.3):

Substituting Eq. (3.15) into Eq. (3.2) gives the conditioned rate expression:

$$\frac{d\alpha}{dt} = c_\alpha \exp\left[-\frac{E_\alpha}{R}\left(\frac{1}{T} - \frac{1}{T_0}\right)\right], \tag{3.16}$$

where

$$c_\alpha = k(T_0)f(\alpha), \tag{3.17}$$

is the effective prefactor of the conditioned problem. The latter is estimated in a similar way as c'_α:

$$c_\alpha = \frac{\Delta\alpha}{\langle J_i \rangle} \exp\left(-\frac{\hat{E}_\alpha}{RT_0}\right). \tag{3.18}$$

Eq. (3.16) is the actual rate expression put forward in this thesis. It has similar properties to Eq. (3.2)-(3.4), i.e. it describes the evolution of α in terms of the parameters c_α and E_α, and the same procedure to determine E_α can be applied, i.e. optimization of Eq. (3.8). However, the robustness of the prefactor c_α is greatly improved. The error in c_α is obtained from the propagation of the error in the activation energy. Following similar steps as those leading to Eq. (3.13) gives:

$$\frac{\delta c_\alpha}{c_\alpha} = \delta E_\alpha \left(-\frac{\langle X_i \rangle}{\langle J_i \rangle} - \frac{1}{RT_0}\right), \tag{3.19}$$

where δE_α is the error in the activation energy given by Eq. (3.12). Eq. (3.19) is the actual relation hereafter used for estimating the error in c_α in the integral method. Applying the same order of magnitude approximation that leads to Eq. (3.14), the above simplifies to:

$$\frac{\delta c_\alpha}{c_\alpha} \sim \frac{\delta E_\alpha}{R}\left(\frac{1}{T_\alpha} - \frac{1}{T_0}\right). \tag{3.20}$$

Hence, the error in the effective prefactor c_α is reduced by $\delta E_\alpha / RT_0$ with respect to the original prefactor c'_α (see Eq. (3.14)). This difference makes c_α more suitable to study and its determination more robust, while the kinetic information it carries is essentially the same as the one in the original prefactor.

Correspondingly for the differential method, instead of Eq. (3.5), the governing equation becomes

$$r_{i,\alpha} = c_\alpha \exp\left[-\frac{E_\alpha}{R}\left(\frac{1}{T_{i,\alpha}} - \frac{1}{T_0}\right)\right], \tag{3.21}$$

which is equivalently solved using a least-square solver, which provides estimated values for the two unknowns c_α and E_α. The errors in these two parameters are obtained from the square root of the diagonal elements of the covariance matrix[154].

3.2.3 Prediction of conversion rate for an arbitrary temperature program

The methodology applied in this thesis can be used to predict conversion as a function of time for an arbitrary temperature program. The prediction (i.e. achieving $\alpha(t)$) is realized by integrating Eq. (3.16) with the constituting functions c_α

and E_α taken as piecewise constant functions. The initial condition to Eq. (3.16) is taken as the first value of α for which the kinetic analysis was performed minus the increment $\Delta\alpha$ used in the integral method, and the time at which this conversion is achieved. For reconstructing runs with a linear heating rate β, the temperature in Eq. (3.16) is simply $T(t) = T(t=0) + \beta t$, while for isothermal runs $T(t) = T_{\text{iso}}$. By using temperature programs included in the derivation of the kinetic parameters a so called reconstruction is performed. By comparing the reconstructed curve with the original experimental curve the validity of the derived kinetic parameters is tested. By using temperature programs not included in the derivation of the kinetic parameters a prediction is performed. The ability to predict mass-loss rates is a much stronger proof of the reliability of the derived kinetic parameters than a successful reconstruction.

3.2.3.1 Predictive methods proposed in the literature

The isoconversional studies on biomass pyrolysis have only determined the apparent activation energy in a strictly model-free manner. To the best of my knowledge there are only a handful of publications (*e.g.*, [40, 57–59]) that derive complete rate expressions isoconversionally. The nuances of each of these fully isoconversional methods and the method used in this thesis are discussed in the following.

To facilitate this comparison, the integrated form of Eq. (3.16), with c_α substituted from Eq. (3.18), is here given for an isothermal temperature program:

$$t_\alpha^{(iso)} - t_{\alpha-\Delta\alpha}^{(iso)} = \frac{\Delta\alpha}{c_\alpha \exp\left[-\frac{E_\alpha}{R}\left(\frac{1}{T_{iso}} - \frac{1}{T_0}\right)\right]} = \frac{\langle J_i \rangle}{e^{-\hat{E}_\alpha/RT_{iso}}}. \tag{3.22}$$

The times $t_\alpha^{(iso)}$ and $t_{\alpha-\Delta\alpha}^{(iso)}$ are the times it takes to reach a conversion α and $\alpha - \Delta\alpha$, respectively, in an isothermal experiment at T_{iso}. As explained, the kinetic parameters (E_α and c_α) determined with the two isoconversional methods are taken as piecewise constant in the $\Delta\alpha$-increments. Eq. (3.22) is the equation used for predictions in this thesis (when purely isothermal predictions are made).

The model-free prediction proposed by Vyazovkin [38], rewriting the original expression to facilitate comparison to Eq. (3.22), has the following form:

$$t_\alpha^{(iso)} - t_{\alpha-\Delta\alpha}^{(iso)} = \frac{1}{\beta_i e^{-E_\alpha/RT_{iso}}} \int_{T_{i,\alpha-\Delta\alpha}}^{T_{i,\alpha}} e^{-E_\alpha/RT} dT. \tag{3.23}$$

Here, $T_{i,\alpha}$ and $T_{i,\alpha-\Delta\alpha}$ are the temperatures at which conversion α, respectively $\alpha - \Delta\alpha$, is reached in a dynamic experiment at a heating rate β_i; this dynamic experiment is one of the several runs used for deriving E_α. By writing Eq. (3.23)

in the time domain and exchanging the written-out integral with the notation J_i, we get

$$t_{\alpha}^{(iso)} - t_{\alpha-\Delta\alpha}^{(iso)} = \frac{J_i(E_\alpha)}{e^{-E_\alpha/RT_{iso}}}. \tag{3.24}$$

The difference between the predictive method derived in this thesis (Eq. (3.22)) and that developed by Vyazovkin [38] (Eq. (3.24)) is the averaging of the right hand side integral in Eq. (3.22). In other words, instead of referring to a single dynamic experiment at β_i, as done in Eq. (3.24) by using $J_i(E_\alpha)$, the method used here considers an average over all experiments used for deriving E_α.

A predictive method developed by Roduit *et al.* [59] is based on the following expression:

$$t_\alpha = \int_0^{t_\alpha} dt = \int_0^{\alpha} \frac{d\alpha}{A_\alpha f(\alpha)\exp\left(-\mathrm{E}_\alpha/\left(\mathrm{RT}_\alpha\right)\right)}. \tag{3.25}$$

Except for the integration boundaries (that can easily be changed into $t_{\alpha-\Delta\alpha}$ and t_α), this expression is identical to the integrated form of the unconditioned rate expression used in this thesis, i.e. Eq. (3.5), where $c'_\alpha = Af(\alpha)$. Roduit *et al.* [59] derived $Af(\alpha)$ from the intercept in the linear Friedman method and the method is thus very sensitive to inaccuracies in the Friedman plot intercept[40, 59].

Farjas and Roura [40] developed the following predictive expression[108]:

$$t_\alpha = t_{\alpha-\Delta\alpha} + \frac{E_\alpha}{R\beta}\frac{p(E_\alpha/RT_\alpha) - p(E_\alpha/RT_{\alpha-\Delta\alpha})}{\exp(-E_\alpha/RT_{iso})}, \tag{3.26}$$

where $p(E/RT)$ is the temperature integral[40, 108]:

$$\int_0^T \exp\left(-\frac{E}{RT}\right) dT = \frac{E}{R} p(\frac{E}{RT}). \tag{3.27}$$

If the temperature integral is transformed into a time integral that is solved numerically then the method by Farjas and Roura [40] is identical to the method by Vyazovkin [38] (Eq. (3.24)). Notice that both Eq. (3.24) and (3.26), in the form reported here, are only applicable for the prediction of isothermal experiments from E_α obtained from dynamic experiments.

An iterative linear integral isoconversional method has been developed by Cai and Chen [57]. As the name suggests, the method consists of the integral form of the rate expression. The temperature integral is approximated and by linearization of the integral rate expression, the apparent activation energy at α can be achieved from the slope of a plot of the left hand side of the linearized expression vs $-1/RT_{i,\alpha}$. The index i denotes an experiment conducted at heating rate β_i. As

common for all isoconversional methods, several experiments at different heating rates are needed to find the apparent activation energy and the method is similar to that of Friedman [98]. The left hand side of the linearized equation is a function of the apparent activation energy, which means that an iterative method is needed: A first guess of E_α gives a slope from which a new E_α is achieved. The new E_α is inserted into the left hand side of the equation and a new plot is achieved. This procedure continues until the apparent activation energy derived from the slope is no longer significantly different from the value inserted into the left hand side of the equation[57]. It is reported that few iterations are usually needed and the accuracy of this method is slightly higher than the already high accuracy of the integral incremental method of Vyazovkin[105]. The method is also reported to be much faster than that of the non-linear integral method of Vyazovkin, which could be an advantage[105]. One possible drawback with this method is the explicit expression of β in the method. This can introduce errors if the sample temperature deviates from the heating rate in the temperature program. Another disadvantage is the need for a first guess of the apparent activation energy. An iterative linear isoconversional method has also been developed by Budrugeac [155]. This method uses time integrals instead of temperature integrals. It gives the same accuracy as the Friedman method on a simulated example and it was said to be computationally faster than the method of Vyazovkin[155]. To defend the use of the incremental method of Vyazovkin in this thesis I like to add that the computational time is actually not that long: As an example, the time it took to process 13 experimental data curves, each with 25×10^3 to 52×10^3 data points, for the Vyazovkin method applied here was ca. 20 s on a laptop computer (ASUS ZenBook UX302, Intel Core i7-4500U CPU, 12.0 GB RAM). Admittedly, the same data was processed considerably faster ($\approx$0.1 s) with the method of Friedman but 20 s should not be considered as computationally slow.

Finally, a much simpler method was implemented by Šimon *et al.* [58] and Dubaj *et al.* [156]. Compared to some of the incremental linear methods (*e.g.*, [155] and [105]), this method uses the experimental data without prior transformation. Additionally, compared to *e.g.* the method of Vyazovkin used in this work, the method of Dubaj *et al.* [156] is based on an apparently simpler minimization problem and the determination of the statistical error in the derived kinetic parameters is straight forward[156]. The method is based on the integrated form of the rate equation written as

$$\beta = \int_{T_1}^{T_{i+1}} \frac{dT}{A\exp(E/RT)} = J(T_i, T_{i+1}, A, E). \tag{3.28}$$

By subtracting the heating rate β from Eq. (3.28) a non-linear implicit regression model is achieved. This model can be transformed into a non-linear orthogonal regression problem which leads to a statistically sound objective function that

through minimization of data at several different heating rates gives the parameters A and E as a function of conversion. Except for the explicit expression of β in the method there are no obvious disadvantages with this method. The explicit expression of heating rate demands experimental data for which the sample temperature can be described with a constant β.

The latter two of the above methods can be adopted to make predictions at arbitrary temperature programs. The nuances of the method used in this thesis and some of the previously published methods can hardly be used as argument enough to call the method used in this thesis new. Nonetheless, the differences such as conditioning of the rate expression, no explicit use of β in the expressions, as well as taking an average of the time integrals used, instead of using a value for a specific temperature program, at least makes this method a step in the right direction.

3.2.4 Implementation

All the numerical routines were implemented in Python, using the modules Scipy and Numpy[157]. Details about the implementations can be found in paper 1-3.

Chapter 4

Results and discussion

This chapter presents a compilation of the results from paper 1-4 in three parts: thermal analysis, kinetic analysis and mass-loss predictions. Note that if not stated otherwise, all the plotted experimental curves are chosen arbitrarily among the repeated runs and illustrate non-smoothed data.

4.1 Thermal analysis

This section presents the main thermal analysis results from paper 1-4.

4.1.1 Thermal lag

Thermal lag and its consequences for kinetic interpretations is discussed on page 14. In this thesis the occurrence of thermal lag was investigated for microcrystalline cellulose, spruce powder and spruce chips by comparing the peak temperatures as a function of heating rate and sample mass. The peak temperature is defined as the temperature for which the maximum mass-loss rate is reached.

The thermal conversion of microcrystalline cellulose was investigated in paper 1. TGA was conducted for three different sample masses (1.6, 4.0 and 9.9 mg) and heating rates ranging from 2-15 K/min. Fig. 4.1 shows a plot of the peak temperatures as a function of heating rate, comparing the three sample masses. It is clear that as the heating rate increases the difference in the peak temperatures between the three sample masses increases. This is a clear indication of thermal lag and it shows that at 10 K/min and a sample mass of 4.0 to 9.9 mg, microcrystalline cellulose is subject to thermal lag. For 9.9 mg there is thermal lag even at 5 K/min. To investigate whether also the lowest sample mass process is affected by thermal lag,

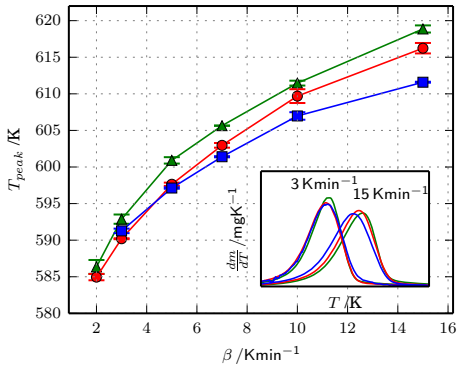

Figure 4.1: Mean peak temperatures for microcrystalline cellulose plotted as a function of heating rate for sample mass 1.6 mg (squares), 4.0 mg (circles) and 9.9 mg (triangles). Bars indicate standard deviation in peak temperatures. *Inset*: Mass-loss rate as a function of sample temperature. A Savitsky-Golay filter was used to smooth the rate curves to increase visibility.

additional runs at 15 K/min with a mass of 2.7 mg were performed (not shown). Such tests showed an increase in the peak temperature compared to a sample mass of 1.6 mg which means that a mass lower than 2.7 mg is needed to prevent thermal lag. Since decreasing the sample mass will decrease the signal to noise ratio the sample mass cannot be decreased to very low levels without a decrease in the data quality. Data quality issues were seen in the kinetic parameters derived from the experiments using 1.6 mg but this, and the thermal lag for the higher sample masses, did not prevent assessing some information about the reaction kinetics for the three sample masses studied.

Similar experiments were conducted for spruce wood in paper 2. The mass-loss rate as a function of heating rate for spruce powder at three different sample masses (1.5, 4 and 10 mg) is seen in Fig. 4.2. Notice that only one repetition per heating rate was performed for the lowest and highest sample mass. The absence of any difference in peak temperature as a function of sample mass suggests that, for wood powder, there is no thermal lag for a 10 mg sample at 100 K/min.

By comparing the influence of sample mass on the peak temperature for microcrystalline cellulose and spruce we realized that the thermal lag must be caused by factors other than just the sample mass. From literature we learned that cellulose pyrolysis exhibits strong endothermic reaction heats, compared to biomass with an overall heat of reaction close to zero[41, 158]. The self-cooling caused by endothermic reactions in the case of cellulose is probably the cause for the varying level of thermal lag seen for these two samples.

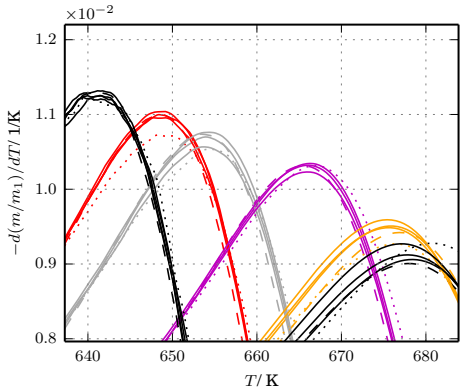

Figure 4.2: Zoom in around the peak temperatures for the normalized mass-loss rate curves for spruce wood. The normalized mass-loss rate curves $(d(m/m_1)/dT)$ are shown as a function of temperature at (from left to right) 10, 15, 20, 40, 80 and 100 K/min for sample mass 4 mg (solid line), 1.5 mg (dotted line) and 10 mg (dashed line). A Savisky-Golay filter was used to smooth the rate curves for increased visibility.

The thermal lag during pyrolysis of spruce chips in the macro-TGA experiments (see page 37 for a description of the experiments) was estimated by comparing conversion times as a function of furnace temperature and sample size (sample mass 160-700 mg). During the extreme conditions experienced by the sample, namely when a centimeter sized chip is introduced into a furnace at a temperature of 574 or 676 K, thermal lag is expected. The experimental mass-loss curves as a function of time are seen in Fig. 4.3 for 574 K and 676 K, respectively. As expected, the thermal lag is clearly visible as a shift of the mass-loss curves to the left as the sample thickness (sample mass) is increased. A longer pyrolysis time is needed to reach the same mass-loss percentage for the larger chips compared to for the smaller chips. These results indicate that at least for the medium and thick chips there is a temperature gradient and thus no true isothermal process. The values of the Biot number and the Pyrolysis number, estimated for each of the three chip sizes at the two mentioned temperatures, suggest that temperature gradients exist for all the studied cases except for the small chip (160 mg) at 574 K.

4.1.2 Char yield

Char is one of the lumped products resulting from pyrolysis. As presented in Section 2.2.1.1, the char yield is strongly influenced by the operation conditions, as

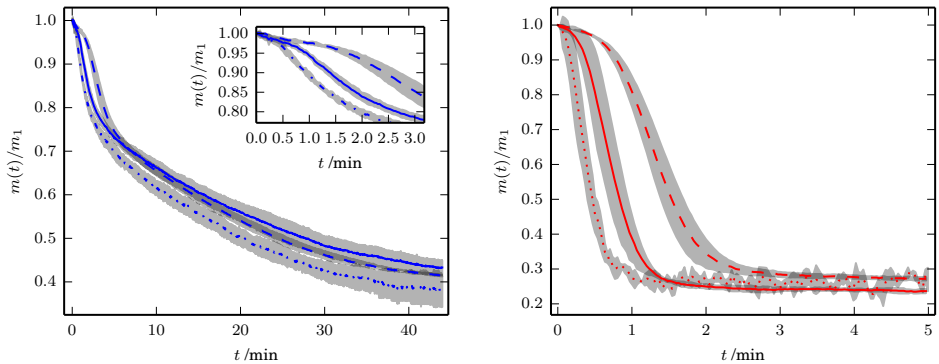

(a) (b)

Figure 4.3: Normalized mass as a function of time at (a) 574 K and (b) 676 K for thin (dash-dotted), medium (solid) and thick (dashed) chips. The inset in (a) shows a magnification of the curves at the start of the process. The lines represent mean values while the shaded areas around the lines represent standard deviations.

well as by the sample properties and dimensions. From TGA, the char yield is obtained as the final solid mass fraction, m_{final}/m_{dry} resulting after devolatilization, given that the main mass loss step has been completed. The definition of char yield used in this thesis is the residual solid mass fraction at close to complete conversion. Except for being characteristic for the sample and pyrolysis process conditions, the char yield is important when using isoconversional analysis, as explained on page 57.

The char yield for the three different sample masses of microcrystalline cellulose as a function of initial dry mass, m_1, and heating rate, β, is seen in Fig. 4.4. Starting with the influence of initial sample mass, Fig. 4.4a shows that there is a significant increase in char yield when the initial sample mass increases from 4.0 mg to 9.9 mg. The difference in char yield between samples with the initial mass 1.6 mg and 4.0 mg was found to be insignificant. The increased scatter in the char yield as the sample mass decreases is a result of the decreased accuracy in the measured mass as the noise to signal ratio increases. Fig. 4.4b shows that there is no consistent trend between the char yield and the heating rate: the differences in char yield at one and the same heating rate is sometimes bigger than the difference between values at different heating rates.

The char yield resulting from pyrolysis of wood powder as a function of heating rate is shown in Fig. 4.5. From this figure we see that for heating rates above 1 K/min, i.e. from 2 to 100 K/min, there is no significant influence of heating rate on

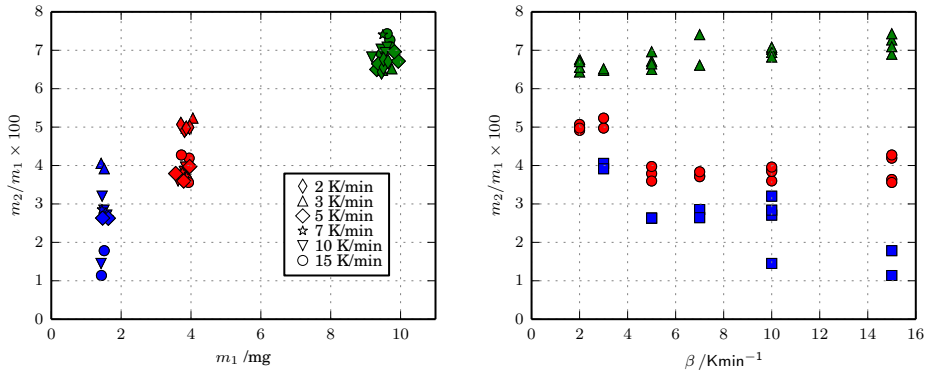

(a) (b)

Figure 4.4: Char yield for microcrystalline cellulose, as a function of initial dry mass m_1 (a) and heating rate β (b). In (a): Different heating rates are indicated by different markers. In (b): initial sample mass 1.6 mg (squares), 4.0 mg (circles) and 9.9 mg (triangles). m_2 is determined at 1023 K.

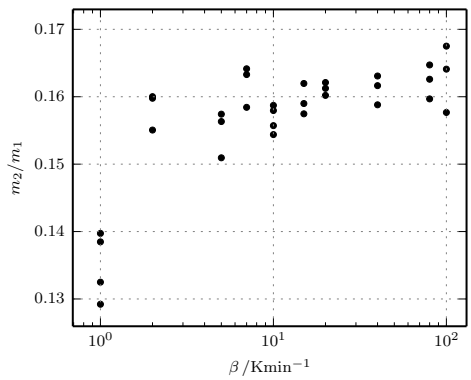

Figure 4.5: Char yield, m_2/m_1, as a function of heating rate β for spruce powder. The char yield is defined at 1000 K. All applied heating rates and repetitions are included. m_1 is the dry sample mass at 433 K.

the char yield. The difference in char yield achieved at 1 K/min compared to at the higher heating rates results from very slow char pyrolysis processes only giving significant contributions after long process times. The same explanation was used by Shen *et al.* [159] who also suggested that the difference could result from a more thermally stable char formed at higher heating rates. In addition, it could be argued that the difference could be due to trace amounts of oxygen in the system. In paper 3 we investigated this by comparing the mass loss at high temperature with data from another thermogravimetric equipment. The results from such analysis do not exclude the possibility that oxygen is responsible for the slow mass-loss at high temperatures, leading to the low char yield at $\beta = 1$ K/min seen in Fig. 4.5. For microcrystalline cellulose such mass-loss phenomena was absent while for the pulp and black liquor precipitates in paper 3, such mass-loss phenomena was seen at high temperatures. For the wood powder in paper 2, the data collected above 1000 K was a function of heating rate.

The char yields for the kraft samples studied in paper 3 are presented in Tab. 4.1. For these samples, the char yield was related to the amount of lignin and ash but there was no clear trend. For example, a higher char yield (20 wt% compared to 16 wt%) was achieved from the pulp sample P2 which had half as much Klason lignin (ash included) as wood. Similarly, sample L1 (62 % Klason lignin) gave 3 % more char than sample L2 (100 % Klason lignin). Notice that despite the small (3-4 %) differences in char yield in the mentioned examples the differences are significant.

Finally, the char yield for the wood chips having three different thicknesses revealed to be independent of sample mass at 574 to 676 K (paper 4). There was an influence of temperature on the char yield though and the char yield for the medium sized chip decreased linearly with temperature in the studied temperature interval. The char yield for 4 mg spruce powder compared to a 4 mg wood cube (both samples pyrolyzed in the Mettler Toledo system) gave different char yields, results that suggest an increased vapor hold-up time, and thus an increased presence of secondary reactions, during pyrolysis of wood chips, compared to wood powders.

4.1.3 Thermal characteristics

TGA gives a means to characterize the thermal decomposition of materials as a function of temperature. In Tab. 4.1 the most relevant characteristics resulting from TGA analysis are collected for the nine samples studied in this thesis. The characteristics are the peak temperature (T_{peak}), the char decomposition temperature (T_2), defined as the temperature where the char yield becomes a function of the heating rate, and the char yield at T_2. From this compilation we see that sample XL1 has the lowest peak temperature and sample L2 has the highest, among all samples. This is consistent with the knowledge that hemicellulose decomposes at

Table 4.1: Initial dry mass (m_1) peak temperatures (T_{peak}) at 2 K/min, char decomposition temperatures (T_2) and char yield (m_2/m_1) at T_2. *At $\beta = 3$ K/min. MCC = microcrystalline cellulose.

Material	T_1/K	m_1/mg	T_{peak}/K	T_2/K	$m_2/m_1 \times 100$
MCC	423	$1.6 \pm 5\%$	591 ± 0.3*	1023	2.6 ± 0.8
		$4.0 \pm 3\%$	585 ± 0.4		4.2 ± 0.6
		$9.9 \pm 2\%$	586 ± 0.9		6.8 ± 0.3
W	433	1.7±7%	613	1000	14.8
		4.0±3%			16.0
		10.0±1%			17.4
	403	$3.9 \pm 3\%$			16.0
P1	403	$3.9 \pm 3\%$	609	900	13.0
P2		$3.9 \pm 2\%$	592	860	20.0
XL1		$3.8 \pm 2\%$	537	910	38.0
XL2		$3.9 \pm 2\%$	545	950	39.0
XL3		$3.9 \pm 2\%$	556	950	36.0
L1		$4.0 \pm 2\%$	615	900	46.0
L2		$3.9 \pm 2\%$	640	1000	43.0

lower temperatures than lignin. Regarding the values of T_2, no trends related to ash or lignin amount was found. Additionally, we see that microcrystalline cellulose (MCC) gives considerably lower char yields than any of the other samples, even after considering the amount of ash in the char. The sample giving the second lowest char yield, after MCC, is the low lignin pulp (P1). The difference in char yield between wood and sample P1 is not as big as one could expect (based on the lignin content), only about 2 % difference in weight. Two of the XL-samples (XL2 and XL3) had the same lignin amount as sample L1 but sample L1 still gave about 10 wt% more char. This could be related to the high xylan content in the XL-samples. This idea is contradicted by the fact that sample XL1, having almost twice as high xylan content as the two other XL-samples, gives practically the same amount of char as sample XL2 and XL3. This indicates that the char amount is a result of many factors and seemingly not linearly related to ash, lignin and xylan amount.

4.2 Kinetic analysis

This section presents the main results from the kinetic analysis in paper 1-4.

4.2.1 Reliability analysis

The reliability of the apparent activation energies derived in this thesis were thoroughly examined to investigate if the features seen in the apparent activation energy trends were kinetic features or artifacts. There are several sources of uncertainties that can lead to artifacts in the derived apparent activation energies. The sources of error investigated in this thesis are due to i) data quality (noise and sampling rate), ii) violation of the isoconversional principle (i.e. different reaction mechanisms as a function of temperature program), iii) modifications of the raw data (wrong definition of conversion) and iv) optimization problems (finding local minima). The influence of all these factors on the derived apparent activation energy was assessed separately, as well as simultaneously by using the derived kinetic parameters (E_α and c_α) to reconstruct the data used for kinetic analysis or to make predictions of the mass-loss rate at extrapolated conditions (i.e. conditions not included in the kinetic analysis). In this thesis, reconstruction was always satisfactory. The results from the more stringent test, i.e. prediction, are presented in Section 4.3 on page 65.

The influence of the data quality on the apparent kinetic parameters was investigated by performing isoconversional analysis on parts of the experimental data. For example, in paper 1 the apparent activation energies derived from the two halves of the experimental data, i.e. excluding half of the repetitions for each heating rate, were compared. The same procedure was used on the spruce data in paper 2. In both of these papers the influence of the included heating rates were also studied. The analysis of parts of the experimental data revealed that the derived parameters did not vary significantly (resulted in a change below 10 % of the original value) as a function of the underlying experimental data. The influence of sampling rate on the accuracy of the derived apparent activation energy was investigated using analytical data with known apparent activation energies and different data resolution. By studying the derived values as well as the derived uncertainty (see Section 3.2) it was found that a higher sampling rate (data resolution) gives more reliable apparent activation energies. From this type of reliability check we learned that the Friedman method is slightly less robust, i.e. the derived apparent activation energies vary more as a function of the underlying data, compared to the method of Vyazovkin. Regarding the error propagation analysis (see Section 3.2), we found that, for both the differential and integral method, it has the tendency to underestimate the uncertainty. Additionally, the uncertainty derived for the differential method is more useful as an indication of the uncertainty in the derived parameters.

Establishing a Friedman plot ($\ln(d\alpha/dt)$ vs $1/T$) is an easy way to check whether the experimental data fulfills the isoconversional principle or not. If there is a linear relationship between the logarithm of the conversion rate at a certain conversion α, as a function of the inverse of the temperature then the isoconversional

principle holds at that conversion. This test was performed for all data collected in this thesis. The results from such analysis suggest that for data where the final char yield is a function of heating rate, the isoconversional principle is violated. Another thing visible from such analysis is that if the definition of conversion is erroneous, then the isoconversional principle will not be satisfied at high conversion. The definition of conversion may be erroneous if there is no clear plateau in the mass-loss at the end of the process, which was the case for some of the samples studied in this thesis. When there is no clear final plateau in the normalized mass then the definition of final mass (m_2) becomes arbitrary. A solution to this problem is to define the final conversion point at a temperature where the final char yield is not a function of heating rate. This prevents an arbitrary definition of conversion, which enables a sound comparison of different samples. Since this approach forces the conversion curves for different heating rates to reach complete conversion at the same temperature, it results in a violation of the isoconversional principle at the highest conversions, visible from a Friedman plot.

Finally, the derived apparent activation energies may be biased due to numerical optimization issues. This possible source of error was investigated by varying the interval in conversion, $\Delta\alpha$, used in both of the isoconversional methods. There was no significant influence of $\Delta\alpha$ on the derived apparent activation energies in the range of $0.01 < \Delta\alpha < 0.08$.

4.2.2 Apparent activation energies

In this thesis, apparent activation energies have been derived as a function of conversion for microcrystalline cellulose, spruce powder and the seven kraft process samples. The influence of sample mass (paper 1), heating rate (paper 2) and sample composition (paper 3) on the derived values have been investigated. The apparent activation energies derived from TGA data reflect the sum of the activation energies for all of the simultaneously proceeding processes. For microcrystalline cellulose the apparent activation energy, derived from 2-15 K/min, was practically constant as a function of conversion for all sample masses but for the lowest sample mass it was significantly higher. This was probably not a result of thermal lag since there was no decreasing trend in apparent activation energies as a function of the two higher sample masses. The difference was likely due to different pyrolysis processes since it was found that the conversion function ($f(\alpha)$) of the two higher sample masses differed from that of the lowest mass (see Section 4.2.3). For spruce we noticed that the apparent activation energy derived from a set of low heating rate experiments (2-10 K/min) differed from those derived using a set of high heating rates (10-100 K/min). Thorough reliability testing of the derived apparent activation energies suggested that the differences between high and low heating rate parameters resulted from differences in data quality. The rate expression derived from the low heating rate data set was more reliable and could

be used to predict the mass-loss rates at extrapolated conditions (see Section 4.3) with higher accuracy.

In paper 3, we derived the apparent activation energy for several samples of different chemical composition, using data from 2-10 K/min. We had hoped to find relationships between the characteristics in the apparent activation energy trends and the sample composition in terms of lignin content, ash content and carbohydrate composition. However, no such trends were found. Since the current thesis is executed with an engineering perspective the values of the apparent kinetic parameters are of secondary importance, as long as they are successful in predicting pyrolysis conversion rates. In cases where one specific thermal property is important the apparent activation energy trend as a function of conversion can be used as a fingerprint for the material. An example of this can be found in the study of Cinar *et al.* [39] where they use these fingerprints to compare the combustion-front propagation behavior of several crude oil samples. Several other examples are found in the book of Vyazovkin [38]. The latter illustrates that the apparent activation energy can be used as a measure of reactivity, where higher apparent activation energies are indications of a slower process. This information, i.e. the reaction rate, is of course already available in the raw data used to establish the kinetic fingerprint, but comparison of different samples can be facilitated by the use of these fingerprints. If using them as a measure of reactivity it is important to remember that the reaction rate is also determined by the effective prefactor, or the frequency factor, in the Arrhenius expression. As will be shown next, the interpretation of the fingerprints is not always straight forward.

The correlation between high activation energy and low reaction rate, i.e. high temperature onset of the reaction, is also seen for the samples in this work. Fig. 4.6, 4.8 and 4.10 show the conversion as a function of temperature in panel (a) and the apparent activation energy as a function of conversion in panel (b) for wood and the two pulp samples, the three xylan-lignin samples and the two lignin samples, respectively. Notice that the (b) panels in these figures contain the exact same information as Fig. 3 in paper 3, but the apparent activation energy is shown as a function of conversion instead of temperature.

Fig. 4.6 (a) illustrates that pulp sample P2 reaches a conversion of 0.4 at a lower temperature than for sample W and P1, and the process for sample P2 is thus faster. This is reflected in panel (b) where sample P2 has lower apparent activation energy up to a conversion of 0.4. As seen from Fig. 4.7, showing the conversion rate as a function of temperature, sample P1 and W have the same reaction rate at approximately 575 K (the curves intersect). From Fig. 4.6 (a) we see that this temperature corresponds to the conversions 0.2 and 0.3, for sample P1 and W, respectively. From Fig. 4.6 (b) we see that indeed, at these conversions the two samples have the same apparent activation energy.

Moving on to the xylan-lignin samples, Fig. 4.8 (a) shows that the three sam-

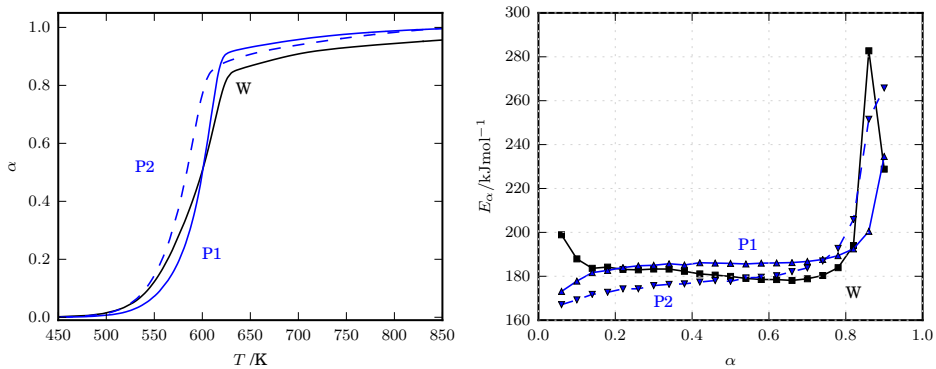

Figure 4.6: Conversion as a function of temperature at 2 K/min (a) and apparent activation energy as a function of conversion (b) for sample W, P1 and P2.

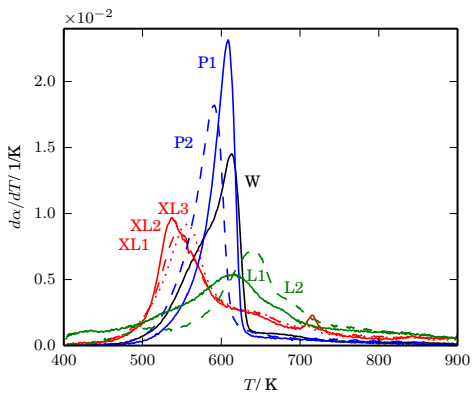

Figure 4.7: Conversion rate as a function of sample temperature for heating rate 2 K/min. W (black), P1 (blue solid line), P2 (blue dashed line), XL1 (red solid line), XL2 (red dashed line), XL3 (red dotted line), L1 (green solid line), L2 (green dashed line). The plotted curves were chosen arbitrarily among the repeated runs. m_1 is the dry sample mass at 403 K. The conversion, α, is defined in Eq. (3.1). A Savitsky-Golay filter was used to increase visibility.

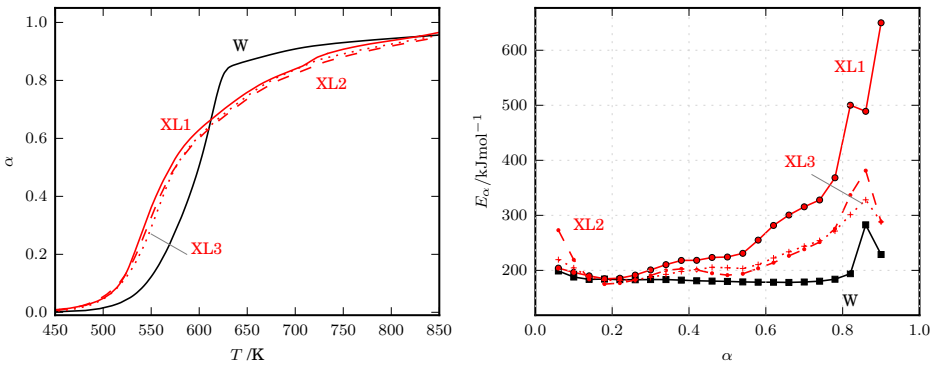

Figure 4.8: Conversion as a function of temperature at 2 K/min (a) and apparent activation energy as a function of conversion (b) for sample W, XL1, XL2 and XL3.

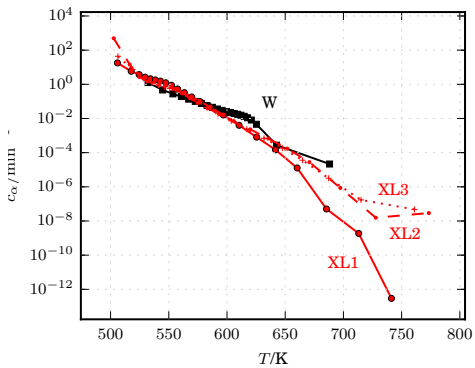

Figure 4.9: Effective prefactor as a function of temperature for the three XL-samples and wood. Linestyles are identical to those in Fig. 4.8 (b); the markers indicate the conversion values α, i.e. the upper limit of the interval $\alpha - \Delta\alpha$ used in the derivation of E_α. The effective prefactor for W is shown for comparison. A heating rate of $\beta = 2$ K/min was used to plot in the temperature domain. $T_0 = 600$ K.

ples have very similar pyrolysis behavior, despite the fact that they are precipitated from black-liquors produced after 50, 150 and 250 min cooking (see Tab. 3.1 on page 29). The XL1 sample decomposes slightly faster and reaches its peak temperature earlier than the other two samples (see Tab. 4.1 or Fig. 4.7). Looking at Fig. 4.8 (b) we see that up until a conversion of 0.2 sample XL1 has lower apparent activation energy than the other samples. Notice though that the apparent activation energy for W is even lower than for sample XL1, despite the fact that wood starts to decompose almost 30 K later (See Fig. 4.7). It is not easy to give an explanation for this behavior. One could claim that noise in the data is responsible, since the influence of noise is larger at low mass-loss signals. Proper testing, and the success of the kinetic parameters to reconstruct the original data (see Section 4.3) contradicts this idea. Remembering that the reaction rate is not only a function of temperature and apparent activation energy, but also the probability of reaction, included as a frequency factor in the Arrhenius temperature function, we understand that, despite proper reliability testing, this specific behavior at low conversion can be related to data quality issues. In Fig. 4.9 we see that the effective prefactor, i.e. the product between the conversion function and the frequency factor, is about one hundred times lower for W compared to the XL-samples. The same compensation is seen for sample XL2: the higher initial E_α is balanced by a higher effective prefactor. Since the effective prefactor is derived dependent on the apparent activation energy and experimental data, (see Eq. (3.18) on page 43) the effective prefactor can balance the mismatch between the experimental data and the apparent activation energy, giving rate expressions that can describe the process. The limited accuracy of the isoconversional methods at low and high conversions (below 0.1 and above 0.9), due to the noise inherently present in experimental data, is well known[35]. It is also for these low and high conversions that the actual value of m_{T2} in the definition of the conversion (see Eq. 3.1) has the most leverage. If using the apparent activation energy trends as fingerprints then the limited accuracy at high and low conversion is important to remember. Continuing with the trends in Fig. 4.8 (b) we see that the apparent activation energy is higher for XL1 than the other three samples until the end of the process. This matches with the reaction rate for sample XL1 which is lower for this sample than for the other samples throughout the rest of the process (see Fig. 4.7). The difference in reaction rate is very small though which makes it hard to motivate the significant difference in apparent activation energy.

Fig. 4.10 shows the conversion as a function of temperature and the apparent activation energy as a function of conversion for the lignin samples, compared to wood. As seen from Fig. 4.10 (a) sample L1 reaches a conversion of 0.2 at a temperature about 50 K lower than that for sample L2. In Fig. 4.10 (b) we see that sample L1 indeed has lower E_α than sample L2 below $\alpha = 0.2$. Actually, the apparent activation energy for sample L1 is lower than for sample L2 up until a conversion of 0.62 for L1 and 0.54 for L2. From Fig. 4.7 we see that at tempera-

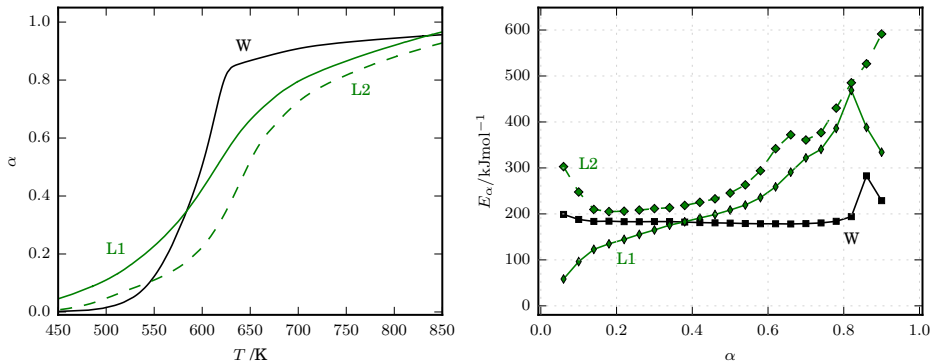

(a) (b)

Figure 4.10: Conversion as a function of temperature at 2 K/min (a) and apparent activation energy as a function of conversion (b) for sample W, L1 and L2.

tures below 625 K (the temperature for which sample L1 reaches 0.62 conversion) the rate of conversion is higher for sample L1 than for sample L2, confirming the trend in the apparent activation energy.

As a final investigation whether the apparent activation energy trends are consistent with the reaction rate or not, Fig. 4.11 (a) shows the conversion curves as a function of temperature together with the apparent activation energy as a function of conversion (b) for sample L2 and XL1. Fig. 4.11 (a) shows that the XL1 sample and the L2 sample decomposes practically at the same rate from 400 to 500 K. At approximately 500 K they have reached 6 % conversion (see Tab. 4.1). In Fig. 4.11 (b) we see that the apparent activation energy at 6 % conversion is 300 kJ/mol for sample L2 and 200 kJ/mol for sample XL1. So, even though the two samples decompose at a similar rate at the same temperature their apparent activation energies are different. At conversions between 0.2 and 0.5, the apparent activation energy for the two processes are similar, which is coherent with the similar conversion rates at these conversions, seen in Fig. 4.11. At higher conversions, above 0.8, the apparent activation energy for sample L2 increases above that for XL1 and as a result, the conversion rate for sample L2 decreases, compared to that for sample XL1. So, except for at the start of the process, the apparent kinetic parameters can be used as a fingerprint for these samples.

It is known that especially at high and low conversions the isoconversional methods have limited accuracy[35] and despite the thorough checking of the reliability of the apparent kinetic parameters (see Section 4.2.1) the high apparent activation energy for L2 at conversion 0.06 may be an artifact. As long as the derived ap-

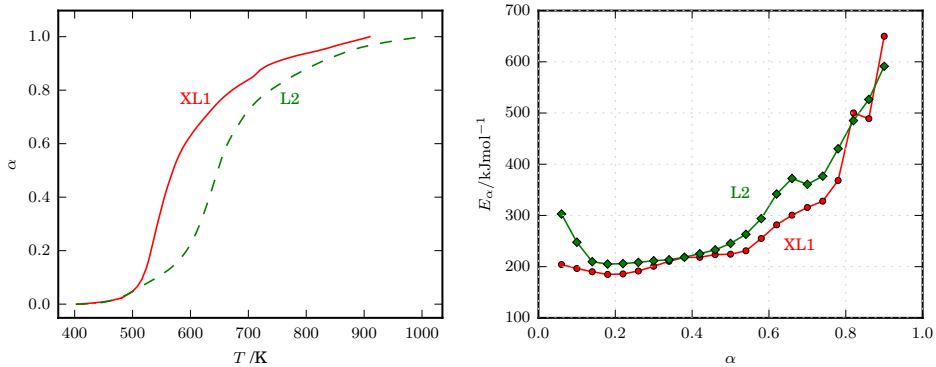

Figure 4.11: Conversion as a function of temperature at 2 K/min (a) and apparent activation energy as a function of conversion (b) for sample L2 and XL1.

parent kinetic parameters can be used for prediction purposes the reason for the individual features in the apparent activation energy trends are here of secondary importance. The results from the prediction studies are shown later in this thesis. A final note on the actual values of the apparent activation energy. It is not uncommon to see very high (above 600 kJ/mol and up to 1000 kJ/mol) apparent activation energies in the literature on thermal analysis kinetics, especially for physical processes like melting and glass transition [38], that happen in very narrow temperature ranges. This reminds us of the fact, stated previously, that the apparent activation energies derived from TGA through isoconversional analysis give an overall picture of the process, and not actual energy boundaries for elementary reaction steps.

4.2.3 The effective prefactor

As shown in Section 3.2, the effective prefactor, c_α, for the conditioned rate equation is the product of the conversion function and the rate constant at a reference temperature. The effective prefactor is derived based on the apparent activation energy (see Eq. (3.18)). Since the apparent activation energy is not a true physical parameter, and the effective prefactor is evaluated from the apparent activation energy, the effective prefactor c_α should not be interpreted as a physical parameter. Physical frequency factors for heterogeneous systems vary between 10^5 and 10^{18} s^{-1}[160, 161]. The actual values for the frequency factors are not given focus in this thesis but a quick estimation of the Arrhenius frequency factor, A, for the low

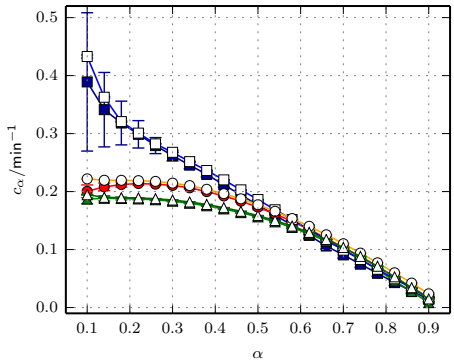

Figure 4.12: Effective prefactor as a function of conversion derived from experiments with sample mass 1.6 mg (squares), 4.0 mg (circles) and 9.9 mg (triangles). The data is for pyrolysis of microcrystalline cellulose (see paper 1). Closed symbols: differential method, open symbols: integral method. Reference temperature, $T_0 = 600$ K.

sample mass experiments of cellulose, assuming a first order reaction results in $A \approx 9 \times 10^{16} \mathrm{s}^{-1}$. The frequency factors were also roughly estimated for the kraft cooking samples in paper 3. We found that, at 50 % conversion and assuming a first order reaction, all the estimated frequency factors were within the limits presented above.

In paper 1 we showed that for processes with apparent activation energies practically independent of conversion the effective prefactor can be used to gain information about the conversion function. In this thesis, the nature of the conversion function was only investigated for microcrystalline cellulose since, using the methodology applied in the current thesis, the conversion function is not needed in order to predict conversion rates. The conversion function could be interesting from a fundamental viewpoint. However, for most biomass that consists of several different macromolecules it is unlikely that a single conversion function can be formulated to describe the process. The effective prefactor for microcrystalline cellulose as a function of conversion is seen in Fig. 4.12. By comparing the trend of the effective prefactor with that of generalized master plot curves, developed as a means to extract information about $f(\alpha)$, we saw that microcrystalline cellulose seems to decompose in different ways as a function of sample mass. It seems like samples of 4-10 mg cellulose decompose through an autocatalytic process at low conversion. At high conversion the decomposition process is instead similar to a first order reaction model. For this sample mass range the decomposition process can thus not be described by a single conversion function, despite the almost

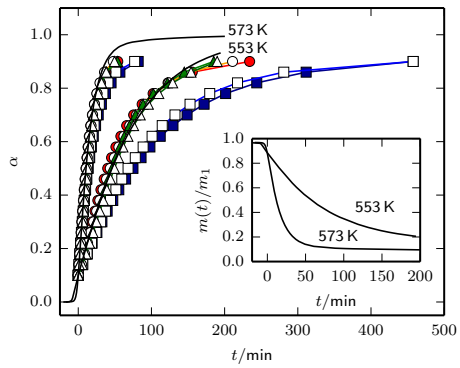

Figure 4.13: Conversion for quasi-isothermal curves as a function of time for microcrystalline cellulose (4.0 mg). Solid thick lines: experiments. Symbols: modeled data with kinetic parameters derived from sample mass 1.6 mg (squares), 4.0 mg (circles) and 9.9 mg (triangles) at heating rate 2-15 K/min (3-15 K/min for the low sample mass). Closed symbols: differential method, open symbols: integral method. Inset: Experimental mass loss curves for the two isotherms. In both panels, time zero is at 10% conversion.

constant apparent activation energy for the whole conversion range. For the low sample mass (1.6 mg) a single step first order reaction seemed more plausible.

4.3 Mass-loss predictions

This section presents the main prediction results from paper 1-4.

The most rewarding part when working with kinetic analysis is to use the derived reaction rate expression to make predictions at extrapolated conditions. If the prediction is successful then, as in this thesis, the quest is complete. If the prediction is not satisfactory, then the hard work of finding out why begins. In this thesis, all the predictions have been satisfactory.

Fig. 4.13 shows the quasi-isothermal experimental curves (solid black lines) of microcrystalline cellulose, together with the predicted curves (markers) derived from dynamic experiments (2 or 3 to 15 K/min) using 1.6, 4.0 and 9.9 mg sample mass. The quasi-isothermal experiments were performed with a sample mass of 4.0 mg and the initial heat-up period of the experiment was not taken into account by the model. Despite this, the two rate expressions derived from 4.0 and 9.9 mg sample mass were able to accurately describe the experiments at 553 K and 573K. The unsatisfactory results from the lowest sample mass could be due to either poor

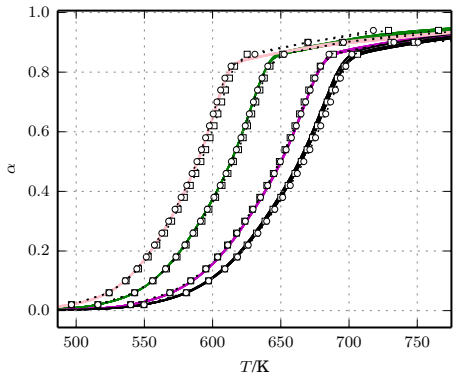

Figure 4.14: Reconstructed and modeled conversion for dynamic experiments of wood powder at heating rates (from left to right): 1, 5, 40 and 100 K/min. Only kinetic data from the integral method is shown. Solid lines: experimental curves (all repetitions shown): symbols: reconstructed and modeled data using kinetics from heating rate 2-10 K/min (circles) and 10-100 K/min (squares). The first marker to the left on each curve represent the initial value ($\alpha = 0.02$).

experimental data or another underlying reaction mechanism.

In our study of spruce powder (paper 2), two models based on dynamic experimental data at 1-10 K/min and 10-100 K/min respectively could successfully predict the mass-loss at 1-100 K/min and at quasi-isothermal conditions (temperatures 539-650 K). Both the differential method of Friedman and the integral method of Vyazovkin gave successful data, but the parameters from the integral method led to slightly more accurate predictions. Fig. 4.14 shows the experimental, modeled and reconstructed dynamic curves while Fig. 4.15 presents a comparison between the predicted and experimental quasi-isothermal curves. As seen from the literature overview in Section 2.3.4 there are only a handful of biomass pyrolysis studies that use the derived rate expression to predict mass-loss rates at extrapolated conditions and usually the prediction is not as accurate as seen in this thesis.

In paper 3 we studied samples with more heterogeneity than spruce wood and the commercial cellulose. Among the samples were black liquor precipitates, by-products from kraft pulp mills. These materials are relevant for upgrading to *e.g.*, char materials and fuels (see Section 1.2). The precipitates had different composition and to gain further knowledge about how pyrolysis properties are related to sample composition, this study also investigated the properties of two pulps of different composition. The different compositions gave different pyrolysis characteristics and as a result, different apparent kinetic parameters. As with microcrystalline cellulose and spruce wood, the derived rate expressions could be used

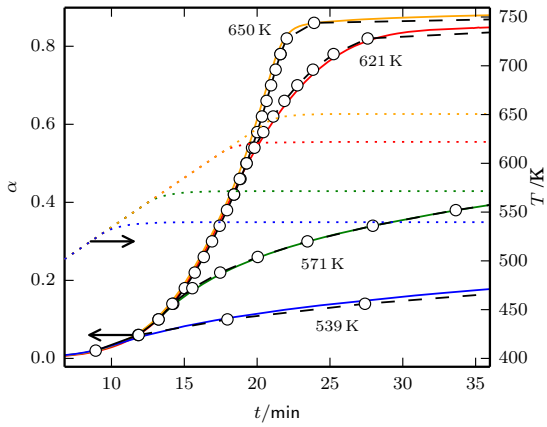

(a)

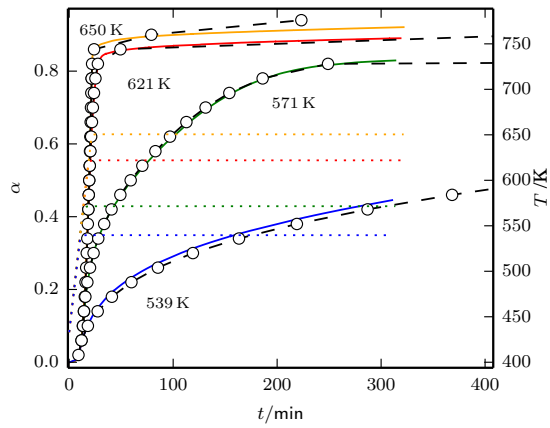

(b)

Figure 4.15: Conversion as a function of time for wood powder during quasi-isothermal pyrolysis at four different temperatures during (a) the first 30 min and (b) 300 min. Both the experimental (solid lines) and the modeled (markers) curves include the dynamic (10 K/min) segment needed to reach the isotherm. Kinetic parameters derived from dynamic experiments at 2-10 K/min, using the integral method, was used. Dotted lines show the evolution of temperature for the four plotted experimental curves.

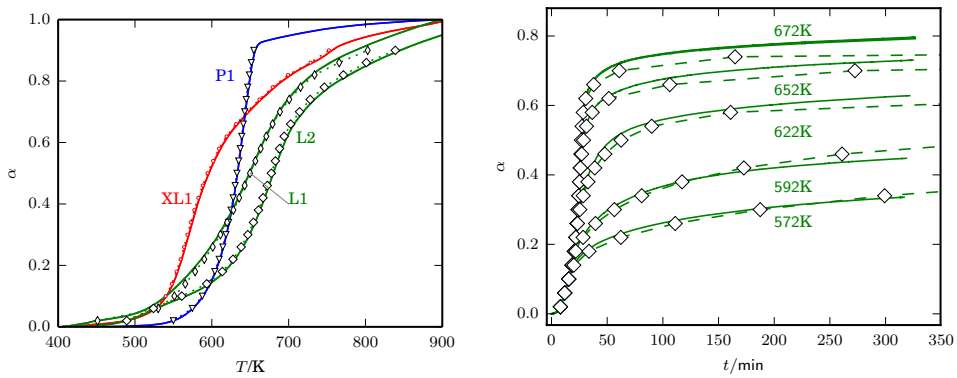

(a) (b)

Figure 4.16: (a) Conversion as a function of temperature for a heating rate of 15 K/min. Solid lines: experiments, markers: model predictions (circles: XL1, triangles: P1, prism: L1, diamond: L2). (b) Conversion as a function of time for the quasi isothermal decomposition of lignin sample L2. Solid lines: experiments, dashed lines with markers: model predictions. Model predictions account for the heating ramp preceding the isothermal segment.

to successfully predict the mass-loss at linear heating rate and quasi-isothermal conditions (only one sample was tested). Fig. 4.16a and 4.16b show the modeled and the experimental curves for dynamic conditions and quasi-isothermal conditions, respectively. The success of the model-free methodology used in this thesis to predict the mass-loss rate for these heterogeneous samples is promising, since the nature of biomass is far from homogeneous.

In our fourth paper we took our research a step closer to industry by performing experiments with industrial grade wood chips at rapid heating. As shown in Fig. 4.3, presenting the mass-loss data as a function of time, the medium and large size chips (300 mg and approximately 700 mg, respectively) were subject to thermal lag at both 574 K and 676 K. Since we did not use any heat transfer model, and did not measure the temperature profile inside the chips, the prediction is based on the temperature measured by the thermocouple situated below the chip (see Section 3.1.5.4). The predicted normalized mass, m_t/m_1, as a function of temperature is shown in Fig. 4.17 for three different hold-up times (1, 2 and 44 min). Only experimental data from the medium size chip is shown. The inset of each subfigure illustrates a parity plot, where dashed and dotted lines correspond to 10 % and 20 % deviation, respectively, between model and experiment. After a dwelling time of one minute, the model predicts a lower normalized mass compared to the

experiments, as seen in Fig. 4.17 (a). This can be explained by the thermal lag experienced by the chips early in the process, resulting in a lower temperature for the chip than that recorded by the thermocouple. After two minutes, illustrated by Fig. 4.17 (b), the deviation between the model and the experiments has decreased, possibly due to less thermal lag. Interestingly though, the model predicts a higher mass than seen in the experiments. This suggests that the chips decompose in a manner different from that for the spruce powder at linear heating rate, and/or that the temperature inside the chip is higher than the measured temperature, due to exothermal reactions. Indeed, at the beginning of the process (below 5 min) the thermocouple situated below the chip recorded some temperatures that were higher than those of the furnace (not shown). This temperature overshoot reached a maximum of 10 K at 676 K and decreased to insignificant levels at temperatures below 637 K. The same phenomena, i.e. that the temperature overshoot increases with increased temperature during pyrolysis of macro particles, has been described by Bates and Ghoniem [162] and references therein. Additional experimental and modeling data is needed to draw a conclusion about the source of the deviation between the predicted and the experimental results. Finally, at a dwelling time of 44 min, Fig. 4.17 (c) illustrates that the model underestimates the final char yield at temperatures above 574 K. This could be a result of an increased presence of secondary char forming reactions in the chips, compared to in the powder. At 574 K the char yield is lower for the chips than according to the prediction.

In paper 4 we also found that the isoconversional reaction rate expression for spruce powder derived in this thesis gave rise to practically the same predicted mass-loss values, as a function of temperature and time, as the rate expressions developed through model-fitting by Tapasvi *et al.* [32]. Since different temperature programs, TGA setups and numerical methods were used to establish these two rate expressions we can conclude that isoconversional methods and model-fitting methods can have equivalent predictive capabilities. The model developed by Tapasvi *et al.* [32] was based on data from nine different temperature programs, i.e. four linear heating rate programs, one isothermal program, two stepwise isothermal programs as well as one controlled reaction rate program and one modulated temperature program. This is five more temperature programs, compared to the four linear heating rate programs used to derive the isoconversional rate expression (paper 2). It would be interesting to compare the amount of experimental data that the model-fitting approach and the isoconversional approach need in order to establish reliable kinetic expressions. Finally, this comparison clarifies that it can be easier to develop an isoconversional rate expression than a model-fitting expression: The model suggested by Tapasvi *et al.* [32] was the result of thorough comparisons of several different reaction models, keeping varying numbers of fitting parameters constant. By using the methodology presented in this thesis the kinetic analysis is performed according to a protocol, enabling fast and easy analysis for many different materials.

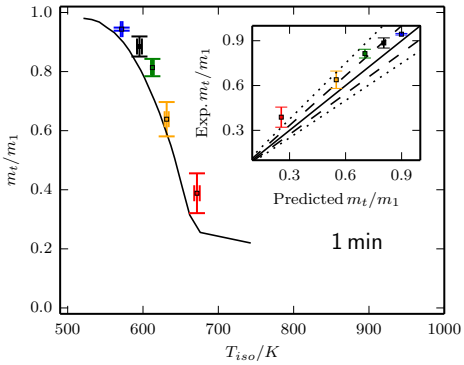

(a) 1 min

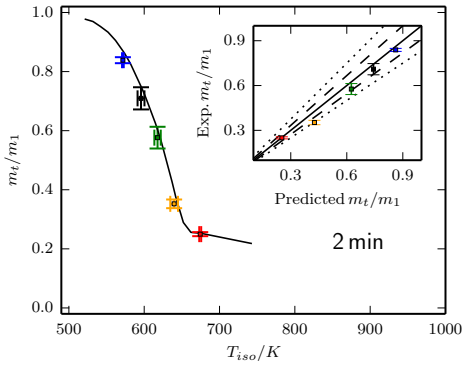

(b) 2 min

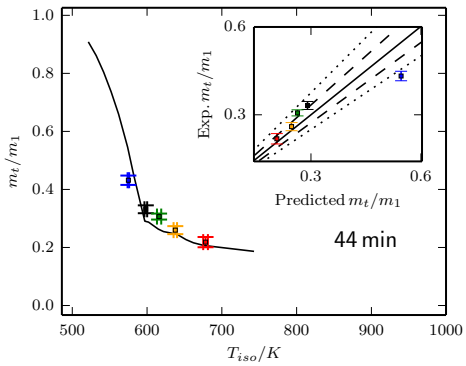

(c) 44 min

Figure 4.17: Modeled and experimental normalized mass after (a) 1, (b) 2, (c) 44 min of dwelling at the isothermal temperature. The curve in the main canvas represents the normalized mass modeled using m_2/m_1= 0.135. Squares are experimental mean normalized masses at the respective dwelling times. The error bars represent the standard deviation in mass and temperature at the plotted dwelling time. The insets show parity plots comparing the normalized mass at the same dwelling time as in the main canvas. The dashed lines represent a deviation from equality by 10 % while the dotted lines represent 20 % deviation.

Chapter 5

Conclusions

In this thesis I have thoroughly investigated the thermal properties of biomass samples of different origin, composition and heterogeneity. These materials were chosen to investigate the applicability of isoconversional analysis to describe the pyrolysis kinetics of these materials in particular, and biomass in general. The aim with this research was to develop a simple yet accurate methodology that has the potential to be used in industry to choose the optimal process parameters needed to reach a certain conversion. The following conclusions can be drawn:

- The methodology applied in this thesis fulfills both of the criteria posed in the aim of this thesis. The method is model-free and as such it is easier to use compared to model-fitting methods where different reaction schemes and conversion functions need to be tested and compared. Additionally, the methodology is accurate when it comes to reconstruction of the underlying experimental data and making predictions at extrapolated conditions. For example, a reaction rate expression developed from TGA data on spruce powder (4 mg) at 1-10 K/min can be used to predict, with more than 80 % accuracy, the final char yield for spruce chips at fast heating rate conditions (597 to 676 K).

- The isoconversional principle is valid between 2 and 15 K/min for all samples studied in this thesis (sample mass 4.0 mg) and between 1 and 100 K/min for wood (sample mass 4.0 mg). In addition, for cellulose it is also valid at quasi-isothermal experiments at 553-573 K, for spruce it is valid at quasi-isothermal conditions at 539-650 K and for lignin (sample L2) at quasi-isothermal conditions at 573 to 673 K (a 10 K/min ramp was used in all the experiments to reach the isotherm). The validity of the isoconversional principle tells us that for these complex materials the reactions

governing the conversion rate are not significantly altered within these process conditions. Since the studied materials constitute a broad collection of properties the success of the isoconversional principle shows promise also for other types of biomass.

- For kinetic evaluation based on mass-loss TGA data the integral incremental method of Vyazovkin gives more reliable kinetic parameters than the non-linear differential method of Friedman, determined based on the accuracy of the predictions. Depending on the desired accuracy, the easier to implement Friedman method can be used for predictions close to the conditions used during kinetic analysis. The application of the Friedman method in combination with the Vyazovkin method has some clear advantages compared to the use of only the method of Vyazovkin. The method of Friedman can be used to easily test the applicability of the isoconversional principle on the experimental data and a better estimation of the uncertainty in the derived apparent activation energy is achieved, giving an indication of *e.g.* the quality of the underlying experimental data. By comparing the results from the Friedman method with the results from the Vyazovkin method one can get an indication on whether the variations in apparent activation energies for different datasets result from different reaction chemistry or from data quality issues.

- Cellulose pyrolysis at 2-15 K/min and 4-10 mg seems to consist of two different processes: At low conversion the degradation behavior followed an autocatalytic process while at high conversion the decomposition seems to be first order. For a lower sample mass (1.6 mg) the autocatalytic behavior was not visible.

- By studying the kraft cooking samples we found that the char yield is related to the amount of lignin in the sample but the relationship is not linear. Factors such as ash and carbohydrate content seem to be important too.

Chapter 6

Recommendations for future work

This section contains some recommendations for how this research can be continued, together with some additional thoughts from the author.

Recommendations

- *Isoconversional analysis can bring the field forward*: A fully model-free isoconversional methodology, as the one used in this thesis, is important to bring the field of biomass pyrolysis forward. If such methods are used and properly tested at extrapolated conditions a library of model-free rate expressions could be established. This is also possible, but more difficult, with model-fitting methods since such library would need to contain not only the kinetic parameters and the conditions for which they are valid, but also the reaction schemes and the conversion functions. A library based on isoconversional methods would contain the apparent activation energy and the effective prefactor as a function of conversion, together with the conditions for which the isoconversional principle holds. Another advantage with a library over model-free isoconversional data is that as such a library grows it may be possible to find trends in the isoconversional fingerprints that may facilitate the optimization of the process parameters as a function of feedstock properties further. Such trends would be important for easy use of feedstock of different origin, which is important for the economy of the process.
- *Complete the pyrolysis model by taking into account mass and heat transfer*: A reaction rate expression is only one of the necessary pieces when

modeling a pyrolysis reactor. Heat and mass transfer models need to be used in combination with the developed kinetic expressions. Additionally, correlations between reaction enthalpy, heating value of the evolved gases and vapors and conversion are needed. With such correlations at hand, the model could be used to set up energy balances important *e.g.* for staged gasification.

- *Increase the knowledge of the chemical processes during pyrolysis*: There are some more sophisticated thermogravimetric methods that could have given additional kinetic information to this thesis. These tests are the so called jump method or "$f(\alpha)$-test"[163], controlled reaction rate method (CRR) and modulated TGA (MTG) (see *e.g.* [32, 51]). Additional analysis methods are also needed, such as *e.g.* evolved gas analysis, and analysis of the solid residue at different conversions, using *e.g.* solid-state NMR (nuclear magnetic resonance spectroscopy) and XRD (X-ray diffraction spectroscopy).

- *Create correlations between biomass types and process conditions*: One important feature for a biomass pyrolysis process is fuel flexibility. This does not only demand technical solutions that allow for heterogeneous feedstock but also a knowledge of how to change the process parameters to gain a homogeneous product stream. By correlating features in the apparent activation energy trends with pyrolysis properties for different groups of biomasses (hardwood, softwood, straw, husks, bark, nut shells etc.) it could be possible to minimize the day-to-day testing of new feedstocks. Isoconversional analysis enable establishing "fingerprints" that can be used to compare fuel properties.

- *Investigate the range for which the developed rate expressions hold*: An important aspect not touched upon in this thesis is the process range for which the derived reaction rate expressions are valid. It is important to know at what conditions the derived kinetic parameters are no longer valid, due to changes in the reaction pathway.

- *Report sample dimensions, especially for cellulose*: Due to the importance of secondary pyrolysis, especially for dense powders such as that used in the study of cellulose (paper 1), studies should report the sample dimensions properly.

- *Expand the test-matrix for the kraft precipitates*: The results from the kraft material study are interesting but hard to interpret and a more well designed study would be helpful. The influence of precipitation pH, washing solvents and cooking times on the thermal properties, together with additional analysis of the sample composition would be valuable.

- *Investigate the trends of apparent activation energies*: Before using the apparent activation energy trends as fingerprints it is important to investigate the behavior of E_α vs α, *e.g.* whether a process with higher E_α at low conversion starts earlier than a process with lower E_α. Perform simulation work to investigate what happens if there are several parallel reactions where one is giving high conversion rate with low E_α and one is giving low conversion rate with high E_α. Will the isoconversional E_α be a sum? Such simulation work will also increase the understanding of the features seen in apparent activation energy trends, which may result in an understanding about the chemical processes present. Such work may also give information about the effective prefactor.

- *Implement and test the non-parametric approach (NPK)*: This method has some interesting features[164] that should be explored.

- *Explore the relationship between IN and OUT properties during pyrolysis (e.g. torrefaction)*: It is one thing to be able to predict mass-loss as a function of temperature and time during torrefaction. To have fuel flexibility we need to understand the following: What chemical processes are giving the torrefied material the characteristic end properties like brittleness and hydrophobicity? What chemical and physical properties of the fresh biomass have the greatest influence on the end properties? How should two different types of biomass (with certain chemical and physical properties) be torrefied individually in order to get similar end properties?

Author's thoughts

Finally I would like to share some of my thoughts about this field, i.e. kinetic modeling based on thermogravimetric data. In this thesis I have tried to illustrate that the parameters that influence the pyrolysis process are many (equipment design, reaction conditions, sample properties, sample composition, impurities, etc.), which complicates the study and comparison of reaction kinetics. The influence of these parameters is seen when we look at the many different reaction schemes developed for cellulose, which is a much less complex substrate than lignocellulosic biomass. It is true that much of the spread in the reaction kinetics may be due to true differences in the reaction mechanism, due to variations in the studied systems, but it is also possible that the spread is caused by insufficient amount of data, poor control of the system parameters or derivation of values based on single temperature programs. There are many studies where the sole goal is to derive kinetic parameters and not to test their validity. This is unfortunate since, without knowing if the kinetic parameters could actually be used to predict pyrolysis rates at extrapolated conditions, it is impossible to know if the wide spread may be due to differences in reaction chemistry or not. Without this information we can not,

with confidence, use the results from such studies to gain additional information. One idea would be to use data mining and genetic algorithms to establish correlations between input parameters, such as biomass characteristics and process conditions, and output parameters, such as char yield, heating value, process time, etc. With the huge amount of data available in the literature such a project should be possible. But then again, much of the literature lack vital information about the reliability of the data.

Another idea is that the spread in the kinetic parameters and the reaction schemes used is not as big as it seems to be. It is possible that two different reaction schemes with different kinetic parameters may actually give rise to the same mass-loss curves as a function of temperature and time. An example of this is the result found in our fourth paper, i.e. that the model developed by Tapasvi *et al.* [32], consisting of three parallel reactions where two reactions were modeled with DAEM and one with a self-accelerating conversion function, predicted the same mass loss as a function of time and temperature as our fully isoconversional model for spruce did. The similarity between these two "reaction schemes" is difficult to see without the extra prediction step.

Finally, I believe that we should move away from using the Arrhenius model since it was developed to describe reaction rates of elementary reactions, not solid decomposition kinetics measured through mass-loss. There are alternative theories developed with the aim to describe solid state reactions, such as *e.g.* the physical model by L'vov[165]. Depending on what the purpose of the developed model is, the data collected from TGA may be too crude. Since a solid, or liquid material has an interface I also believe that we need to incorporate the surface effects into our models to be able to gain understanding about the reaction kinetics, and not only success in predicting conversions at extrapolated conditions close enough to our experiments.

In this thesis I made it my task to try to illustrate and bring up the limitations and difficulties related to deriving apparent kinetic parameters from thermogravimetric data using isoconversional analysis. In this way we can move forward. The isoconversional methods that I have used can provide predictive power for the studied materials but they do not give us much detailed understanding, yet.

Chapter 7

Bibliography

[1] L. Zhang, C. C. Xu, P. Champagne, Overview of recent advances in thermochemical conversion of biomass, Energy Convers. Manage. 51 (2010) 969–982, doi:10.1016/j.enconman.2009.11.038.

[2] S. V. Vassilev, D. Baxter, L. K. Andersen, C. G. Vassileva, An overview of the chemical composition of biomass, Fuel 89 (2010) 913–933, doi:10.1016/j.fuel.2009.10.022.

[3] A. Bauen, G. Berndes, M. Junginger, M. Londo, F. Vuille, Bioenergy – A sustainable and reliable energy source A review of status and prospects, Tech. rep., IEA Bioenergy: ExCo:2009:06 (2009).

[4] M. Broström, A. Nordin, L. Pommer, C. Branca, C. D. Blasi, Influence of torrefaction on the devolatlization and oxidation kinetics of wood, J Anal Appl Pyrol 96 (2012) 100–109, doi:10.1016/j.jaap.2012.03.011.

[5] P. McKendry, Energy production from biomass (part 3): gasification technologies, Bioresour. Technol. 83 (2002) 55–63, doi:10.1016/s0960-8524(01)00120-1.

[6] J. Koppejan, S. Sokhansanj, S. Melin, S. Madrali, Status overview of torrefaction technologies, Tech. Rep. Task 32: Final report, IEA Bioenergy (2012).

[7] A. Dufour, P. Girods, E. Masson, S. Normand, Y. Rogaume, A. Zoulalian, Comparison of two methods of measuring wood pyrolysis tar, J. Chromatogr. A 1164 (2007) 240–247, doi:10.1016/j.chroma.2007.06.049.

[8] Y. L. Brech, L. Jia, S. Cissé, G. Mauviel, N. Brosse, A. Dufour, Mechanisms of biomass pyrolysis studied by combining a fixed bed reactor with advanced gas analysis, J. Anal. Appl. Pyrolysis 117 (2016) 334–346, doi:10.1016/j.jaap.2015.10.013.

[9] P. Spath, D. Dayton, Preliminary screening - Technical and economic assessment of synthesis gas to fuels and chemicals with emphasis on the potential for biomass-derived syngas, NREL National Renewable Energy Laboratory (2003) NREL/TP–510–34929.

[10] M. Strandberg, I. Olofsson, L. Pommer, S. Wiklund-Lindström, K. Åberg, A. Nordin, Effects of temperature and residence time on continuous torrefaction of spruce wood, Fuel Process. Technol. 134 (2015) 387–398, doi:10.1016/j.fuproc.2015.02.021.

[11] P. Bergman, Combined torrefaction and pelletisation: The TOP process, Tech. rep., ECN-C-05-073 (2005).

[12] P. Bergman, J. Kiel, A. Boersma, R. R. Zwart, Torrefaction for co-firing in existing coal-fired power stations "BIOCOAL", Tech. rep., ECN-C-05-013 (2005).

[13] Prins, K. Ptasinski, F. Janssen, More efficient biomass gasification via torrefaction, Energy 31 (2006) 3458–3470, doi:10.1016/j.energy.2006.03.008.

[14] R. W. R. Zwart, H. Boerrigter, A. van der Drift, The impact of biomass pretreatment on the

feasibility of overseas biomass conversion to Fischer-Tropsch products, Energy Fuels 20 (2006) 2192–2197.

[15] J. Kiel, M. Ciepilk, J. Pels, W. van de Kamp, A. Saraber, R. van Eijk, Biomass co-firing in high percentages-Dutch R&D consortium pushing the limits, in 4th International Conference on Clean Coal Technologies in conjunction with the 3rd International Freiberg Conference on IGCC & XtL Technologies, ECN.

[16] M. van der Stelt, H. Gerhauser, J. Kiel, K. Ptasinski, Biomass upgrading by torrefaction for the production of biofuels: A review, Biomass Bioenergy 35 (2011) 3748 – 3762, doi: 10.1016/j.biombioe.2011.06.023.

[17] A. Uslu, A. P. C. Faaij, P. C. A. Bergman, Pre-treatment technologies, and their effect on international bioenergy supply chain logistics. Techno-economic evaluation of torrefaction, fast pyrolysis and pelletisation, Energy 33 (2008) 1206–1223, doi:10.1016/j.energy.2008.03.007.

[18] W.-H. Chen, P.-C. Kuo, Isothermal torrefaction kinetics of hemicellulose, cellulose, lignin and xylan using thermogravimetric analysis, Energy 36 (2011) 6451 – 6460, doi: 10.1016/j.energy.2011.09.022.

[19] M. Cremers, J. Koppejan, J. Middelkamp, J. Witkamp, S. Sokhansanj, S. Melin, S. Madrali, Status overview of torrefaction-A review of the commercialisation of biomass torrefaction, IEA Bioenergy (2015), ISBN:978 - 1 - 910154 - 23 - 6.

[20] D. Neves, H. Thunman, A. Matos, L. Tarelho, A. Gómez-Barea, Characterization and prediction of biomass pyrolysis products, Prog. Energy Combust. Sci. 37 (2011) 611 – 630, doi: 10.1016/j.pecs.2011.01.001.

[21] C. Li, K. Suzuki, Tar property, analysis, reforming mechanism and model for biomass gasification—An overview, Renewable Sustainable Energy Rev. 13 (2009) 594–604, doi: 10.1016/j.rser.2008.01.009.

[22] P. Brandt, E. Larsen, U. Henriksen, High Tar Reduction in a Two-Stage Gasifier, Energy Fuels 14 (2000) 816–819, doi:10.1021/ef990182m.

[23] S. Heidenreich, P. U. Foscolo, New concepts in biomass gasification, Prog. Energy Combust. Sci. 46 (2015) 72–95, doi:10.1016/j.pecs.2014.06.002.

[24] W. Lan, G. Chen, X. Zhu, X. Wang, B. Xu, Progress in techniques of biomass conversion into syngas, J. Energy Inst. 88 (2015) 151–156, doi:10.1016/j.joei.2014.05.003.

[25] M. J. Antal, E. Croiset, X. Dai, C. DeAlmeida, W. S.-L. Mok, N. Norberg, J.-R. Richard, M. A. Majthoub, High-Yield Biomass Charcoal, Energy Fuels 10 (1996) 652–658, doi: 10.1021/ef9501859.

[26] J. A. Caballero, J. A. Conesa, New approach to thermal analysis kinetics by considering several first order reactions, Thermochim. Acta 525 (2011) 40–49, doi:10.1016/j.tca.2011.07.019.

[27] J. E. White, W. J. Catallo, B. L. Legendre, Biomass pyrolysis kinetics: A comparative critical review with relevant agricultural residue case studies, J. Anal. Appl. Pyrolysis 91 (2011) 1–33, doi:10.1016/j.jaap.2011.01.004.

[28] S. Vyazovkin, K. Chrissafis, M. L. Di Lorenzo, N. Koga, M. Pijolat, B. Roduit, N. Sbirrazzuoli, J. J. Suñol, ICTAC Kinetics Committee recommendations for collecting experimental thermal analysis data for kinetic computations, Thermochim. Acta 590 (2014) 1–23, doi: 10.1016/j.tca.2014.05.036.

[29] A. K. Burnham, R. K. Weese, Kinetics of thermal degradation of explosive binders Viton A, Estane, and Kel-F, Thermochim. Acta 426 (2005) 85–92, doi:10.1016/j.tca.2004.07.009.

[30] A. K. Burnham, L. N. Dinh, A comparison of isoconversional and model-fitting approaches to kinetic parameter estimation and application predictions, J. Therm. Anal. Calorim. 89 (2007) 479–490, doi:10.1007/s10973-006-8486-1.

[31] S. Vyazovkin, A. K. Burnham, J. M. Criado, L. A. Pérez-Maqueda, C. Popescu, N. Sbirrazzuoli, ICTAC Kinetics Committee recommendations for performing kinetic computations on thermal analysis data, Thermochim. Acta 520 (2011) 1–19, doi:10.1016/j.tca.2011.03.034.

[32] D. Tapasvi, R. Khalil, G. Várhegyi, K.-Q. Tran, M. Grønli, Ø. Skreiberg, Thermal Decomposition Kinetics of Woods with an Emphasis on Torrefaction, Energy Fuels 27 (2013) 6134–6145, doi:10.1021/ef4016075.

[33] J. Cai, W. Wu, R. Liu, An overview of distributed activation energy model and its application in the pyrolysis of lignocellulosic biomass, Renew. Sustainable Energy Rev. 36 (2014) 236–246, doi:10.1016/j.rser.2014.04.052.

[34] A. Sharma, V. Pareek, D. Zhang, Biomass pyrolysis-A review of modelling, process parameters and catalytic studies, Renewable Sustainable Energy Rev. 50 (2015) 1081–1096, doi:10.1016/j.rser.2015.04.193.

[35] A. K. Burnham, R. L. Braun, Global Kinetic Analysis of Complex Materials, Energy Fuels 13 (1999) 1–22, doi:10.1021/ef9800765.

[36] G. Várhegyi, P. Szabó, M. J. Antal, Kinetics of Charcoal Devolatilization, Energy Fuels 16 (2002) 724–731, doi:10.1021/ef010227v.

[37] B. Chen, L. M. Castanier, A. R. Kovscek, Consistency Measures for Isoconversional Interpretation of In-Situ Combustion Reaction Kinetics, Energy Fuels 28 (2014) 868–876, doi:10.1021/ef4020235.

[38] S. Vyazovkin, Isoconversional Kinetics of Thermally Stimulated Processes, Springer Cham Heidelberg New York Dordrecht London (2015, ISBN 978-3-319-14174-9), doi:10.1007/978-3-319-14175-6.

[39] M. Cinar, B. Hasçaki, L. M. Castanier, A. R. Kovscek, Predictability of Crude Oil In-Situ Combustion by the Isoconversional Kinetic Approach, SPE Journal 16 (2011) 537–547, doi:10.2118/148088-pa.

[40] J. Farjas, P. Roura, Isoconversional analysis of solid-state transformations A critical review. Part III. Isothermal and non isothermal predictions, J. Therm. Anal. Calorim. 109 (2012) 183–191, doi:10.1007/s10973-011-1642-2.

[41] C. D. Blasi, Modeling chemical and physical processes of wood and biomass pyrolysis, Prog. Energy Combust. Sci. 34 (2008) 47–90, doi:10.1016/j.pecs.2006.12.001.

[42] A. Anca-Couce, A. Berger, N. Zobel, How to determine consistent biomass pyrolysis kinetics in a parallel reaction scheme, Fuel 123 (2014) 230–240, doi:10.1016/j.fuel.2014.01.014.

[43] F. Shafizadeh, C. P. P. S., Wood Technology: Chemical Aspects, vol. 43 of *ACS Symposium Series*, chap. 5 Thermal Deterioration of Wood, Americal Chemical Society (1977) pp. 57–81, doi:10.1021/bk-1977-0043.ch005.

[44] M. G. Grønli, G. Várhegyi, C. Di Blasi, Thermogravimetric Analysis and Devolatilization Kinetics of Wood, Ind. Eng. Chem. Res. 41 (2002) 4201–4208, doi:10.1021/ie0201157.

[45] N. Prakash, T. Karunanithi, Advances in Modeling and Simulation of Biomass Pyrolysis, Asian Network for Scientific Information 2 (2009) 1–27.

[46] A. Roberts, A review of kinetics data for the pyrolysis of wood and related substances, Combust. Flame 14 (1970) 261–272, doi:10.1016/s0010-2180(70)80037-2.

[47] C. Şerbănescu, Kinetic analysis of cellulose pyrolysis: a short review, Chem. Pap. 68 (2014) 847–860, doi:10.2478/s11696-013-0529-z.

[48] J. Lédé, Cellulose pyrolysis kinetics: An historical review on the existence and role of intermediate active cellulose, J. Anal. Appl. Pyrolysis 94 (2012) 17 – 32, doi:10.1016/j.jaap.2011.12.019.

[49] A. K. Burnham, X. Zhou, L. J. Broadbelt, Critical Review of the Global Chemical Kinetics of Cellulose Thermal Decomposition, Energy Fuels 29 (2015) 2906–2918, doi:10.1021/acs.energyfuels.5b00350.

[50] J. G. Reynolds, A. K. Burnham, Pyrolysis Decomposition Kinetics of Cellulose-Based Materials by Constant Heating Rate Micropyrolysis, Energy Fuels 11 (1997) 88–97, doi:10.1021/ef960086a.

[51] V. Mamleev, S. Bourbigot, M. L. Bras, J. Yvon, J. Lefebvre, Model-free method for evaluation of activation energies in modulated thermogravimetry and analysis of cellulose decomposition, Chem. Eng. Sci. 61 (2006) 1276 – 1292, doi:10.1016/j.ces.2005.07.040.

[52] V. Mamleev, S. Bourbigot, J. Yvon, Kinetic analysis of the thermal decomposition of cellulose: The main step of mass loss, J. Anal. Appl. Pyrolysis 80 (2007) 151–165, doi:10.1016/j.jaap.2007.01.013.

[53] L. Cabrales, N. Abidi, On the thermal degradation of cellulose in cotton fibers, J. Therm. Anal. Calorim. 102 (2010) 485–491, doi:10.1007/s10973-010-0911-9.

[54] R. Capart, L. Khezami, A. K. Burnham, Assessment of various kinetic models for the pyrolysis of a microgranular cellulose, Thermochim. Acta 417 (2004) 79–89, doi: 10.1016/j.tca.2004.01.029.

[55] P. E. Sánchez-Jiménez, L. A. Pérez-Maqueda, A. Perejón, J. M. Criado, Generalized master plots as a straightforward approach for determining the kinetic model: The case of cellulose pyrolysis, Thermochim. Acta 552 (2013) 54 – 59, doi:10.1016/j.tca.2012.11.003.

[56] R. Moriana, Y. Zhang, P. Mischnick, J. Li, M. Ek, Thermal degradation behavior and kinetic analysis of spruce glucomannan and its methylated derivatives, Carbohydr. Polym. 106 (2014) 60–70, doi:10.1016/j.carbpol.2014.01.086.

[57] J. Cai, Y. Chen, Iterative linear integral isoconversional method: Theory and application, Bioresour. Technol. 103 (2012) 309 – 312, doi:10.1016/j.biortech.2011.10.008.

[58] P. Šimon, P. S. Thomas, J. Okuliar, A. S. Ray, An Incremental Integral Isoconversional Method, J. Therm. Anal. Calorim. 72 (2003) 867–874, doi:10.1023/a:1025022416344.

[59] B. Roduit, P. Folly, B. Berger, J. Mathieu, A. Sarbach, H. Andres, M. Ramin, B. Vogelsanger, Evaluating SADT by advanced kinetics-based simulation approach, J. Therm. Anal. Calorim. 93 (2008) 153–161, doi:10.1007/s10973-007-8865-2.

[60] D. Tavast, Improved Usage of Wood Raw Material through Modification of the Kraft Process, Licentiate thesis, KTH Royal Institute of Technology, Stockholm, Sweden (2015), ISBN:978-91-7595-586-5.

[61] J. Zakzeski, P. C. A. Bruijnincx, A. L. Jongerius, B. M. Weckhuysen, The Catalytic Valorization of Lignin for the Production of Renewable Chemicals, Chem. Rev. 110 (2010) 3552–3599, doi: 10.1021/cr900354u.

[62] A. Van Heiningen, Converting a kraft pulp mill into an integrated forest biorefinery, Pulp Pap. Can. 107 (2006) 141–146.

[63] Lundberg, Converting a kraft pulp mill into a multi-product biorefinery - Part 1: Energy aspects, Nord. Pulp Pap. Res. J. 28 (2013) 480–488, doi:10.3183/npprj-2013-28-04-p480-488.

[64] M. Hamaguchi, J. Saari, E. Vakkilainen, Bio-oil and Biochar as Additional Revenue Streams in South American Kraft Pulp Mills, BioResources 8 (2013) 3399–3413.

[65] A. J. Ragauskas, M. Nagy, D. H. Kim, C. A. Eckert, J. P. Hallett, C. L. Liotta, From wood to fuels: Integrating biofuels and pulp production, Ind. Biotechnol. 2 (2006) 55–65, doi: 10.1089/ind.2006.2.55.

[66] N. M. L. Hansen, D. Plackett, Sustainable Films and Coatings from Hemicelluloses: A Review, Biomacromolecules 9 (2008) 1493–1505, doi:10.1021/bm800053z.

[67] W.-J. Liu, H. Jiang, H.-Q. Yu, Thermochemical conversion of lignin to functional materials: a review and future directions, Green Chem. doi:10.1039/c5gc01054c.

[68] J. Luterbacher, D. Martin Alonso, J. Dumesic, Targeted chemical upgrading of lignocellulosic biomass to platform molecules, Green Chem. doi:10.1039/c4gc01160k.

[69] P. Tomani, The lignoboost process, Cell Chem Technol 44 (2010) 53–58.

[70] E. Sjöström, Chapter 3 - WOOD POLYSACCHARIDES, in Wood Chemistry, Academic Press, San Diego, second edn. (1993) pp. 51 – 70, doi:10.1016/B978-0-08-092589-9.50007-3.

[71] D. Mohan, C. U. Pittman Jr., P. H. Steele, Pyrolysis of wood/biomass for bio-oil: A critical review, Energy Fuels 20 (2006) 848–889.

[72] S. V. Vassilev, D. Baxter, L. K. Andersen, C. G. Vassileva, T. J. Morgan, An overview of the organic and inorganic phase composition of biomass, Fuel 94 (2012) 1 – 33, doi: 10.1016/j.fuel.2011.09.030.

[73] J. Klinger, E. Bar-Ziv, D. Shonnard, Unified kinetic model for torrefaction–pyrolysis, Fuel Process. Technol. 138 (2015) 175–183, doi:10.1016/j.fuproc.2015.05.010.

[74] J. Orfão, F. Antunes, J. Figueiredo, Pyrolysis kinetics of lignocellulosic materials-three independent reactions model, Fuel 78 (1999) 349–358, doi:10.1016/S0016-2361(98)00156-2.

[75] H. Yang, R. Yan, H. Chen, D. H. Lee, C. Zheng, Characteristics of hemicellulose, cellulose and lignin pyrolysis, Fuel 86 (2007) 1781–1788.

[76] M. J. Antal Jr., G. Varhegyi, Cellulose pyrolysis kinetics: The current state of knowledge, Ind. Eng. Chem. Res. 34 (1995) 703–717.

[77] A. Anca-Couce, Reaction mechanisms and multi-scale modelling of lignocellulosic biomass pyrolysis, Prog. Energy Combust. Sci. 53 (2016) 41–79, doi:10.1016/j.pecs.2015.10.002.
[78] P. Morf, P. Hasler, T. Nussbaumer, Mechanisms and kinetics of homogeneous secondary reactions of tar from continuous pyrolysis of wood chips, Fuel 81 (2002) 843–853, doi:10.1016/s0016-2361(01)00216-2.
[79] P. Hasler, T. Nussbaumer, Gas cleaning for IC engine applications from fixed bed biomass gasification, Biomass Bioenergy 16 (1999) 385–395, doi:10.1016/s0961-9534(99)00018-5.
[80] G. Maschio, C. Koufopanos, A. Lucchesi, Pyrolysis, a promising route for biomass utilization, Bioresour. Technol. 42 (1992) 219–231, doi:10.1016/0960-8524(92)90025-s.
[81] X. Shi, J. Wang, A comparative investigation into the formation behaviors of char, liquids and gases during pyrolysis of pinewood and lignocellulosic components, Bioresour. Technol. 170 (2014) 262–269, doi:10.1016/j.biortech.2014.07.110.
[82] T. Hosoya, H. Kawamoto, S. Saka, Pyrolysis gasification reactivities of primary tar and char fractions from cellulose and lignin as studied with a closed ampoule reactor, J. Anal. Appl. Pyrolysis 83 (2008) 71–77, doi:10.1016/j.jaap.2008.06.002.
[83] A. M. Emsley, G. C. Stevens, Kinetics and mechanisms of the low-temperature degradation of cellulose, Cellulose 1 (1994) 26–56, doi:10.1007/BF00818797.
[84] Y.-C. Lin, J. Cho, G. A. Tompsett, P. R. Westmoreland, G. W. Huber, Kinetics and Mechanism of Cellulose Pyrolysis, J. Phys. Chem. C 113 (2009) 20097–20107, doi:10.1021/jp906702p.
[85] V. Mamleev, S. Bourbigot, M. L. Bras, J. Yvon, The facts and hypotheses relating to the phenomenological model of cellulose pyrolysis: Interdependence of the steps, J. Anal. Appl. Pyrolysis 84 (2009) 1 – 17, doi:10.1016/j.jaap.2008.10.014.
[86] A. Demirbaş, Biomass resource facilities and biomass conversion processing for fuels and chemicals, Energy Convers. Manage. 42 (2001) 1357–1378, doi:10.1016/s0196-8904(00)00137-0.
[87] W. Hemminger, S. Sarge, Definitions, Nomenclature, Terms and Literature, in Principles and Practice, Elsevier BV (1998) pp. 1–73, doi:10.1016/s1573-4374(98)80004-6.
[88] P. K. Chatterjee, Application of thermogravimetric techniques to reaction kinetics, Journal of Polymer Science Part A: General Papers 3 (1965) 4253–4262, doi:10.1002/pol.1965.100031221.
[89] M. J. Antal, G. Várhegyi, E. Jakab, Cellulose Pyrolysis Kinetics: Revisited, Ind. Eng. Chem. Res. 37 (1998) 1267–1275, doi:10.1021/ie970144v.
[90] S. Vyazovkin, Modification of the integral isoconversional method to account for variation in the activation energy, J. Comput. Chem. 22 (2001) 178–183, doi:10.1002/1096-987X(20010130)22:2<178::AID-JCC5>3.0.CO;2-.
[91] L. Vlaev, N. Nedelchev, K. Gyurova, M. Zagorcheva, A comparative study of non-isothermal kinetics of decomposition of calcium oxalate monohydrate, J. Anal. Appl. Pyrolysis 81 (2008) 253–262, doi:10.1016/j.jaap.2007.12.003.
[92] E. Simons, A. Newkirk, New studies on calcium oxalate monohydrateA guide to the interpretation of thermogravimetric measurements, Talanta 11 (1964) 549–571, doi:10.1016/0039-9140(64)80066-7.
[93] D. Dollimore, The application of thermal analysis in studying the thermal decomposition of solids, Thermochim. Acta 203 (1992) 7–23, doi:10.1016/0040-6031(92)85181-t.
[94] C. D. Blasi, Modeling intra- and extra-particle processes of wood fast pyrolysis, AIChE Journal 48 (2002) 2386–2397, doi:10.1002/aic.690481028.
[95] C. D. Blasi, C. Branca, Temperatures of Wood Particles in a Hot Sand Bed Fluidized by Nitrogen, Energy Fuels 17 (2003) 247–254, doi:10.1021/ef020146e.
[96] P. Šimon, Considerations on the single-step kinetics approximation, J. Therm. Anal. Calorim. 82 (2005) 651–657, doi:10.1007/s10973-005-0945-6.
[97] P. Šimon, Single-step kinetics approximation employing non-Arrhenius temperature functions, J. Therm. Anal. Calorim. 79 (2005) 703–708, doi:10.1007/s10973-005-0599-4.
[98] H. L. Friedman, Kinetics of thermal degradation of char-forming plastics from thermogravimetry. Application to a phenolic plastic, J Polym Sci Pol Sym 6 (1964) 183–195, doi:10.1002/polc.5070060121.

[99] M. Starink, The determination of activation energy from linear heating rate experiments: a comparison of the accuracy of isoconversion methods, Thermochim. Acta 404 (2003) 163–176, doi:10.1016/s0040-6031(03)00144-8.

[100] J. M. Criado, P. E. Sánchez-Jiménez, L. A. Pérez-Maqueda, Critical study of the isoconversional methods of kinetic analysis, J. Therm. Anal. Calorim. 92 (2008) 199–203, doi:10.1007/s10973-007-8763-7.

[101] T. Ozawa, A New Method of Analyzing Thermogravimetric Data, Bull. Chem. Soc. Jpn. 38 (1965) 1881–1886, doi:10.1246/bcsj.38.1881.

[102] J. H. Flynn, L. A. Wall, A quick, direct method for the determination of activation energy from thermogravimetric data, J. Polym. Sci. B Polym. Lett. 4 (1966) 323–328, doi:10.1002/pol.1966.110040504.

[103] J. H. Flynn, L. A. Wall, General treatment of the thermogravimetry of polymers, J. RES. NATL. BUR. STAN. SECT. A. 70A (1966) 487, doi:10.6028/jres.070a.043.

[104] J. J. M. Órfão, Review and evaluation of the approximations to the temperature integral, AIChE J. 53 (2007) 2905–2915, doi:10.1002/aic.11296.

[105] J. Cai, S. Chen, A new iterative linear integral isoconversional method for the determination of the activation energy varying with the conversion degree, J. Comput. Chem. 30 (2009) 1986–1991, doi:10.1002/jcc.21195.

[106] P. Budrugeac, An iterative model-free method to determine the activation energy of non-isothermal heterogeneous processes, Thermochim. Acta 511 (2010) 8–16, doi:10.1016/j.tca.2010.07.018.

[107] P. Farjas, J.and Roura, Isoconversional analysis of solid state transformations: A critical review. Part I. Single step transformations with constant activation energy, J. Therm. Anal. Calorim. 105 (2011) 757–766, doi:10.1007/s10973-011-1446-4.

[108] P. Budrugeac, Applicability of non-isothermal model-free predictions for assessment of conversion vs. time curves for complex processes in isothermal and quasi-isothermal conditions, Thermochim. Acta 558 (2013) 67–73, doi:10.1016/j.tca.2013.02.001.

[109] T. S. T. Akahira, Method of determining activation deterioration constant of electrical insulating materials, Res. Report Chiba Inst. Technol. (Sci. Technol.) 16 (1971) 22–31.

[110] I. Milosavljevic, E. M. Suuberg, Cellulose Thermal Decomposition Kinetics: Global Mass Loss Kinetics, Ind. Eng. Chem. Res. 34 (1995) 1081–1091, doi:doi: 10.1021/ie00043a009.

[111] J. A. Conesa, J. Caballero, A. Marcilla, R. Font, Analysis of different kinetic models in the dynamic pyrolysis of cellulose, Thermochim. Acta 254 (1995) 175–192, doi:10.1016/0040-6031(94)02102-T.

[112] R. Bilbao, J. Arauzo, M. L. Salvador, Kinetics and Modeling of Gas Formation in the Thermal Decomposition of Powdery Cellulose and Pine Sawdust, Ind. Eng. Chem. Res. 34 (1995) 786–793, doi:10.1021/ie00042a010.

[113] J. Banyasz, S. Li, J. Lyons-Hart, K. Shafer, Gas evolution and the mechanism of cellulose pyrolysis, Fuel 80 (2001) 1757 – 1763, doi:10.1016/S0016-2361(01)00060-6.

[114] W. DEJONG, A. PIRONE, M. WOJTOWICZ, Pyrolysis of Miscanthus Giganteus and wood pellets: TG-FTIR analysis and reaction kinetics, Fuel 82 (2003) 1139–1147, doi:10.1016/s0016-2361(02)00419-2.

[115] R. Radmanesh, Y. Courbariaux, J. Chaouki, C. Guy, A unified lumped approach in kinetic modeling of biomass pyrolysis, Fuel 85 (2006) 1211–1220, doi:10.1016/j.fuel.2005.11.021.

[116] A. K. Sadhukhan, P. Gupta, R. K. Saha, Modelling and experimental studies on pyrolysis of biomass particles, J. Anal. Appl. Pyrolysis 81 (2008) 183 – 192, doi:10.1016/j.jaap.2007.11.007.

[117] D. Pyle, C. Zaror, Heat transfer and kinetics in the low temperature pyrolysis of solids, Chem. Eng. Sci. 39 (1984) 147 – 158, doi:10.1016/0009-2509(84)80140-2.

[118] C. Zaror, D. Pyle, The pyrolysis of biomass: A general review, Sadhana 5 (1982) 269–285.

[119] S. Völker, T. Rieckmann, The Potential of Multivariate Regression in Determining Formal Kinetics of Biomass Pyrolysis, in A. V. Bridgwater (Ed.), Progress in Thermochemical Biomass Conversion, chap. 87, Wiley-Blackwell (2008) pp. 1076–1090, doi:10.1002/9780470694954.ch87.

[120] J. J. Manyà, E. Velo, L. Puigjaner, Kinetics of Biomass Pyrolysis: A Reformulated Three-Parallel-Reactions Model, Ind. Eng. Chem. Res. 42 (2003) 434–441, doi:10.1021/ie020218p.
[121] C. Branca, A. Albano, C. D. Blasi, Critical evaluation of global mechanisms of wood devolatilization, Thermochim. Acta 429 (2005) 133 – 141, doi:10.1016/j.tca.2005.02.030.
[122] E. Mészáros, G. Várhegyi, , E. Jakab, B. Marosvölgyi, Thermogravimetric and Reaction Kinetic Analysis of Biomass Samples from an Energy Plantation, Energy Fuels 18 (2004) 497–507, doi:10.1021/ef034030+.
[123] C. J. Gómez, L. Puigjaner, Slow Pyrolysis of Woody Residues and an Herbaceous Biomass Crop: A Kinetic Study, Ind. Eng. Chem. Res. 44 (2005) 6650–6660, doi:10.1021/ie050474c.
[124] A. G. Barneto, J. A. Carmona, J. E. M. Alfonso, R. S. Serrano, Simulation of the thermogravimetry analysis of three non-wood pulps, Bioresour. Technol. 101 (2010) 3220–3229, doi:10.1016/j.biortech.2009.12.034.
[125] N. Sonoyama, J. ichiro Hayashi, Characterisation of coal and biomass based on kinetic parameter distributions for pyrolysis, Fuel 114 (2013) 206–215, doi:10.1016/j.fuel.2012.04.023.
[126] F. Yao, Q. Wu, Y. Lei, W. Guo, Y. Xu, Thermal decomposition kinetics of natural fibers: Activation energy with dynamic thermogravimetric analysis, Polym. Degrad. Stab. 93 (2008) 90–98, doi:10.1016/j.polymdegradstab.2007.10.012.
[127] Y.-H. Park, J. Kim, S.-S. Kim, Y.-K. Park, Pyrolysis characteristics and kinetics of oak trees using thermogravimetric analyzer and micro-tubing reactor, Bioresour. Technol. 100 (2009) 400–405, doi:10.1016/j.biortech.2008.06.040.
[128] L. Gašparovič, Z. Koreňová, L. Jelemenský, Kinetic study of wood chips decomposition by TGA, Chem. Pap. 64 (2010) 174–181, doi:10.2478/s11696-009-0109-4.
[129] K. Slopiecka, P. Bartocci, F. Fantozzi, Thermogravimetric analysis and kinetic study of poplar wood pyrolysis, Appl. Energy 97 (2012) 491–497, doi:10.1016/j.apenergy.2011.12.056.
[130] T. Chen, J. Wu, Z. Zhang, M. Zhu, L. Sun, J. Wu, D. Zhang, Key thermal events during pyrolysis and CO2-gasification of selected combustible solid wastes in a thermogravimetric analyser, Fuel 137 (2014) 77–84, doi:10.1016/j.fuel.2014.07.077.
[131] W. Wu, Y. Mei, L. Zhang, R. Liu, J. Cai, Effective Activation Energies of Lignocellulosic Biomass Pyrolysis, Energy Fuels 28 (2014) 3916–3923, doi:10.1021/ef5005896.
[132] J. Cai, S. Yang, T. Li, Logistic distributed activation energy model – Part 2: Application to cellulose pyrolysis, Bioresour. Technol. 102 (2011) 3642 – 3644, doi:10.1016/j.biortech.2010.11.073.
[133] M. Antal, W. Mok, J. Roy, A. Raissi, D. Anderson, Pyrolytic sources of hydrocarbons from biomass, J. Anal. Appl. Pyrolysis 8 (1985) 291–303, doi:10.1016/0165-2370(85)80032-2.
[134] A. G. W. Bradbury, Y. Sakai, F. Shafizadeh, A kinetic model for pyrolysis of cellulose, J. Appl. Polym. Sci. 23 (1979) 3271–3280, doi:10.1002/app.1979.070231112.
[135] S. Kim, Y. Eom, Estimation of kinetic triplet of cellulose pyrolysis reaction from isothermal kinetic results, Korean J. Chem. Eng. 23 (2006) 409–414, doi:10.1007/BF02706742.
[136] H. S. Barud, C. A. Ribeiro, J. M. V. Capela, M. S. Crespi, S. J. L. Ribeiro, Y. Messadeq, Kinetic parameters for thermal decomposition of microcrystalline, vegetal, and bacterial cellulose, J. Therm. Anal. Calorim. 105 (2010) 421–426, doi:10.1007/s10973-010-1118-9.
[137] S. M. Shaik, C. Koh, P. N. Sharratt, R. B. Tan, Influence of acids and alkalis on transglycosylation and beta-elimination pathway kinetics during cellulose pyrolysis, Thermochim. Acta 566 (2013) 1–9, doi:10.1016/j.tca.2013.05.003.
[138] S. Hu, A. Jess, M. Xu, Kinetic study of Chinese biomass slow pyrolysis: Comparison of different kinetic models, Fuel 86 (2007) 2778–2788, doi:10.1016/j.fuel.2007.02.031.
[139] M. Miranda, C. Bica, S. Nachtigall, N. Rehman, S. Rosa, Kinetical thermal degradation study of maize straw and soybean hull celluloses by simultaneous DSC–TGA and MDSC techniques, Thermochim. Acta 565 (2013) 65–71, doi:10.1016/j.tca.2013.04.012.
[140] R. Moriana, F. Vilaplana, S. Karlsson, A. Ribes, Correlation of chemical, structural and thermal properties of natural fibres for their sustainable exploitation, Carbohydr. Polym. 112 (2014) 422–431, doi:10.1016/j.carbpol.2014.06.009.
[141] S. Beis, S. Mukkamala, N. Hill, J. Joseph, C. Baker, B. Jensen, E. Stemmler, M. Wheeler,

B. Frederick, A. van Heiningen, A. Berg, W. DeSisto, Fast pyrolysis of lignins, BioResources 5 (2010) 1408–1424.

[142] D. Ferdous, A. K. Dalai, S. K. Bej, R. W. Thring, Pyrolysis of Lignins: Experimental and Kinetics Studies, Energy Fuels 16 (2002) 1405–1412, doi:10.1021/ef0200323.

[143] T. Mani, P. Murugan, N. Mahinpey, Determination of Distributed Activation Energy Model Kinetic Parameters Using Simulated Annealing Optimization Method for Nonisothermal Pyrolysis of Lignin, Ind. Eng. Chem. Res. 48 (2009) 1464–1467, doi:10.1021/ie8013605.

[144] G. Jiang, D. J. Nowakowski, A. V. Bridgwater, A systematic study of the kinetics of lignin pyrolysis, Thermochim. Acta 498 (2010) 61–66, doi:10.1016/j.tca.2009.10.003.

[145] B. Jankovic, The comparative kinetic analysis of Acetocell and Lignoboost lignin pyrolysis: The estimation of the distributed reactivity models, Bioresour. Technol. 102 (2011) 9763 – 9771, doi:10.1016/j.biortech.2011.07.080.

[146] J. Cai, W. Wu, R. Liu, G. W. Huber, A distributed activation energy model for the pyrolysis of lignocellulosic biomass, Green Chem. 15 (2013) 1331, doi:10.1039/c3gc36958g.

[147] S. Wang, B. Ru, H. Lin, W. Sun, Pyrolysis behaviors of four O-acetyl-preserved hemicelluloses isolated from hardwoods and softwoods, Fuel 150 (2015) 243–251, doi:10.1016/j.fuel.2015.02.045.

[148] S. Wu, D. Shen, J. Hu, H. Zhang, R. Xiao, Intensive Interaction Region during Co-pyrolysis of Lignin and Cellulose: Experimental Observation and Kinetic Assessment, BioResources 9 (2014) 2259–2273.

[149] R. García, C. Pizarro, A. G. Lavín, J. L. Bueno, Biomass proximate analysis using thermogravimetry, Bioresour. Technol. 139 (2013) 1–4, doi:10.1016/j.biortech.2013.03.197.

[150] S. W. Dean, K. B. Cantrell, J. H. Martin, K. S. Ro, Application of Thermogravimetric Analysis for the Proximate Analysis of Livestock Wastes, J. ASTM Int. 7 (2010) 102583, doi:10.1520/jai102583.

[151] P. Šimon, Considerations on the single-step kinetics approximation, J. Therm. Anal. Calorim. 82 (2005) 651–657, doi:10.1007/s10973-005-0945-6.

[152] S. Vyazovkin, Kinetic concepts of thermally stimulated reactions in solids: A view from a historical perspective, Int. Rev. Phys. Chem. 19 (2000) 45–60, doi:10.1080/014423500229855.

[153] J. R. Taylor, An introduction to error analysis, University Science Books, Sausalito California, 2 edn. (1997).

[154] D. Montgomery, G. Runger, Applied Statistics and Probability for Engineers, John Wiley & Sons, 5 edn. (2010).

[155] P. Budrugeac, An iterative model-free method to determine the activation energy of heterogeneous processes under arbitrary temperature programs, Thermochim. Acta 523 (2011) 84 – 89, doi:10.1016/j.tca.2011.05.003.

[156] T. Dubaj, Z. Cibulková, P. Šimon, An incremental isoconversional method for kinetic analysis based on the orthogonal distance regression, J. Comput. Chem. 36 (2014) 392–398, doi:10.1002/jcc.23813.

[157] T. E. Oliphant, Python for Scientific Computing, Comput. Sci. Eng. 9 (2007) 10–20, doi:10.1109/mcse.2007.58.

[158] Q. Chen, R. Yang, B. Zhao, Y. Li, S. Wang, H. Wu, Y. Zhuo, C. Chen, Investigation of heat of biomass pyrolysis and secondary reactions by simultaneous thermogravimetry and differential scanning calorimetry, Fuel 134 (2014) 467–476, doi:10.1016/j.fuel.2014.05.092.

[159] D. Shen, S. Gu, A. Bridgwater, The thermal performance of the polysaccharides extracted from hardwood: Cellulose and hemicellulose, Carbohydr. Polym. 82 (2010) 39–45, doi:10.1016/j.carbpol.2010.04.018.

[160] H. F. Cordes, Preexponential factors for solid-state thermal decomposition, The Journal of Physical Chemistry 72 (1968) 2185–2189, doi:10.1021/j100852a052.

[161] R. Baetzold, Preexponential factors in surface reactions, J. Catal. 45 (1976) 94–105, doi:10.1016/0021-9517(76)90059-2.

[162] R. B. Bates, A. F. Ghoniem, Modeling kinetics-transport interactions during biomass torrefaction: The effects of temperature, particle size, and moisture content, Fuel 137 (2014) 216–229,

doi:10.1016/j.fuel.2014.07.047.

[163] M. Pijolat, M. Soustelle, Experimental tests to validate the rate-limiting step assumption used in the kinetic analysis of solid-state reactions, Thermochim. Acta 478 (2008) 34 – 40, doi: 10.1016/j.tca.2008.08.013.

[164] J. D. Sewry, M. E. Brown, "Model-free" kinetic analysis?, Thermochim. Acta 390 (2002) 217–225, doi:10.1016/S0040-6031(02)00083-7.

[165] A. Galwey, What can we learn about the mechanisms of thermal decompositions of solids from kinetic measurements?, J. Therm. Anal. Calorim. 92 (2008) 967–983, 10.1007/s10973-007-8413-0.

It is the mark of an educated mind to be able to entertain a thought without accepting it.

– Aristotle

Chapter 8

Acknowledgments

Finally, let me thank those who stood behind me during these years.

First, let me acknowledge the funding of this project, which was received from the Swedish Energy Agency and the academic and industrial partners within the Swedish Gasification Centre. Secondly, I want to thank my supervisors for this turbulent but successful ride! Thank you Klas Engvall for giving me the freedom to define the scope of this project. Thank you Per Alvfors for accepting the responsibility for my administrative supervision. Thank you Matthäus U Bäbler for helping me out when I got stuck and for becoming my scientific supervisor. Your office door is always open and I have felt welcome to discuss the research issues with you. Thank you Rosana Moriana for introducing me to the thermal analysis lab and becoming my scientific supervisor. Your positive words have encouraged me and you have always done your best to help. Thank you. The outcome of this thesis work would not have been the same without the input from all of you. I also want to thank those who I have had the chance to collaborate with or received work related help from, i.e. Raquel Bohn Lima, Daniel Tavast, Elisabet Brännvall, Staffan Sandin, Kentaro Umeki, Páscoa Dos Santos Magaia, Antonia Svärd, Peter Gille, Tommy Zavalis, Sergey Vyazovkin, Tibor Dubaj, Therese Vikström, Gustav Häggström, Kawnish Kirtania, Angel David Garcia Llamas and Albert Bach Oller. Thank you for the fruitful collaborations and advices.

To all of you who I did not collaborate with but met in the corridors of TR 42 during all these years: I am very happy to have had you as colleagues and friends. I have learned many different things from you. You have been my sounding board,

my source of laughter and my inspiration. Thank you for the nice lunch breaks, the board game nights, the beer brewing, the afterworks, the dinners and the dota games. A special thanks to Ann Ekqvist, Janne Vedin, Kiki Price, Inger Odnevall Wallinder and Ulla Jacobsson. I could always count on you.

Some of you have supported me from outside the walls of KTH. You are very dear to me and we should really meet more often! Thank you for supporting me :). A special thanks to the lovely people at KTH-hallen! Thank you for pushing me to my limit with a smile.

My amazing family! I know that you are as happy as I am that this chapter is finally closed. Thank you for the endless support, the warm hugs and the restful holidays. I love you. Let us enter the next chapter together! I also want to thank Rasmus' family, now also mine :). You are very important and dear to me and you have helped and supported me throughout rain and sunshine. Thank you.

Rasmus, my dearest and closest friend. It still amazes me how our love, strong nine years ago, can continue to get stronger every day. Thank you for being my guiding light throughout these years. Without you I would have lost my way. Tack min skatt! It will be interesting to see how our life together evolves, now that, for the first time since we got together, we will do different things. If I don't get a postdoc that is ;).

The music that I have been listening to during all the hours in the office has also helped and inspired me. I want to thank the following artists, among others, for my everyday ear candy: Slayer, Queen, Watain, Kate Bush, Tool, Mastodon, Electric Wizard, Pallbearer, Fleetwood Mac, Rush, Justice, Death in June, Alcest, Air, Jesu, Drudkh, Sade, Queensrÿche, Gojira, Burst, Doom:VS, BEAST!, Jex Thoth, Jimi Hendrix, Laibach, Enslaved, Summoning, Bolt Thrower, Meshuggah, ISIS, Dio, Faith No More, Metallica, YOB, Daft Punk, Depeche Mode, Kraftwerk, Primus, Marduk, Behemoth, Wolves in the throne room, Deru, Arcana, Ministry, Pink Floyd, Avatarium, Dargaard, Cathedral, Wodensthrone, Reverend Bizarre, Ahab, Evoken, Tyranny, Triptykon, Opeth, Katatonia, Amon Amarth, Ghost B.C., Type O Negative, Entombed, Morbid Angel, Vader, Autopsy, Arch Enemy, Dark Tranquility, Alice In Chains, A Perfect Circle, Bathory, Devil Townsend Project, Bring Me The Horizon, Aeon Zen, God Is An Astronaut, Immortal, Megadeth, Scepticism, Emperor, Nasum, Lycia, Fields Of The Nephilim, Cult Of Luna, Ulver, Judas Priest, Dissection, Leprous, Swallow The Sun, Mourning Beloveth, Testament and Anthrax.